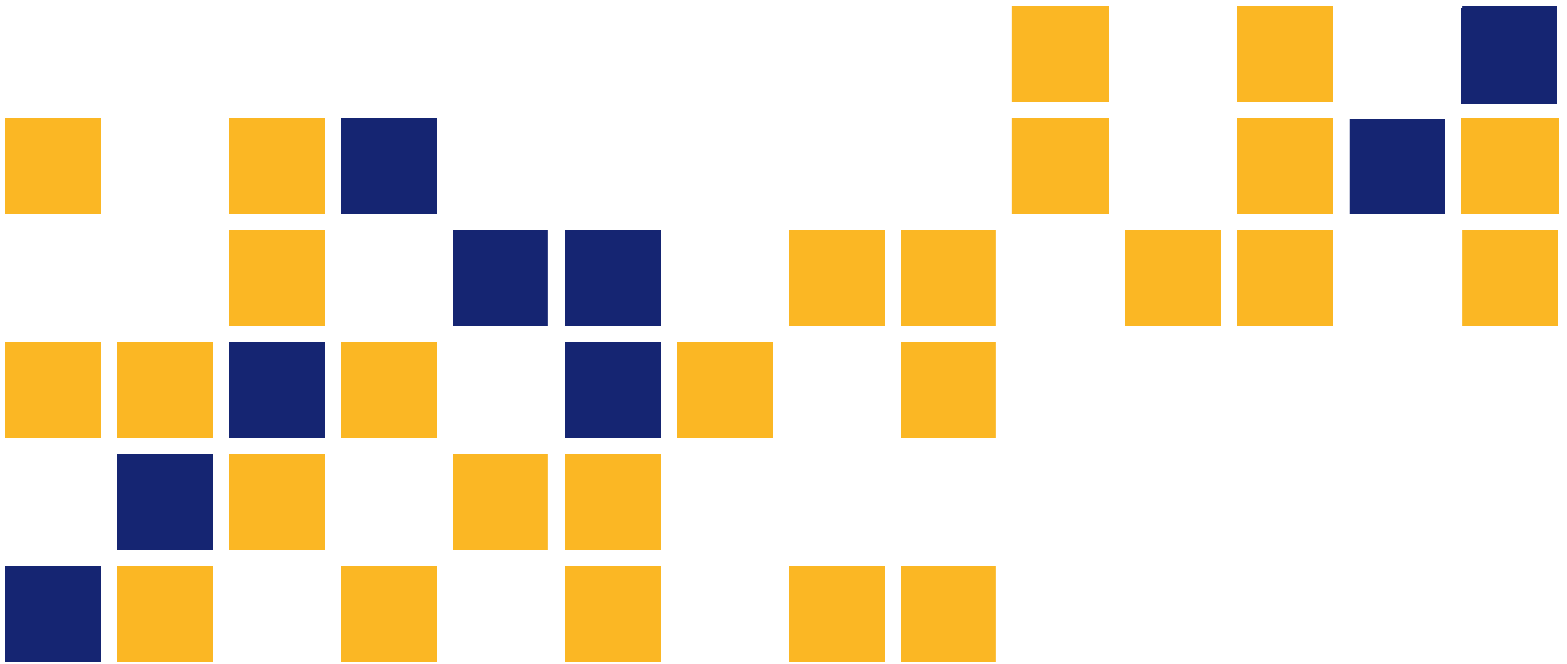


Air Void Clustering

Kyle A. Riding, Ph.D., P.E.
Asad Esmaeily, Ph.D., P.E.
Jan Vosahlik

Kansas State University Transportation Center



1 Report No. K-TRAN: KSU-13-6	2 Government Accession No.	3 Recipient Catalog No.	
4 Title and Subtitle Air Void Clustering		5 Report Date June 2015	
		6 Performing Organization Code	
7 Author(s) Kyle A. Riding, Ph.D., P.E., Asad Esmaily, Ph.D., P.E., Jan Vosahlik		7 Performing Organization Report No.	
9 Performing Organization Name and Address Kansas State University Transportation Center Department of Civil Engineering 2118 Fiedler Hall Manhattan, Kansas 66506		10 Work Unit No. (TRAIS)	
		11 Contract or Grant No. C1942	
12 Sponsoring Agency Name and Address Kansas Department of Transportation Bureau of Research 2300 SW Van Buren Topeka, Kansas 66611-1195		13 Type of Report and Period Covered Final Report August 2012–August 2014	
		14 Sponsoring Agency Code RE-0597-01	
15 Supplementary Notes For more information write to address in block 9. Appendices are available in a separate PDF. http://kdotapp.ksdot.org/kdotlib/kdotlib2.aspx or library@ksdot.org .			
<p>Air void clustering around coarse aggregate in concrete has been identified as a potential source of low strengths in concrete mixes by several Departments of Transportation around the country. Research was carried out to (1) develop a quantitative measure of air void clustering around aggregates; (2) investigate whether air void clustering can be reproduced in a laboratory environment; (3) determine if air void clustering contributes to lower compressive strengths in concrete mixes; and (4) identify potential factors that may cause clustering. Five types of coarse aggregate and five different air entraining agents were included in the laboratory study to determine if aggregate type or chemical composition of the air entraining agent directly relates to air void clustering. A total of 65 mixes were made, implementing the frequently used technique of retempering that has been previously associated with air void clustering around aggregates. Cylinders for compressive strength testing as well as samples for total air void analysis in the hardened concrete were made. Compressive strength at 7 and 28 days was determined, and automated testing for total air void analysis (including a new method of clustering evaluation) was performed on all mixes. This study found that it is possible to reproduce air void clustering in laboratory conditions. However, the results have shown that retempering does not always cause air void clustering. It was also observed that air void clustering is not responsible for a decrease in compressive strength of retempered concrete, as neither aggregate type nor chemical composition of the air entraining agent had a significant impact on severity of void clustering around coarse aggregate particles. It was found that the total air content and an inhomogeneous microstructure of the cement paste, not air void clustering, were responsible for lower strengths.</p>			
17 Key Words Air void clustering, Air entraining agents, Retempering, Air void analysis, Compressive strength, Coarse aggregate		18 Distribution Statement No restrictions. This document is available to the public through the National Technical Information Service www.ntis.gov .	
19 Security Classification (of this report) Unclassified	20 Security Classification (of this page) Unclassified	21 No. of pages 115 + Appendices	22 Price

This page intentionally left blank.

Air Void Clustering

Final Report

Prepared by

Kyle A. Riding, Ph.D., P.E.

Asad Esmaeily, Ph.D., P.E.

Jan Vosahlik

Kansas State University Transportation Center

A Report on Research Sponsored by

**THE KANSAS DEPARTMENT OF TRANSPORTATION
TOPEKA, KANSAS**

and

**KANSAS STATE UNIVERSITY TRANSPORTATION CENTER
MANHATTAN, KANSAS**

June 2015

© Copyright 2015, **Kansas Department of Transportation**

PREFACE

The Kansas Department of Transportation's (KDOT) Kansas Transportation Research and New-Developments (K-TRAN) Research Program funded this research project. It is an ongoing, cooperative and comprehensive research program addressing transportation needs of the state of Kansas utilizing academic and research resources from KDOT, Kansas State University and the University of Kansas. Transportation professionals in KDOT and the universities jointly develop the projects included in the research program.

NOTICE

The authors and the state of Kansas do not endorse products or manufacturers. Trade and manufacturers names appear herein solely because they are considered essential to the object of this report.

This information is available in alternative accessible formats. To obtain an alternative format, contact the Office of Public Affairs, Kansas Department of Transportation, 700 SW Harrison, 2nd Floor – West Wing, Topeka, Kansas 66603-3745 or phone (785) 296-3585 (Voice) (TDD).

DISCLAIMER

The contents of this report reflect the views of the authors who are responsible for the facts and accuracy of the data presented herein. The contents do not necessarily reflect the views or the policies of the state of Kansas. This report does not constitute a standard, specification or regulation.

Abstract

Air void clustering around coarse aggregate in concrete has been identified as a potential source of low strengths in concrete mixes by several Departments of Transportation around the country. Research was carried out to (1) develop a quantitative measure of air void clustering around aggregates; (2) investigate whether air void clustering can be reproduced in a laboratory environment; (3) determine if air void clustering contributes to lower compressive strengths in concrete mixes; and (4) identify potential factors that may cause clustering. Five types of coarse aggregate and five different air entraining agents were included in the laboratory study to determine if aggregate type or chemical composition of the air entraining agent directly relates to air void clustering. A total of 65 mixes were made, implementing the frequently used technique of retempering that has been previously associated with air void clustering around aggregates. Cylinders for compressive strength testing as well as samples for total air void analysis in the hardened concrete were made. Compressive strength at 7 and 28 days was determined, and automated testing for total air void analysis (including a new method of clustering evaluation) was performed on all mixes. This study found that it is possible to reproduce air void clustering in laboratory conditions. However, the results have shown that retempering does not always cause air void clustering. It was also observed that air void clustering is not responsible for a decrease in compressive strength of retempered concrete, as neither aggregate type nor chemical composition of the air entraining agent had a significant impact on severity of void clustering around coarse aggregate particles. It was found that the total air content and an inhomogeneous microstructure of the cement paste, not air void clustering, were responsible for lower strengths.

Acknowledgements

The authors wish to acknowledge the financial support of the Kansas Department of Transportation (KDOT) for this research. Dr. Heather McLeod and Randy Billinger were the KDOT project monitors for this project. The advice and assistance of Jennifer Distlehorst, Rodney Montney, and Andrew Jenkins is also gratefully acknowledged.

Table of Contents

Abstract	v
Acknowledgements	vi
Table of Contents	vii
List of Tables	ix
List of Figures	x
Chapter 1: Introduction	1
1.1 Research Background	1
1.2 Scope of Research.....	1
Chapter 2: Literature Review	2
2.1 Air Entrainment	2
2.2 Freeze-Thaw Resistance	3
2.3 Air-Void System Characterization.....	4
2.4 Mechanism of Air Entrainment	6
2.5 Factors Affecting Air Entrainment in Concrete.....	8
2.5.1 Cement	8
2.5.2 Supplementary Cementitious Materials	9
2.5.3 Admixtures.....	9
2.5.4 Aggregate.....	9
2.5.5 Water	9
2.5.6 Concrete Workability and Slump.....	10
2.5.7 Mixing Procedures	10
2.5.8 Transport, Construction Techniques, and Field Conditions	10
2.6 Effects of Air Entrainment on Concrete Properties	12
2.7 Air Void Clustering In Entrained Concrete	13
Chapter 3: Materials.....	16
3.1 Cementitious Materials	16
3.2 Aggregate.....	17
3.3 Air Entraining Admixtures	20
3.4 Testing Matrix.....	21
3.5 Mix Design	23
Chapter 4: Laboratory Study.....	25
4.1 Mixing Procedure	25
4.2 Material Testing and Evaluation Methods.....	28
4.2.1 Fresh Concrete Properties Testing	28
4.2.2 Compressive Strength	28
4.2.3 Air Void Analysis of Hardened Concrete	29

Chapter 5: Field Testing.....	42
5.1 Introduction.....	42
5.2 Methods	42
5.3 Materials, Mix Design, and Retempering	42
Chapter 6: Results	44
6.1 Fresh Concrete Properties	44
6.2 Compressive Strength.....	46
6.3 Air Void Content of Hardened Concrete	50
6.4 Air Void Clustering	53
6.5 Field Samples.....	57
Chapter 7: Discussion	60
7.1 Retempering.....	60
7.2 Aggregate Type.....	72
7.3 Type of Air Entraining Agent.....	84
7.4 Visual Rating of Air Void Clustering.....	92
7.5 Field Testing	93
Chapter 8: Conclusions and Recommendations	95
8.1 Conclusions.....	95
8.2 Recommendations.....	96
8.3 Future Research Needs	96
References.....	97

Due to file size, Appendices A to C are available in a separate file located at:

<http://kdotapp.ksdot.org/kdotlib/kdotlib2.aspx>

or by contacting the KDOT Library at library@ksdot.org or 785-291-3463.

List of Tables

Table 2.1: Air Entraining Agents.....	6
Table 3.1: Cement Chemical Composition – X-Ray Fluorescence	16
Table 3.2: Compound Calculations According to ASTM C150 (2012).....	17
Table 3.3: Coarse Aggregate Properties	18
Table 3.4: Fine Aggregate Properties	19
Table 3.5: Air Entraining Agents.....	20
Table 3.6: Labeling System	21
Table 3.7: Testing Matrix	22
Table 3.8: Testing Matrix – Control Mixes	23
Table 3.9: Mix Designs.....	24
Table 3.10: AEA Dosages.....	24
Table 5.1: Mix Design – 1PT0835A.....	43
Table 6.1: Fresh Concrete Properties.....	46
Table 6.2: Fresh Concrete Properties – Field Testing.....	57
Table 7.1: Compressive Strength – Comparative Analysis	67
Table 7.2: High Density Zones in Lincoln Quartzite.....	82

List of Figures

Figure 3.1: Aggregate Gradation	18
Figure 3.2: Fine Aggregate Gradation	19
Figure 4.1: Lancaster Shear Mixer.....	25
Figure 4.2: Mixing Procedure.....	26
Figure 4.3: Stored Hardened Air Void Samples	27
Figure 4.4: Compressive Strength Setup	29
Figure 4.5: Hardened Air Void Analysis Mold	30
Figure 4.6: Cutting of Specimens	31
Figure 4.7: Polishing Disks.....	32
Figure 4.8: Polishing Setup.....	32
Figure 4.9: Flattening the Sample.....	33
Figure 4.10: Scanner Settings	34
Figure 4.11: Scanning Setup.....	35
Figure 4.12: Image Scans.....	36
Figure 4.13: Aggregate Detection.....	37
Figure 4.14: Voids Detection.....	38
Figure 4.15: Clustering Zone	40
Figure 6.1: Air Content (Fresh) – Lincoln Quartzite	44
Figure 6.2: Air Content (Fresh) – Granite	45
Figure 6.3: Air Content (Fresh) – Limestone and SD Quartzite.....	45
Figure 6.4: Compressive Strength at 7 Days – Lincoln Quartzite	47
Figure 6.5: Compressive Strength at 7 Days – Granite	47
Figure 6.6: Compressive Strength at 7 Days – Limestone and SD Quartzite.....	48
Figure 6.7: Compressive Strength at 28 Days – Lincoln Quartzite	48
Figure 6.8: Compressive Strength at 28 Days – Granite	49
Figure 6.9: Compressive Strength at 28 Days – Limestone and SD Quartzite.....	49
Figure 6.10: Air Content (Hardened) – Lincoln Quartzite	50
Figure 6.11: Air Content (Hardened) – Granite.....	51
Figure 6.12: Air Content (Hardened) – Limestone and SD Quartzite	51
Figure 6.13: Spacing Factor – Lincoln Quartzite.....	52
Figure 6.14: Spacing Factor – Granite.....	52
Figure 6.15: Spacing Factor – Limestone and SD Quartzite	53
Figure 6.16: Clustering Index – Lincoln Quartzite.....	54
Figure 6.17: Clustering Index – Granite	54
Figure 6.18: Clustering Index – Limestone and SD Quartzite.....	55
Figure 6.19: Clustering Index (Visual Rating) – Lincoln Quartzite	55

Figure 6.20: Clustering Index (Visual Rating) – Granite	56
Figure 6.21: Clustering Index (Visual Rating) – Limestone and SD Quartzite.....	56
Figure 6.22: Compressive Strength at 7 Days – Field Testing	57
Figure 6.23: Compressive Strength at 28 Days – Field Testing	58
Figure 6.24: Hardened Air Void Content – Field Testing	58
Figure 6.25: Clustering Index – Field Testing	59
Figure 7.1: Slump Before and After Retempering.....	61
Figure 7.2: Fresh Air Content Before and After Retempering	61
Figure 7.3: Air Content vs Unit Weight.....	62
Figure 7.4: Clustering Index – Before and After Retempering	63
Figure 7.5: Clustering Index – After Retempering and Control Mixes	64
Figure 7.6: Compressive Strength at 7 Days	65
Figure 7.7: Compressive Strength at 28 Days	65
Figure 7.8: Clustering Index vs Compressive Strength at 7 Days	68
Figure 7.9: Clustering Index vs Compressive Strength at 28 Days	69
Figure 7.10: Visual Clustering Rating vs Compressive Strength at 7 Days	70
Figure 7.11: Visual Clustering Rating vs Compressive Strength at 28 Days	70
Figure 7.12: Fresh Air Content vs Compressive Strength at 7 Days	71
Figure 7.13: Fresh Air Content vs Compressive Strength at 28 Days	72
Figure 7.14: Slump Change After Retempering	73
Figure 7.15: Increase in Air Content after Retempering by Aggregate Type.....	74
Figure 7.16: Clustering Index – Non-Washed Lincoln Quartzite.....	75
Figure 7.17: Clustering Index – Washed Lincoln Quartzite	75
Figure 7.18: Clustering Index – Granite	75
Figure 7.19: Clustering Index – Limestone	76
Figure 7.20: Clustering Index – SD Quartzite	76
Figure 7.21: Clustering Index vs Compressive Strength – Non-Washed Lincoln Quartzite.....	77
Figure 7.22: Clustering Index vs Compressive Strength – Washed Lincoln Quartzite	77
Figure 7.23: Clustering Index vs Compressive Strength – Granite	78
Figure 7.24: Clustering Index vs Compressive Strength – Limestone	78
Figure 7.25: Clustering Index vs Compressive Strength – SD Quartzite	79
Figure 7.26: AEA Dosage vs Air Content – Lincoln Quartzite	80
Figure 7.27: Higher Density Zones.....	81
Figure 7.28: Compressive Strength – Lincoln Quartzite	83
Figure 7.29: Increase in Slump After Retempering by Used AEA.....	84
Figure 7.30: Increase in Air Content After Retempering by Used AEA	85
Figure 7.31: Clustering Index – Daravair 1000	86
Figure 7.32: Clustering Index – AEA-92S	86

Figure 7.33: Clustering Index – Daravair M.....	87
Figure 7.34: Clustering Index – Polychem SA-50.....	87
Figure 7.35: Clustering Index – Darex II.....	88
Figure 7.36: Clustering Index – Average by AEA	88
Figure 7.37: Compressive Strength vs Change in Clustering Index – Daravair 1000.....	89
Figure 7.38: Compressive Strength vs Change in Clustering Index – AEA-92S	90
Figure 7.39: Compressive Strength vs Change in Clustering Index – Daravair M	90
Figure 7.40: Compressive Strength vs Change in Clustering Index – Polychem SA-50	91
Figure 7.41: Compressive Strength vs Change in Clustering Index – Darex II	91
Figure 7.42: Compressive Strength vs Change in Fresh Air Content – Darex II	92
Figure 7.43: Visual Clustering Evaluation.....	93

Chapter 1: Introduction

1.1 Research Background

Discovery of air entrainment was arguably one of the most significant milestones in the history of the concrete industry. In use since the 1930s, entrainment of small air voids allows concrete structures and pavements to better withstand the impact of aggressive environments, especially in cold climates. Since the 1970s, concerns have arisen regarding air void clustering around coarse aggregate particles. Clusters of entrained air bubbles were observed primarily during the summer construction season (May through August) in retempered mixes or mixes that use a non-organic air entraining admixture. Air void clustering has been blamed for low compressive strengths in concrete pavement (Cross, Duke, Kellar, & Johnston, 2000; Distlehorst, 2009).

1.2 Scope of Research

From July 2013 to July 2014, a laboratory study was conducted by the Department of Civil Engineering at Kansas State University (KSU), Manhattan, Kansas, to answer questions related to air void clustering. Extensive testing was conducted in order to answer the following questions:

1. Is air void clustering reproducible under laboratory conditions using materials frequently utilized on concrete pavement construction projects in Kansas?
2. What effect does concrete mix retempering have on air void clustering?
3. Is air void clustering directly associated with loss of compressive strength in retempered or non-retempered concrete?
4. How does the chemical composition of air entraining agents (AEA) affect air void clustering?
5. How does the aggregate type affect air void clustering?
6. What is the effect of aggregate cleanness on air void clustering?

Chapter 2: Literature Review

2.1 Air Entrainment

Similar to other breakthroughs in the concrete industry (such as reinforced concrete), air entrained concrete was discovered accidentally. In the mid-1930s, beef tallow was used as a grinding aid in cement production in New York State (Torrans & Ivey, 1968). Concrete made from this cement showed significantly improved resistance to freezing and thawing when exposed to water. Subsequent research attributed improved freeze-thaw performance to the incorporation of a fine air void system in the cement paste.

Currently, air-entrained concrete is required in cold climates or environments that include freezing water to protect concrete from freeze-thaw damage (Kosmatka, Kerkhoff, & Panarese, 2003). However, entrained air voids are not the only air bubbles found in concrete. Powers and Helmuth (1953), pioneers in the research of air-entrained concrete, defined three groups of voids in concrete:

- Gel pores: These are the smallest pores that can be found in cement paste (0.5-10 nanometers [nm]); water in these pores usually does not freeze. Gel pores represent approximately 28% of the total volume of hydration products (Pigeon & Pleau, 1995).
- Capillary pores: The size of these pores varies from 50 nm to 10 microns (μm). Capillary pores fill spaces between cement grains and hydration products originally occupied by water. Gel and capillary pores are randomly distributed throughout the concrete mass, separated with cement hydration products so water can move through the pores with changes in ambient conditions (Pigeon & Pleau, 1995).
- Air entrained voids: These voids are larger by order of magnitude than the gel or capillary pores. Entrained air void size typically ranges between 10 to 1,000 microns (Kosmatka et al., 2003; Walker, Lane, & Stutzman, 2006). Air bubbles, defined as entrained air voids, are “artificially” stabilized in concrete by adding AEAs to the concrete mix.

In addition to these three main groups of pores, two other types of air voids can be found in hardened concrete: entrapped voids (pores formed by air with radii larger than 1,000 micrometers) and water voids (irregularly shaped air voids primarily formed by water). These two void types weaken the concrete, instead of offering benefits (Walker et al., 2006).

2.2 Freeze-Thaw Resistance

A quality air void system in hardened concrete significantly improves its freeze-thaw resistance. Several theories explaining the principle of how air entrained concrete improves freeze-thaw durability have been developed. The first theory adopted the basic explanation of water behavior under freezing conditions, i.e., expansion of water volume when transforming from liquid to solid phase. Unfortunately, this theory did not account for the micro scale air void system in concrete, thereby neglecting some important factors (such as void size, capillary effects, or air void distribution in cement paste). Consequently, Powers and Willis (1950) introduced the hydraulic pressure theory. According to this theory, capillary pores become filled as the water present in the pores freezes and increases its volume. Remaining water that has no room to freeze is forced out from the pores and must move to available free spaces in the cement paste. Air voids provide such a location. Hydraulic pressure drives this motion, thereby obeying the water flow rules of Darcy's law. When the distance to the next available pore is too long or the freezing rate is too fast, hydraulic pressure within the cement paste may exceed available tensile strength, causing tensile crack formation in the paste. This theory was the first to provide a mathematical relationship between paste properties, freezing rate, and air void spacing (Pigeon & Pleau, 1995).

The original theory by Powers and Willis (1950), however, was found to be inconsistent with experimental data, so a modified theory known as the osmotic pressure theory was introduced (Powers & Helmuth, 1953). This theory accounts for the effect of dissolved alkalis in water within the pores. Because these ions are present in the solution and the capillary pores are very small (50 nm to 10 μm), the freezing point of water in these pores is lower than 32°F (0°C). During freezing, the concentration of dissolved chemicals in water increases as part of the water freezes. Water will keep freezing until the freezing point of the remaining concentrated pore

solution equals that of the concrete temperature. In other words, equilibrium between the ice and water solution is reached at that temperature. Considering the effect of pore size on freezing temperature (the lower the pore size, the lower the freezing temperature of water in the pore), the balanced temperature level is lower in smaller pores and, therefore, equilibrium is not preserved. Thus, water from smaller pores (including gel pores) moves to larger pores in order to reestablish a balanced state; this motion creates internal pressure that may cause cracking in the cement paste. If a sufficient air void system is created in concrete, ice formed in these voids more readily attracts water than capillary pores and protects the paste from damage.

Litvan (1973) elaborates on the assumption that water cannot freeze inside capillary pores due to changes in vapor pressure, and states that water must travel through the paste to the air void in order to freeze. Therefore, if it requires a longer period of time for water to travel to an air void than to freeze in the pore, internal pressure from the water traveling through the pores can cause damage.

One of the newest theories questions many assumptions made by previous explanations and adds several factors that have not been considered previously, such as the effect of the chemical composition of the air entraining agent used (Chatterji, 2003). However, despite the large number of hypotheses explaining air void action in concrete during a freeze-thaw event, a comprehensive theory clarifying the entire phenomena is still lacking.

2.3 Air-Void System Characterization

Spacing factor and total air void content are two parameters used to describe the air-void system. Spacing factor was developed by Powers and Willis (1950) as part of the hydraulic pressure theory. Two formulas, each developed using a specific idealized system, calculate the spacing factor. The first formula, given by Equation 2.1, is valid for values of p/A smaller than 4.342, while the second formula, defined by Equation 2.2, is valid for values of p/A greater than or equal to 4.342 (Garboczi et al., 2014).

$$L = \frac{p}{\alpha A} \quad \text{Equation 2.1}$$

$$L = \frac{3}{\alpha} \left[1.4 \left(\frac{p}{A} + 1 \right)^{\frac{1}{3}} - 1 \right] \quad \text{Equation 2.2}$$

Where:

L=	Spacing factor
p=	Paste volume
A=	Air void volume
α =	Specific surface area of voids

The first idealized system (small values of p/A ratio) is composed of air voids uniformly covered with a thick layer of paste; the layer thickness (or shell) is the spacing factor. The second system utilizes the cubic lattice approach, in which mono-sized air voids are equally distributed in the space at vertices of a cubic array. The dimensions of the unit cell are such that they reflect the air/paste ratio. The spacing factor then represents the distance from the center of a unit cell to the nearest air void surface (Garboczi et al., 2014; Peterson, 2008).

Freeze-thaw resistance clearly increases with lower spacing factors. Typically, a spacing factor of 200 microns (0.008 inches) and specific surface of 25 mm²/mm³ (600 inch²/inch³) are considered acceptable values for freeze-thaw resistant air entrained concrete (Pigeon & Pleau, 1995). In order to calculate spacing factor, analysis of a hardened concrete sample must be conducted. A 5-8% total air content by volume of concrete is typically required for freeze-thaw durable concrete design (Chatterji, 2003; KDOT, 2007). Air content in concrete can be determined on a fresh concrete sample utilizing the Pressure Method (ASTM C231, 2010), Volumetric Method (ASTM C173, 2014), or Gravimetric Method (ASTM C138, 2012), or on a hardened concrete sample (ASTM C457, 2012).

Fresh concrete air content, possibly the most common air void characteristic utilized daily in field applications, is often used as a prompt indicator of air system quality. However, total air content is not always the most accurate parameter of freeze-thaw resistance because

research has shown that the total volume of air voids and other parameters, such as uniform distribution of air voids in the cement matrix, are equally important factors in freeze-thaw resistant concrete (Whiting & Nagi, 1998).

2.4 Mechanism of Air Entrainment

To achieve the required air entrainment in concrete, AEAs are added to a concrete mix. Chemicals which can be utilized as AEAs are often byproducts of various chemical industries. Pigeon & Pleau (1995) classified AEAs into four groups:

1. Sodium salts of wood resin
2. Salts of fatty acids
3. Salts of sulphonated hydrocarbon
4. Alkyl-benzyl sulphonates

The classification system provided by Kosmatka et al. (2003; adapted from Naranjo, 2007) is shown in Table 2.1.

Table 2.1: Air Entraining Agents

Classification	Performance Characteristics
Wood resin and rosin	Quick air generation. Minor air gain with initial mixing. Air loss with prolonged mixing. Mid-size air bubbles formed. Compatible with most other admixtures.
Tall oil	Slower air generation. Air may increase with prolonged mixing. Smallest air bubbles of all agents. Compatible with most other admixtures.
Synthetic detergents	Quick air generation. Minor air loss with mixing. Coarser bubbles. May be incompatible with some high range water reducing admixtures. Also applicable to cellular concretes.
Vegetable oil acids	Slower air generation than wood rosins. Moderate air loss with mixing. Coarser air bubbles relative to wood rosin. Compatible with most other admixtures.

Source: Kosmatka et al. (2003); Adapted from Naranjo (2007), page 7.

Every AEA is a mixture of surfactants (substances reducing fluid surface tension) that must be soluble in water. Most modern AEAs are anionic, although cationic, nonionic, or amphoteric agents can also be used (Du & Folliard, 2005).

The process of air generation in concrete is complex, but two partial sub-processes can be easily distinguished: air bubble formation and air bubble stabilization. Two primary processes to generate air voids in concrete have been proposed (Ramachandran, 1997):

1. Folding of air by a vortex action (similar action to stirring a liquid).
2. Three-dimensional screen formed by fine aggregates when the concrete mass falls and cascades onto itself during mixing.

Concrete mixing is a living process in which air bubbles come into existence and simultaneously vanish unless stabilized. Three fundamental mechanisms may lead to the collapse of air bubbles (Du & Folliard, 2005):

1. Diffusion of air from a small bubble (high internal pressure) to a larger one (lower internal pressure).
2. Bubble coalescence due to capillary flow, leading to rupture of lamellar film between adjacent bubbles (typically slower than Mechanism 1, occurring even in stabilized systems). This mechanism often occurs in fresh concrete due to vibration.
3. Rapid hydrodynamic drainage of the liquid between bubbles, leading to rapid collapse. This mechanism is not likely to occur in fresh concrete because air bubbles are immersed in fresh concrete.

AEA molecules are responsible for various tasks during the mixing process, as symbolically introduced in Equation 2.3 and described as follows (Du & Folliard, 2005):

1. Because AEA molecules are typically composed of a hydrophilic head on one end and hydrophobic tail (usually negatively charged) on the other end, a portion of the AEA dosage is adsorbed by solid surfaces of the cement particles, primarily due to an electric attraction to the hydrophobic tail of the surfactant.

2. Another portion of AEA molecules dissolved in the bulk liquid phase has a primary purpose to reduce the surface tension of water (Pigeon & Pleau, 1995). Surface tension acts as an energy barrier against the stabilization of air bubbles; therefore, the surface tension reduction is necessary. Reduction allows for breakdown of large voids into smaller voids.
3. Once generated, air voids must be stabilized in the cement matrix. AEA concentrates at the liquid/air interfaces and forms an elastic film around the air bubbles, thereby protecting bubbles against collapse.

$$A = A_s + A_l + A_b$$

Equation 2.3

Where:	A=	AEA dosage
	A _s =	Portion of AEA adsorbed on solid surfaces
	A _l =	Portion of AEA in the bulk liquid phase
	A _b =	Portion of AEA in the liquid/air interface

2.5 Factors Affecting Air Entrainment in Concrete

Many factors affect AEA performance, the air entrainment process, and the quality of the air void system in concrete. Development of the air system is a complex process that has been studied for decades and is still not fully understood.

2.5.1 Cement

As the fineness of cement particles increases, the total surface area required to react with an AEA increases. Therefore, the amount of available surfactants in the system is reduced (as shown in Equation 2.3) and, consequently, the level of air entrainment is reduced (Kosmatka et al., 2003). A low-alkali cement may require 20-40% more AEA dosage than a high-alkali cement in order to achieve equivalent air content, because air content typically increases as cement alkali level increases (Pomeroy, 1987; Whiting & Nagi, 1998).

2.5.2 Supplementary Cementitious Materials

In general, increased AEA dosage is required to achieve targeted air content when any supplementary cementitious material (SCM) is used, due to its fineness and increased surface area of particles absorbing AEA molecules (Kosmatka et al., 2003).

2.5.3 Admixtures

Research has shown that use of additional concrete admixtures in conjunction with an AEA, such as water reducers, retarders, or super-plasticizers, can improve air entrainment and increase total air content. However, increased spacing factor has been associated with the usage of specific types of admixtures (Kosmatka et al., 2003).

2.5.4 Aggregate

If the amount of fine aggregates increases, the total amount of air content typically decreases, because sand particles provide reduced shear action due to their smaller size compared to particles that are of larger size (Du & Folliard, 2005). However, aggregate particles with sizes ranging from 0.0234 to 0.0059 inches (sieves #30 and #100, respectively) help with the retention of small air bubbles. In addition, the aggregate manufacturing process (natural or crushed) is important as well. Crushed rock provides increased shear action, thereby generating smaller air bubbles and higher air content than natural rock (Du & Folliard, 2005).

2.5.5 Water

Air content increases with higher water-to-cement (w/c) ratio (Kosmatka et al., 2003). Research has shown that increasing the w/c from 0.4 to 0.8 leads to an approximate 3% increase of air content (Whiting & Nagi, 1998).

Mixing water quality can also significantly impact the quality of the air entraining systems; in order to reduce mix cost, some contractors reuse mixing water (i.e., wash water from mixing trucks). This reuse can result in decreased air content and decrease in the air void system quality. In addition, hard water can decrease air content (Kosmatka et al., 2003; Whiting & Nagi, 1998).

2.5.6 Concrete Workability and Slump

Yield stress of fresh concrete is closely related to slump; an increase in slump reduces yield stress. As discussed, internal stress and viscosity acts as an energy barrier to air void creation. Therefore, increased slump results in an increase of the total amount of air voids in the system, and vice versa (Du & Folliard, 2005). Whiting and Nagi (1998) suggested that a slump increase of 1 inch leads to approximately a 0.5% increase in air content.

2.5.7 Mixing Procedures

The order of added materials also significantly affects the total amount of air content. Simultaneous batching provides less air content than batching of cement prior to adding an AEA (Whiting & Nagi, 1998). Highest air content is typically achieved when maximum mixer capacity is used, since small loads in the mixer cause less stirring and larger blade impact. However, exceeding allowable mixer capacity causes air content loss (Whiting & Nagi, 1998; Kosmatka et al., 2003).

Short mixing periods can also reduce air content; the minimal recommended mixing time is 75 seconds. If truck mixers are used, air content rises during the first 15 minutes of mixing (Whiting & Nagi, 1998). Optimal mixing speed is approximately 20 rotations per minute. At higher mixing speeds, air content may decrease due to stronger impact of the mixing blades (Kosmatka et al., 2003).

Other properties of the mixing system, such as mixing system age, total power of the mixer, and blade quality, strongly influence efficient generation of the air void system (Du & Folliard, 2005).

2.5.8 Transport, Construction Techniques, and Field Conditions

Usually 1-2% of air content loss can be contributed to transport. Mixes with high air content (above 6%) experience even greater loss of air while being transported from the ready-mix plant to the construction site (Whiting & Nagi, 1998). Use of belt conveyors reduces air content by an average of 1%, and loss in air due to pumping is approximately 2-3% (Kosmatka et al., 2003).

Internal vibration can cause loss of air if the concrete is over-vibrated or if vibrators with working frequency higher than 10,000 vibrations per minute are used (Whiting & Nagi, 1998).

Finishing typically has a minimal effect on the air void system. However, if excessive or improper finishing (finishing with bleed water still on surface, sprinkling water on surface before finishing) occurs, air content in the surface layer can decrease (Whiting & Nagi, 1998).

Retempering (i.e., withholding mixing water in the plant and adding it on site) is a common practice used by contractors to meet prescribed performance specification (typically slump or air void content). Outside temperatures can exceed 90°F during the summer construction season (May through August in the United States), typically leading to loss of concrete workability and decreased air content. Research has shown that the loss of workability is primarily caused by evaporation, absorption of water by aggregates, or hydration during transportation (Naranjo, 2007). To prevent this workability loss, concrete suppliers sometimes withhold a portion of the mixing water and add that water into the mix at the project location prior to placing (and sampling) the concrete. Retempering is thought to have no effect on spacing factor (Kosmatka et al., 2003). AEAs are occasionally used in addition to water while retempering, despite the fact that higher dosages of AEAs may be needed for jobsite admixture additions (Whiting & Nagi, 1998). The suggestion has been made (Kozikowski, Vollmer, Taylor, & Gebler, 2005; Naranjo, 2007; Walker et al., 2006) that retempering can also affect air void clustering and subsequently compressive strength; this issue is discussed later in this review.

In general, higher temperatures result in lower air void content. Du and Folliard (2005) offered the following explanations:

1. Higher temperature leads to a higher viscosity of the entire system. Higher viscosity requires more energy to form air voids; therefore, the total amount of generated air in the mix is reduced.
2. Polyvalent cations, such as Ca^{2+} , Al^{3+} , react with AEAs containing alkali salts or wood rosin and form insoluble salts that help stabilize entrained air. Rising temperatures cause these salts to coagulate and precipitate; therefore, the foaming ability of an AEA is reduced. In addition, significant amounts of electrolytes in the solution reduce air bubble

stability by reducing repulsion acting between layers formed around air bubble surfaces.

3. Higher ambient temperatures accelerate the cement hydration process; therefore, more solid surface areas in the concrete mix are generated. These surfaces absorb part of the surfactant dosage, thereby reducing the amount of available surfactants in the system. Therefore, the amount of created air content is also reduced, as demonstrated in Equation 2.3.
4. Increased temperature decreases the amount of air that is able to solute in water. Vaporizing air joins existing air bubbles and they together form larger air bubbles. These large bubbles are susceptible to destruction during the mixing process. Therefore, under high temperature conditions, the amount of entrained air content is lowered and larger air bubbles are formed.

2.6 Effects of Air Entrainment on Concrete Properties

Air entrainment in concrete positively and negatively affects concrete properties. In addition to improved freeze-thaw resistance, air entrainment in concrete increases slump and subsequent workability because small air bubbles in concrete act as a lubricant and reduce friction between cement particles and aggregate. Research has shown that an increased air content of 0.5-1% can increase slump by approximately 1 inch (Whiting & Nagi, 1998). Concrete with entrained air also demonstrates improved resistance to bleeding and segregation, and less vibration time is required to consolidate air entrained concrete (Kosmatka et al., 2003).

Compressive strength of air entrained concrete is typically expected to be less than the strength of corresponding concrete (with identical w/c ratio) without air. A given increase in air content will result in a larger percentage decrease in compressive strength in high strength concrete than the same increase in air content in normal strength concrete. Loss in compressive strength ranges from 2-6% for every percent increase in air content. Similarly, flexural strength decreases by 2-4% for every percent of air in concrete (Whiting & Nagi, 1998).

2.7 Air Void Clustering In Entrained Concrete

Air void clustering around coarse aggregate particles in air entrained concrete and related loss in concrete compressive strength has recently been identified in the concrete industry community, but not fully investigated. Clustering was observed in pavement projects and reported by Departments of Transportation (DOTs) in Delaware, Michigan, New Jersey, Virginia, and South Dakota (Cross et al., 2000), as well as by the Kansas Department of Transportation (KDOT; Distlehorst, 2009).

An extensive examination of air void clustering was conducted by the South Dakota Department of Transportation (SDDOT). During the summer construction season of 1997, SDDOT experienced an unusual failing rate of concrete cylinders during compressive strength testing. A detailed investigation was performed and investigators concluded that low compressive strength could be attributed to a weak bond between the cement paste and aggregate particles and could be associated with the formation of air void clusters around those particles. Air void clustering was observed in mixes that utilized a synthetic AEA. Foam tests of AEAs showed a difference in foaming performance of synthetic AEAs and vinsol (non-synthetic) resin agents. Results proved that synthetic AEAs drain faster than natural admixtures, resulting in thinner bubble walls and low quality cement paste on aggregate surfaces. Researchers hypothesized that these factors led to the lowered compressive strength of the concrete cylinders (Cross et al., 2000).

KDOT has reported similar issues with loss of compressive strength of concrete cylinders made from pavement concrete during a pavement reconstruction project on US Highway 54 in Meade, Kansas. Some of the cylinders that were sampled in 2006 and 2007 failed to meet the required minimum rejectable quality strength of 20 MPa (2900 psi) at 28 days. Further investigation showed that failed samples had higher air content (on average 14.4%) than cylinders that passed the strength requirement (average air content 8.5%). Air void clustering in all tested samples was quantified using the method developed by Kozikowski et al. (2005). Failed cylinders experienced higher clustering index ratings than samples that did not fail. However, compressive strength loss caused directly by air void clustering has not been proven (Distlehorst, 2009).

An extensive research study regarding clustering was carried out in 2004 in the Portland Cement Association (PCA) laboratories (Kozikowski et al., 2005). A wide range of variables was investigated and several conclusions were made:

- Similar to Cross et al. (2000), no air void clustering was observed in concrete mixes in which vinsol (organic) resin admixtures were used.
- It was reported that clustering likely occurs in concrete mixes with late addition of water (i.e., retempering), especially when synthetic agents are used.
- Total mixing time of retempered concrete was found to be another significant factor affecting clustering rate; severity of air-void clustering increased with increased mixing time.
- Aggregate shape/mineralogy may also significantly impact strength loss due to clustering.

A rating system was developed to describe the extent of air void clustering. Each coarse aggregate greater than 6 mm was assigned to one of four categories, depending on the visual rating of clustering (no clustering, minor clustering, moderate clustering, and severe clustering). Then the number of aggregates in the category was multiplied by the category number (0-3) and totals from each category were averaged over the number of examined particles. Results indicated that for ratings greater than 1.0, air void clustering may negatively affect compressive strength of concrete, although experimental data did not provide strong evidence for ratings ranging from 1.0 to 1.5.

Both previously discussed research programs (Cross et al., 2000; Kozikowski et al., 2005) independently concluded that use of synthetic AEAs may lead to an increased rate of air void clustering and air void clustering could possibly reduce compressive strength of concrete.

However, a recent research project in this field questioned the influence of air void clustering on concrete strength reduction. Laboratory experiments and field concrete tests were conducted, and reduction in concrete strength discovered in laboratory tests was attributed to increased air content due to retempering. Clusters of air voids were also observed in field concrete tests, but due to the lack of data, whether or not a correlation existed between clustering

and concrete strength was impossible to establish (Naranjo, 2007). Nevertheless, similar to the projects discussed, results indicated that late addition of water in concrete significantly impacts the rate of air void clustering.

Since lower compressive strength was initially reported during the construction summer season, it is possible that temperature may be a key factor to the clustering issues. To the authors' knowledge, no research has been conducted considering temperature effects.

Chapter 3: Materials

3.1 Cementitious Materials

ASTM C150 (2012) Type I/II cement, obtained from a local construction materials supplier and produced by the Monarch Cement Company in Humbolt, KS, was used for all concrete mixes in this research study. Due to the complexity of laboratory testing, three loads of cement were received: June 2013 (Cement A), March 2014 (Cement B), and May 2014 (Cement C). Once received, cement was removed from original packaging and stored in sealed, 55-gallon plastic barrels under room temperature conditions (72°F). Cement composition was analyzed by X-ray fluorescence by the KDOT Materials Research Center (MRC) in July 2014, and results are presented in Table 3.1. Analysis showed that the samples had very similar composition. Table 3.2 shows adjusted potential phase composition calculated according to ASTM C150.

Table 3.1: Cement Chemical Composition – X-Ray Fluorescence

Component	Cement A	Cement B	Cement C
SiO ₂ (%)	21.9	21.4	21.2
Al ₂ O ₃ (%)	4.2	4.3	4.3
Fe ₂ O ₃ (%)	3.3	3.4	3.4
CaO (%)	63.7	63.6	63.5
MgO (%)	1.8	2.1	2.2
SO ₃ (%)	2.6	2.6	2.6
Loss on Ignition (%)	1.09	1.40	1.38
Na ₂ O (%)	0.15	0.14	0.14
K ₂ O (%)	0.50	0.47	0.47
Insoluble Residue (%)	0.10	0.08	0.06

Table 3.2: Compound Calculations According to ASTM C150 (2012)

Component	Cement A	Cement B	Cement C
Al ₂ O ₃ / Fe ₂ O ₃	1.3	1.3	1.3
C3S	52.5	55.8	56.3
C23	22.9	19.2	18.3
C3A	5.5	5.5	5.5
C ₃ S + C ₃ A	58.0	61.3	61.8
Total Alkali as Na ₂ O _{eq}	0.48	0.45	0.45

3.2 Aggregate

Four types of coarse aggregate, identified by KDOT as frequently used on Kansas concrete pavement projects and listed on the KDOT prequalified material list, were used in this study (KDOT, 2014):

1. A calcium cemented sandstone commonly referred to as Lincoln quartzite (APAC–Shears, Lincoln, KS);
2. Granite (Martin Marietta Materials, Johnson County, Oklahoma);
3. Limestone (Bayer Construction, Manhattan, KS); and
4. South Dakota (SD) quartzite (L.G. Everist, Sioux Falls, SD).

Concerns arose regarding the performance of unwashed Lincoln quartzite because KDOT had experienced unexpected behavior of this material (low compressive strength in some concrete test cylinders and cores). Therefore, laboratory testing was performed on mixes containing washed and non-washed Lincoln quartzite. To determine gradation, specific gravity, and water absorption, each aggregate was sampled and tested in KSU laboratories following procedures specified in ASTM C127 (2012) and ASTM C136 (2006). Aggregate gradation curves are shown in Figure 3.1 and other properties are summarized in Table 3.3.

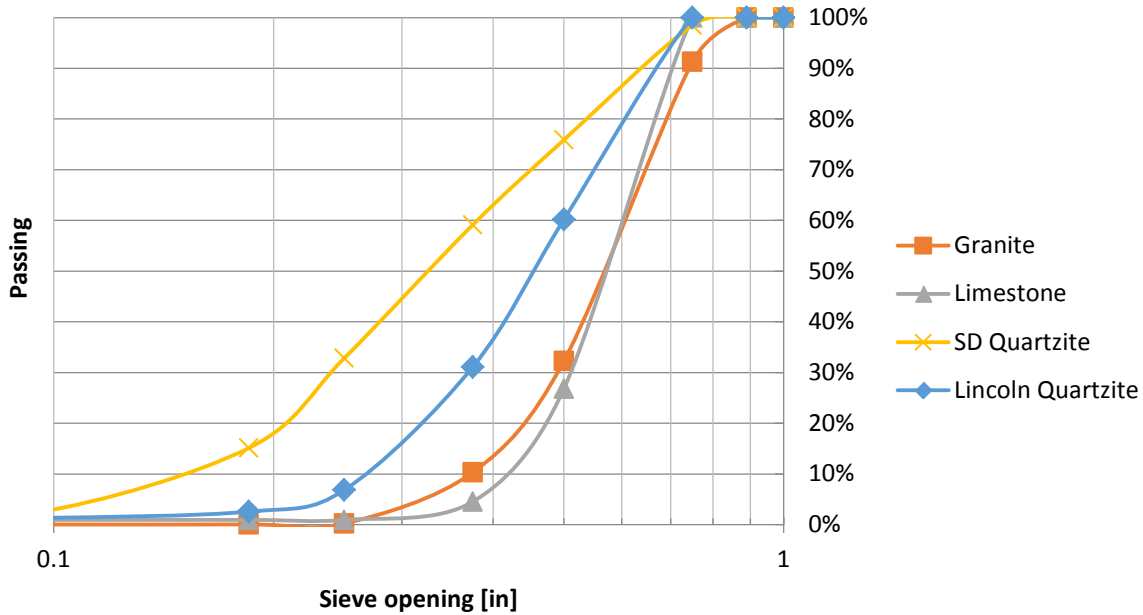


Figure 3.1: Aggregate Gradation

Table 3.3: Coarse Aggregate Properties

Component	Granite	Limestone	SD Quartzite	Lincoln Quartzite
Bulk Specific Gravity	2.69	2.54	2.63	2.60
Bulk Specific Gravity (SSD)	2.69	2.60	2.64	2.63
Apparent Specific Gravity	2.70	2.70	2.65	2.68
Water Absorption (%)	1.10	2.30	0.27	1.25

Local sand (Midwest Concrete Materials, Manhattan, KS) which met ASTM C33 FA and KDOT FA-A specifications was used in all mixes as fine aggregate (KDOT, 2007). Sand was sampled and tested following ASTM C136 (2006) and ASTM C128 (2012) procedures. Gradation curve is presented in Figure 3.2 and other material properties are shown in Table 3.4.

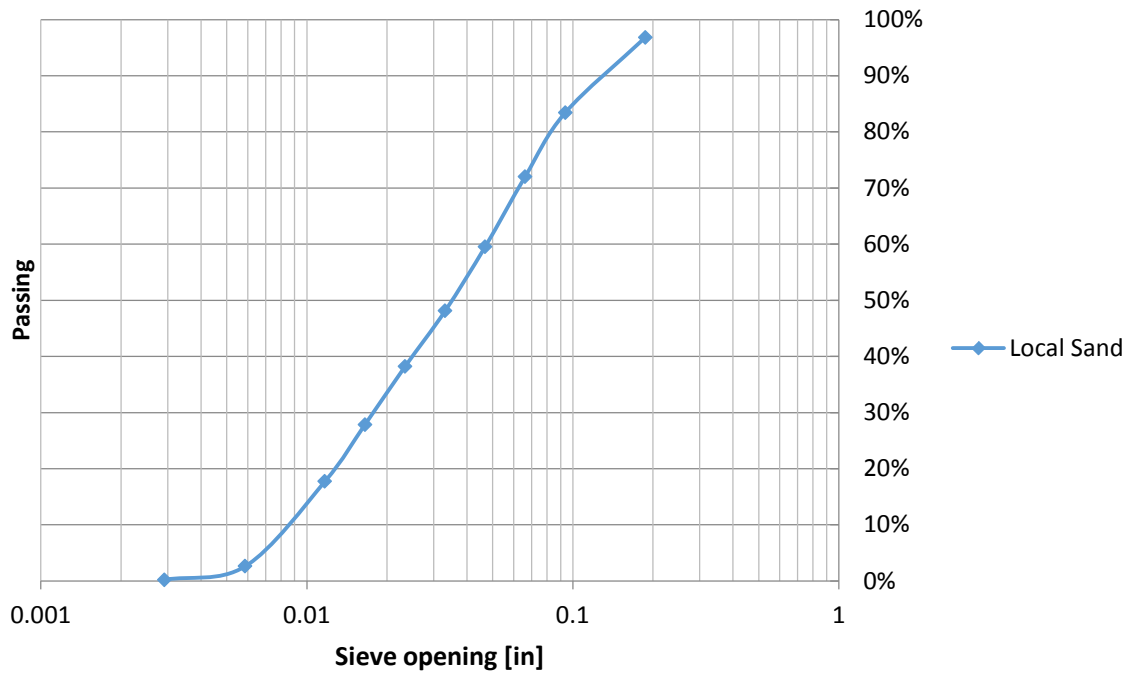


Figure 3.2: Fine Aggregate Gradation

Table 3.4: Fine Aggregate Properties

Component	Sand
Bulk Specific Gravity	2.65
Bulk Specific Gravity (SSD)	2.67
Apparent Specific Gravity	2.67
Water Absorption (%)	0.70

3.3 Air Entraining Admixtures

In July 2013, an email survey was conducted among KDOT districts to determine AEAs used on concrete pavement projects in Kansas. Consequently, five AEAs were selected for use in this laboratory study. However, in addition to the frequent occurrence of the admixture in KDOT projects being a factor for agent selection, the chemical nature of a given admixture was also considered, with the objective to encompass a wide range of AEAs in terms of chemical composition for the study. Using a classification of AEAs developed by Whiting and Nagi (1998), selected AEAs are presented in Table 3.5.

Table 3.5: Air Entraining Agents

Classification	Chemical Description	Selected AEA	Manufacturer
Vinsol® resin	Alkali or alkanolamine salt of a mixture of tricyclic acids, phenolics, and terpenes	Daravair M	WR Grace
Wood rosin	Alkali or alkanolamine salt of tricyclic acids – major components	Daravair 1000	WR Grace
Tall oil	Alkali or alkanolamine salt of fatty acids - major component	Darex II	WR Grace
Vegetable oil acids	Coconut fatty acids, alkanolamine salt	Polychem SA-50	General Resource Technology
Synthetic detergents	Alkyl-aryl sulfonates and sulfates	AEA-92S	Euclid Chemicals

3.4 Testing Matrix

Five AEAs and four coarse aggregates were chosen to be used in the study. Based on selected materials, a testing matrix was established which contained a total of 65 mixes; 50 test mixes (25 mixes with no retempering and 25 retempered mixes) and 15 control mixes. Control mixes were mixes with identical w/c ratios as the retempered mixes and were included in the matrix to investigate the effect retempering may have on clustering and compressive strength.

In order to maintain organization of the testing process, a labeling system was developed and implemented. Each sample used in the study was labeled following a two or three numeral-letter mask (e.g., 2-V, 2-V-R, or 2-V-C). The Arabic numeral refers to the aggregate used in a given mix while the Roman numeral represents the AEA, as shown in Table 3.6. A letter “R” that occurs at the end of a label indicates that the mixture was retempered, and a letter “C” indicates a control mix. Therefore, 2-V-R stands for a retempered mix with washed Lincoln quartzite and Darex II.

The complete testing matrix is presented in Table 3.7 and Table 3.8.

Table 3.6: Labeling System

Aggregate	Denotation	Admixture	Denotation
Non-Washed Lincoln Quartzite	1	Daravair 1000	I
Washed Lincoln Quartzite	2	AEA-92s	II
Granite	3	Daravair M	III
Limestone	4	Polychem SA-50	IV
SD Quartzite	5	Darex II	V

Table 3.7: Testing Matrix

Mix ID		AEA Type	Coarse Aggregate
1	I	Daravair 1000	Lincoln Quartzite - Non-Washed
1	II	AEA-92s	Lincoln Quartzite - Non-Washed
1	III	Daravair M	Lincoln Quartzite - Non-Washed
1	IV	Polychem SA-50	Lincoln Quartzite - Non-Washed
1	V	Darex II	Lincoln Quartzite - Non-Washed
2	I	Daravair 1000	Lincoln Quartzite - Washed
2	II	AEA-92s	Lincoln Quartzite - Washed
2	III	Daravair M	Lincoln Quartzite - Washed
2	IV	Polychem SA-50	Lincoln Quartzite - Washed
2	V	Darex II	Lincoln Quartzite - Washed
3	I	Daravair 1000	Granite
3	II	AEA-92s	Granite
3	III	Daravair M	Granite
3	IV	Polychem SA-50	Granite
3	V	Darex II	Granite
4	I	Daravair 1000	Limestone
4	II	AEA-92s	Limestone
4	III	Daravair M	Limestone
4	IV	Polychem SA-50	Limestone
4	V	Darex II	Limestone
5	I	Daravair 1000	SD Quartzite
5	II	AEA-92s	SD Quartzite
5	III	Daravair M	SD Quartzite
5	IV	Polychem SA-50	SD Quartzite
5	V	Darex II	SD Quartzite

Table 3.8: Testing Matrix – Control Mixes

Mix ID		AEA Type	Coarse Aggregate
1	I-C	Daravair 1000	Lincoln Quartzite - Non-Washed
1	II-C	AEA-92s	Lincoln Quartzite - Non-Washed
1	III-C	Daravair M	Lincoln Quartzite - Non-Washed
1	IV-C	Polychem SA-50	Lincoln Quartzite - Non-Washed
1	V-C	Darex II	Lincoln Quartzite - Non-Washed
2	I-C	Daravair 1000	Lincoln Quartzite - Washed
2	II-C	AEA-92s	Lincoln Quartzite - Washed
2	III-C	Daravair M	Lincoln Quartzite - Washed
2	IV-C	Polychem SA-50	Lincoln Quartzite - Washed
2	V-C	Darex II	Lincoln Quartzite - Washed
3	I-C	Daravair 1000	Granite
3	II-C	AEA-92s	Granite
3	III-C	Daravair M	Granite
3	IV-C	Polychem SA-50	Granite
3	V-C	Darex II	Granite

3.5 Mix Design

Two mix designs that varied in w/c ratios were adopted in this study. Batches with Lincoln quartzite were initially mixed utilizing w/c ratio of 0.40 and later retempered to increase the w/c to 0.43. All other mixtures had an initial w/c of 0.42, which increased to 0.45 after late water addition. The target air content for all mixes before retempering was $6.5\% \pm 1.5\%$ in accordance with current KDOT requirements (KDOT, 2007). The target slump range was 1-3 inches. Mixes before retempering are referred to as “original” in this report, while mixtures after water addition are referred to as “retempered.”

To investigate the effect of air void clustering and retempering on compressive strength, 15 control mixtures with the same w/c ratio of the retempered mixes (0.43 and 0.45) were mixed. Their target air content corresponded to the air content of the retempered mixes (with 0.5% tolerance). These mixes are referred to as “control” mixes.

All mixes contained 580 lbs of cement per cubic yard and a 65:35 ratio of coarse to fine aggregate. The total weight of aggregates in each mix was adjusted to account for specific

gravities of each type of coarse aggregate. The dosage of AEAs also varied among mixes; the required dosage of a given AEA (i.e. the dosage that resulted in $6.5\% \pm 1\%$ of total air content) for each mix was determined by trial-and-error. In general, approximately 0.5-1.5 fl oz per 100 lbs of cement was required to achieve targeted air content. Mix designs are presented in Table 3.9 and dosages of the AEA used are presented in Table 3.10.

Table 3.9: Mix Designs

Aggregate Concrete Component	Lincoln Quartzite	Granite	Limestone	SD Quartzite
Cement (lbs/yd ³)	580	580	580	580
Coarse Aggregate (lbs/yd ³)	1951	2008	1939	1961
Fine Aggregate (lbs/yd ³)	1078	1068	1068	1068
Water (lbs/yd ³)	249	244	244	244
Original w/c	0.40	0.42	0.42	0.42
Retempered w/c	0.43	0.45	0.45	0.45

Table 3.10: AEA Dosages

Aggregate AEA	Non-Washed Lincoln Quartzite	Washed Lincoln Quartzite	Granite	Limestone	SD Quartzite
Daravair 1000	1.2	1.0	1.1	2.8	1.0
AEA 92s	0.9	0.9	0.9	1.1	0.8
Daravair M	0.9	0.8	0.6	1.4	0.9
Polychem SA-50	1.2	1.1	1.0	1.2	1.0
Darex II	0.9	0.9	1.1	1.8	1.1

Note: fl oz per 100 lbs of cement

Chapter 4: Laboratory Study

4.1 Mixing Procedure

Valid ASTM Standards for making and testing concrete in the laboratory were followed for this study: C138 (2012), C143 (2012), C172 (2010), C192 (2013), and C231 (2010).

Prior to mixing, all materials were moved into the mixing laboratory to ensure they were at room temperature (72°F) at the moment of mixing. In addition, all aggregates were placed in the oven (200°F) and dried to constant mass before being placed in the mixing laboratory to cool to room temperature. This procedure allowed for identification of the volume of water that had to be added to maintain the desired w/c ratio due to the aggregates' absorption capability.

A Lancaster shear mixer (Figure 4.1) was used to perform mixing. The volume of all regular mixes was designed to be 1.8 ft³, while the control mixes were 1.05 ft³ (1.05 ft³ corresponds to the volume of concrete left in the mixer after the Phase 1 of mixing).



Figure 4.1: Lancaster Shear Mixer

A simplified version of the mixing procedure described by Naranjo (2007) was used in this study. The procedure consisted of two mixing phases, as illustrated in Figure 4.2.

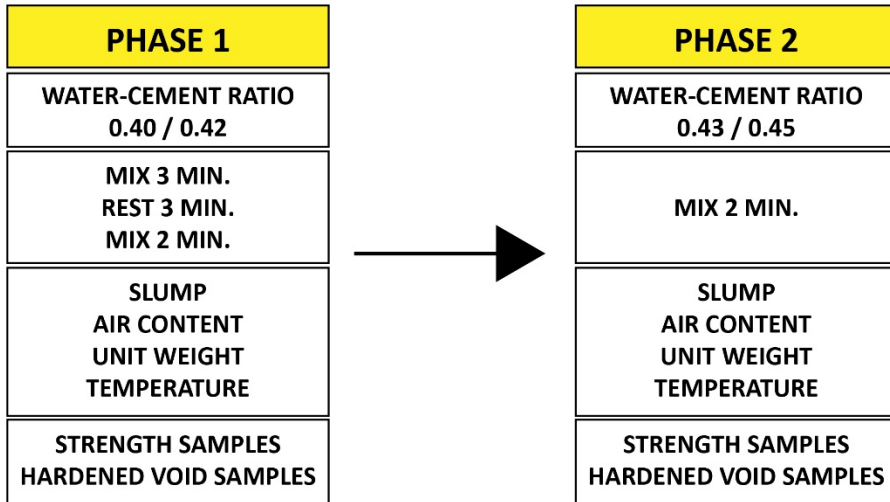


Figure 4.2: Mixing Procedure

Phase 1: Fine and coarse aggregate were placed in the mixing pan with approximately half of the mixing water containing an added dispersed AEA. Aggregates with water and AEA were then mixed until blended, and then the cement and the remainder of the mixing water were added to the mix. As prescribed by current standards (ASTM C192, 2013), the concrete was mixed for 3 minutes, followed by a 3-minute resting period, followed by an additional 2 minutes of mixing. After mixing was complete, 105 lbs of concrete was removed from the mixing pan, while the remaining concrete was covered with plastic wrap to prevent moisture loss. The removed concrete was then used to measure slump, total air content, unit weight, and temperature. Once all required tests were performed, six 4x8 inch cylinders and two food boxes (see Figure 4.5) were cast in order to obtain specimens for future testing: cylinders for compressive strength (three for 7-day strength, three for 28-day strength) and two food boxes for hardened air void analysis.

Phase 2: The second phase typically occurred 30-45 minutes after the initial stage once all tests were completed and specimens cast. At the beginning of this stage, additional water was added to the mix, the mixer was turned on, and the concrete was mixed for another 2 minutes. Tests similar to the first stage were then run, and six 4x8 inch cylinders and two food boxes were cast. The second stage was typically completed within 20-30 minutes from initiation.

Control mixes were mixed following only the Phase 1 procedure (with corresponding w/c ratios – 0.43 or 0.45).

Casted samples were labeled and left undisturbed in the laboratory. After an initial 24-hour period, compressive strength specimens were unmolded and moved to a room with constant temperature of 72°F and relative humidity of 99% (“fog room”). Hardened air void samples were removed from paper molds, labeled, and stored on shelves in the cement laboratory at KSU (Figure 4.3).



Figure 4.3: Stored Hardened Air Void Samples

4.2 Material Testing and Evaluation Methods

4.2.1 Fresh Concrete Properties Testing

Slump, air content, unit weight, and temperature were four fresh concrete properties measured for each mix. Provisions of ASTM Standards C138 (2012) and ASTM C143 (2012) were obeyed. Because a two-stage mixing procedure was adopted for most mixtures in this study, concrete properties were always determined for both the original and retempered mix. Standard testing equipment which met the requirements of both ASTM C138 and ASTM C143 was used, including an Oakton Templog thermometer (Serial Number 502399).

4.2.2 Compressive Strength

ASTM C39 (2012), ASTM C192 (2013), and ASTM C1231 (2014) were followed to perform all tasks associated with concrete compressive strength testing. Standard 4x8 inch plastic molds (Deslauriers, Inc.) were used to make concrete specimens. Cylinders were covered with plastic lids immediately after they were formed and left undisturbed in the laboratory under constant temperature (72°F) for the first 24 hours. Cylinders were then removed from the plastic molds using compressed air, labeled, and stored in the curing room (72°F, 99% relative humidity).

Specimens were tested for compressive strength at 7 and 28 days after casting. Steel retaining cups, rubber compression pads, and a Forney compression machine were utilized for the testing. Test setup is shown in Figure 4.4. Each tested set of cylinders was composed of three samples, and total compressive strength was calculated as an average of the three obtained values.



Figure 4.4: Compressive Strength Setup

4.2.3 Air Void Analysis of Hardened Concrete

Samples for air void analysis of hardened concrete were cast into paper boxes typically used as food containers (Figure 4.5). Compared to the rounded cylinders typically used for hardened air void analysis, cutting and other operations on the specimens were easier and more convenient when rectangular molds were used. A total of four specimens were made for each mix from the main testing matrix: two with original concrete mix, two with retempered mix. Two boxes were cast for each control mix.



Figure 4.5: Hardened Air Void Analysis Mold

Once cast, samples were left undisturbed for a 24-hour period and then removed from paper molds, labeled, and stored. Since air void structure is formed during the mixing period and does not change after the concrete sets, samples were not stored under any specific conditions.

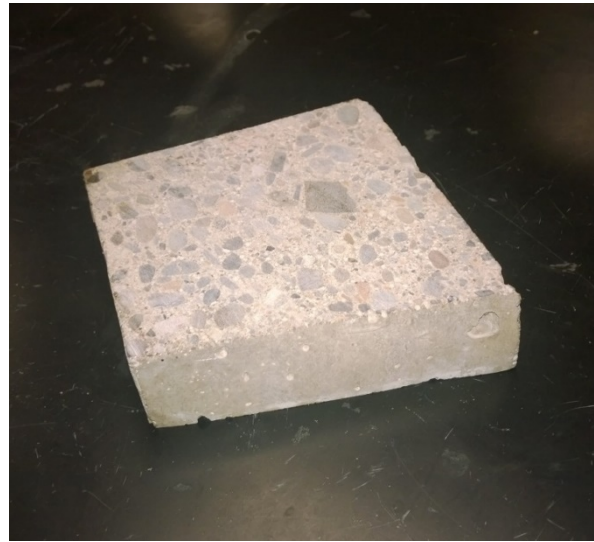
An automatic method of air void system investigation using a flatbed scanner was implemented to carry out analysis of all hardened concrete samples. The method introduced by Peterson (2008) was implemented with several modifications to adjust its usability. Analysis was carried out following the subsequent steps.

4.2.3.1 Cutting of Specimens

Samples were cut using a Covington Engineering concrete saw shown in Figure 4.6a. Upon completion of the cutting process, concrete slices of uniform thickness, approximately 1 inch, were prepared (Figure 4.6b). Once cut, all samples were washed using water and compressed air to remove all cutting residues.



(a)



(b)

Figure 4.6: Cutting of Specimens

(a) Cutting Setup; (b) Cut Sample

4.2.3.2 Surface Polishing

A horizontal polishing table (ASW Diamond SW-1800), equipped with diamond nickel-plated disks (ASW Diamond NT-80, NT-100) and flexible resin processing disks (ASW Diamond PP360, PP600), was used to polish all samples. Disks are shown in Figure 4.7. The polishing table presented in Figure 4.8 was adjusted with a custom-made mounting setup (including two Fischer Scientific DynaMix electric motors), allowing four samples to be polished simultaneously and ensuring that the expected polished surface quality was achieved. Polishing procedure was derived from the procedure developed by Ley (2007).



Figure 4.7: Polishing Disks



Figure 4.8: Polishing Setup

Cut and washed samples were attached to plastic cylinders (5.5 inch diameter, 2 inch height) using a hot glue gun. The cylinders were designed to hold the samples on the lapping wheel. Once the glue dried, a 60:40 solution of acetone and clear lacquer was applied to the sample surface to stabilize the cement paste during polishing. The surface was allowed to dry. Water with a small amount of dish soap (approximately 0.15 fl oz per 5 gallons) was used to lubricate samples and disks during polishing; the amount of water applied to the disk depended on its fineness and was determined by the operator.

Samples were first polished using the nickel-plated disk with 80 grit, followed by the 100 grit disk. The primary purpose of the two disks was to completely flatten the sample; flatness was ensured by (a) drawing an orthogonal grid with construction crayon to determine whether the sample was polished uniformly, and (b) performing a flatness check using a machinist rule (Figure 4.9).



Figure 4.9: Flattening the Sample
(a) Orthogonal Grid; (b) Machinist Rule Flatness Check

As soon as all specimens passed the flatness check, brown and red polymer disks with 1200 and 2200 mesh, respectively, were mounted on the polishing table. The brown disk was responsible for removing all scratches produced on the sample during previous processing, while the red disk was used to complete the entire polishing procedure. Every time the polishing disk was changed, samples were cleaned with water to remove the polishing residues left on the sample. Once all samples were polished to shine like a sheet of glass, they were removed from the plastic cylinders, thoroughly cleaned with water, and dried. Specimens were then placed in plastic bags to protect from further scratching and stored in a desiccator to prevent surface carbonation.

4.2.3.3 Scanning

Immediately prior to scanning, specimens were submerged in an acetone bath for 3-5 minutes to remove lacquer from all voids if present. Samples were then dried using a hairdryer.

Scanning was carried out using an EPSON Perfection V600 Photo scanner, and controlled by default scanning software provided with the scanner – Epson Scan (Ver. 3.83US). Resolution of 4800 dpi with 24-bit color settings was used, and all software image adjustments, with the exception of the unsharp mask option, were disabled (Figure 4.10). The area of the sample scanned was always larger than the minimum area required for conventional hardened air void analysis (ASTM C457, 2012).

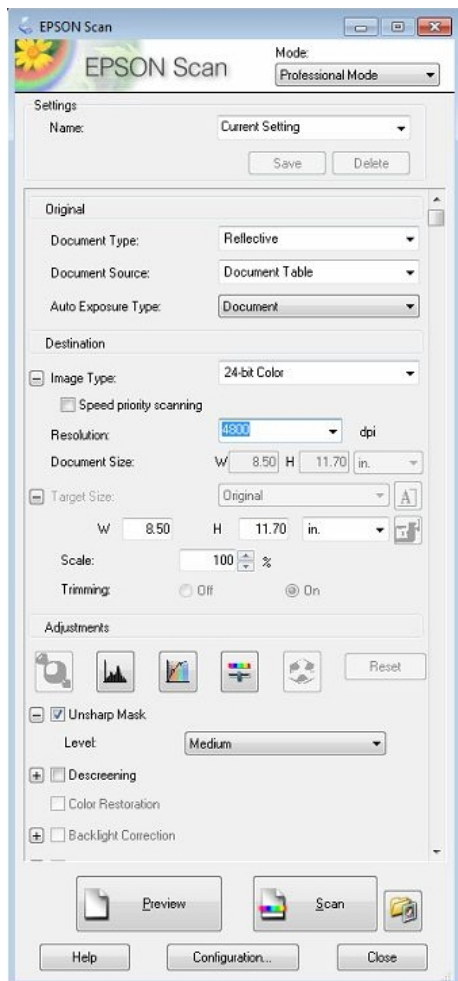


Figure 4.10: Scanner Settings

First, a dried sample was scanned (referred to as Image 1). In order to assist with future image alignment, the sample was placed on the scanning table and aligned to the bottom-right corner using glued thin glass slides, as shown in Figure 4.11. Second, the specimen was sprayed with a solution (1:1) of a 90%-phenolphthalein in alcohol and distilled water in order to color the cement paste. Phenolphthalein works as a pH indicator. As long as the pH level of paste exceeded 11 (ensured by keeping the sample in vacuum before scanning), the color changed to purple-pink. Only a thin layer of solution was applied to eliminate excessive amounts of fluid coloring aggregate particles. The sample was dried using a hairdryer, and pores were cleaned with compressed air to remove any excess solution from the air voids.

Finally, an orange powder (Strait-Line Marking Chalk) was used to fill all air voids in the investigated sample. The powder was uniformly distributed over the sample surface using a microscope slide and then pressed into pores by a rubber stopper. This process was repeated two times to ensure all voids were completely filled. A steel razorblade was used to remove excess powder from the sample and, if needed, the surface was dusted with a fingertip covered by a laboratory glove and lightly-oiled. The specimen was then rescanned (referred to as Image 2). All scanned images are shown in Figure 4.12.



Figure 4.11: Scanning Setup

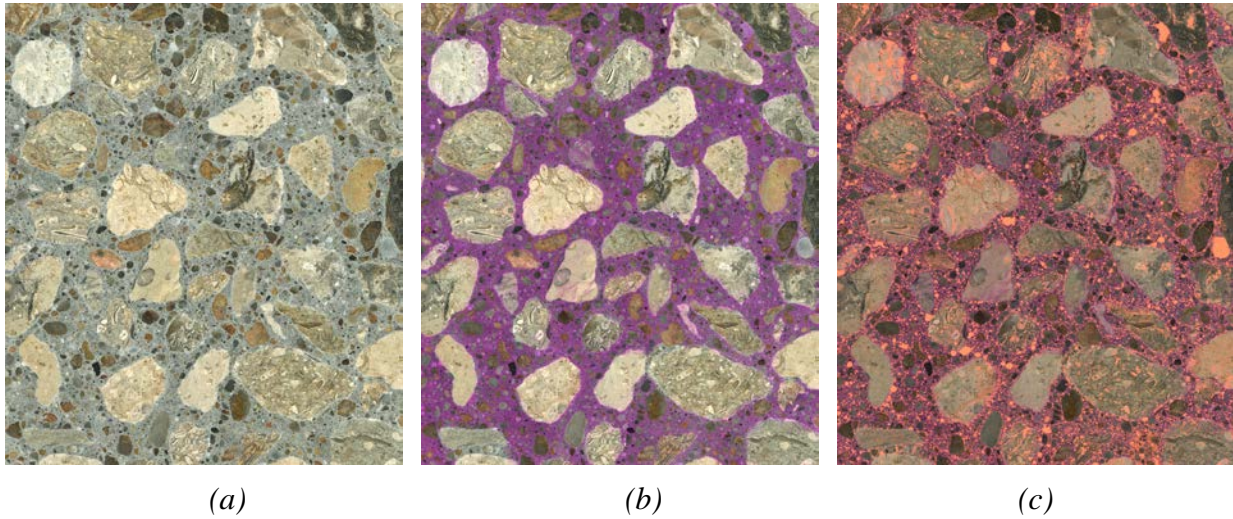


Figure 4.12: Image Scans

(a) Image 1 – No Surface Treatment; (b) Phenolphthalein-Stained Surface; (c) Image 2 – Orange Powder Pressed into Air Voids

4.2.3.4 Raw Image Alignment

All three images had to be aligned with respect to each other in order to conduct the entire analysis. As mentioned, every time the sample was scanned, it was always placed on the exact same location on the scanning table. However, since the resolution was 4800 dpi (i.e., 1 pixel is approximately 5 microns), a slight misalignment can cause error in analysis. Therefore, the determination was made that an image processing technique should be used to precisely align the three images. Adobe Photoshop software and its automatic “Load files into stack” script was utilized, and eventually an alignment with a maximal error of 1-2 pixels was achieved. Once aligned, all three images were cropped to remove border image portions no longer overlapping the other two images because of a shift or rotation the image experienced during alignment.

4.2.3.5 Phase Detection

First, Image 1 and Image 2 were combined using the difference filter (Figure 4.13b). This filter subtracted respective color values from each image and used the resultant value to create a composite image; black color (value of 0) indicates no difference between two images. The black color corresponds to aggregate particles since only the paste experienced a color change. Binary

threshold operation was applied to the image to extract aggregate particles. This operation caused all pixels with value higher than the selected threshold value to be white, while all pixels with lower values became black; therefore, the image's color mode was switched from 24-bit RGB (three channels and 256 possible color value in each channel) to a binary image (single channel with two possible color values, black or white, for each pixel). At the conclusion of this step, aggregate particles were detected (Figure 4.13b).

Unfortunately, this process sometimes tended to overestimate the total paste content because some aggregate particles were not always fully detected. Ideally, no change in color in aggregate should occur (therefore all aggregate would be colored black by the difference filter). However, light color aggregate (especially limestone and sandstone) were sometimes slightly colored by the phenolphthalein solution and, therefore, the colored portions of aggregate particle were missed.

Once the difference filter was applied, aggregate (black) particles less than 50 pixels were removed. Those particles were typically a noise created during the image processing. All remaining particles were then filled with black color if they contained some white pixels (air voids).

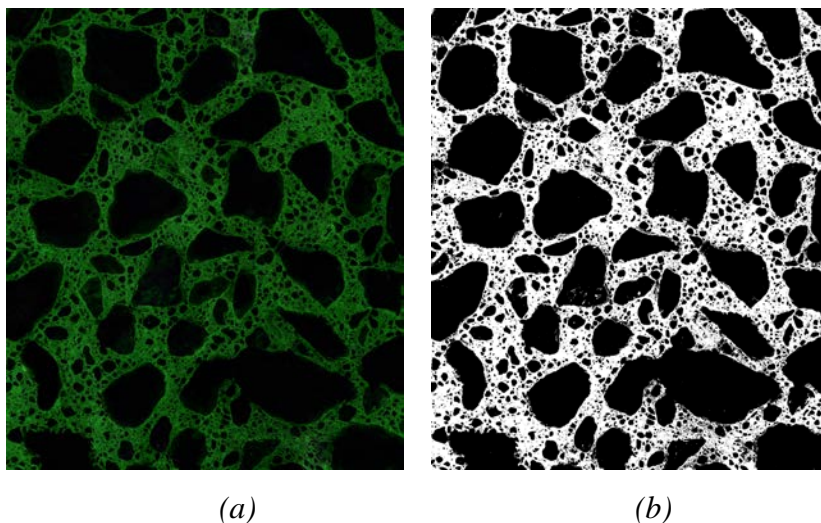


Figure 4.13: Aggregate Detection

(a) Image 1 and Image 2 Combined – Difference Filter Applied; (b) Aggregate Particles Detected by Threshold Operation

Second, Image 2 was utilized to detect air voids as the applied orange powder highlighted all pores present in the sample, i.e., entrained and entrapped air voids as well as air pores present in aggregate particles. Brightness levels of the image were adjusted using Adobe Photoshop, resulting in an image with a dark (black) background and red-orange air voids. Subsequently, air voids were selected based on color, extracted from the dark background, changed to a white color, and copied into a new image with a gray background. This new image utilized a single channel indexed color mode (often referred to as grayscale mode), allowing each pixel to have a color value from 0 to 255 (Figure 4.14).

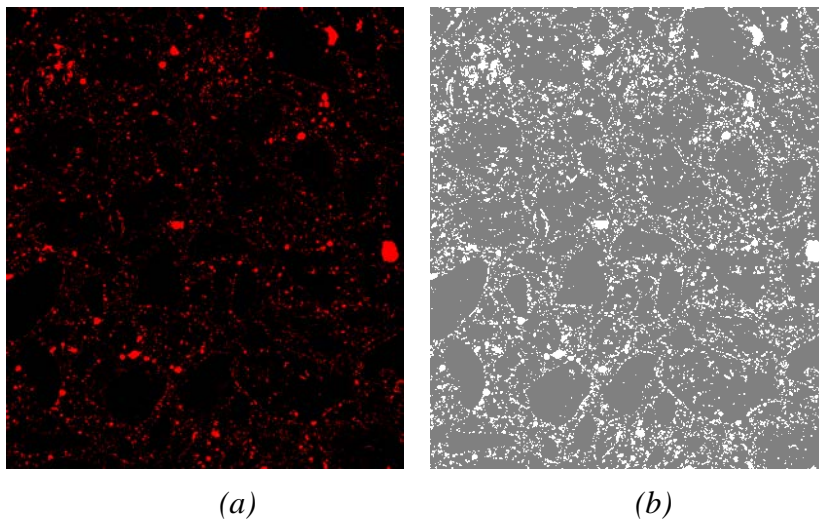


Figure 4.14: Voids Detection

(a) Image 2 after Brightness Adjustments; (b) Grayscale Image with Detected Pores

4.2.3.6 False Color Image

The false color image, created using the binary image shown in Figure 4.13b and Figure 4.14a, used the grayscale mode with black color representing aggregate, white color corresponding to air voids, and gray color indicating cement paste. Air pores in aggregate particles were eliminated as the “hard mix” blend mode was applied between the used images in Photoshop.

4.2.3.7 Air Void Analysis

A new software application, KSU Void Analyzer, was developed to facilitate air void analysis of previously generated images. To create this application, .NET Framework 4.5 with 64-bit architecture, Microsoft Visual Studio 2012, and C# programming language were used. In order to perform advanced image processing tasks, AForge, EmguCV, and ClipperLibrary frameworks (all available under the GPU/GPL license) were incorporated into the KSU Void Analyzer.

KSU Void Analyzer provided all information obtained using conventional analysis methods, such as total air void content, spacing factor, and total areas of concrete phases such as aggregate, cement paste, and air. In addition, information such as sizes, centroid locations, and other properties could be obtained from the software.

Spacing factor was obtained by performing the linear traverse method (ASTM C457, 2012) on the false color image as if it was a real hardened concrete sample. Since the voids in the aggregates were removed during the false color image creation, they were not counted as air voids but were considered part of the aggregate. However, analysis was performed by computer software rather than a human operator. The software iterated through the sample from left to right, investigating every pixel. Total length of traverse, traverse length through air, and traverse length through paste were recorded in order to calculate the spacing factor.

4.2.3.8 Air Void Clustering Evaluation

To investigate the effect air void clustering may have on the compressive strength of concrete, an evaluation method was implemented in the software that could quantify air clustering severity. This method utilized existing false-color images and information obtained in previous steps of the analysis, particularly location of air void centroids and areas of aggregate particles. Since analysis of each aggregate would be extremely demanding computationally, only particles with an area of more than 20,000,000 pixels (0.86 inch²) were investigated.

As a first step, an equidistant line derived from boundaries of selected aggregate particles was formed, creating a layer of a uniform thickness (0.26 mm) immediately surrounding the analyzed particle. The layer was then searched for the presence of air voids by iterating through

all detected air voids and their centroids, and determining whether the air void centroid lies within the investigated layer. The thickness of the searched layer was not selected randomly; it corresponded to the value of 100 pixels for the used resolution. But more importantly, by selecting 0.26 mm as the width of the clustering layer, it was ensured that only air voids smaller than 0.52 mm in diameter were included in the analysis, as larger air bubbles are typically considered to be entrapped voids rather than entrained air (as shown in Figure 4.15). The total percentage of detected air voids within the investigated area was then recorded and local values of air content were compared to the total air void content of the analyzed sample. Clustering index was defined as a ratio of air void content of the investigated layer to the total air void content of the entire sample.

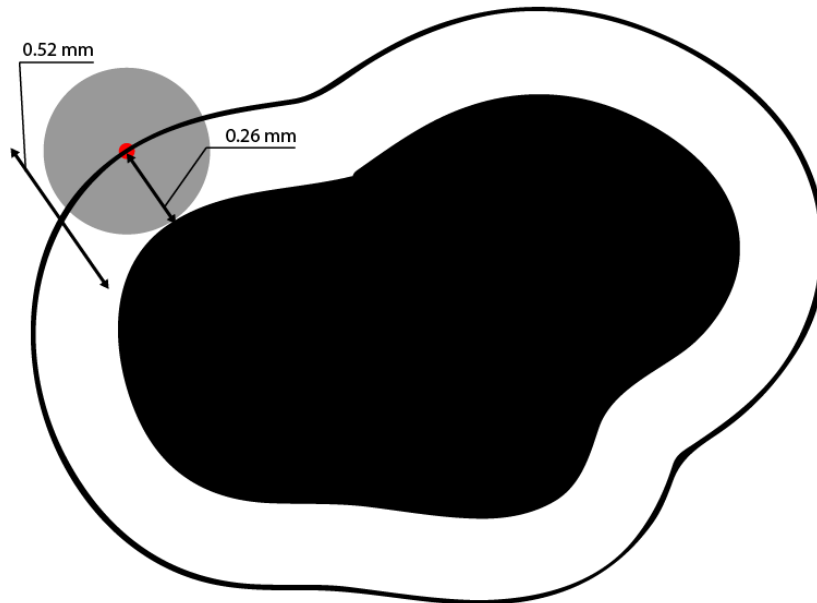


Figure 4.15: Clustering Zone

4.2.3.9 Air Void Clustering Rating

A clustering evaluation method developed by Kozikowski et al. (2005) was also used to estimate the extent of air void clustering. This method was performed by an independent operator from the person performing the hardened air void sample image analysis. Twenty or more of the largest aggregate particles in each sample were selected for rating. Those particles were then investigated under a microscope and assigned to a category represented with a number from 0 to 3 based on severity of void clustering. Once all particles were rated, the number of particles in each category were multiplied by the category number and then averaged over the total number of particles. Therefore, a single number indicating the air void level was generated.

Chapter 5: Field Testing

5.1 Introduction

Two ongoing construction projects under the supervision of KDOT, with the retempering practice implemented, were visited in the summer of 2014.

The first site (Site I) was located in northwest Topeka, KS, in Shawnee County, where a new interchange at US-24 and Menoken Road was being constructed. Site I was visited and samples were taken on June 20, 2014, when the deck on Bridge 282 was being placed.

The second site (Site II) was located approximately 15 miles south of Topeka, near Carbondale, KS, in Osage County. This project, visited and sampled on July 7, 2014, included the reconstruction/replacement of the highway on the south bridge approach to Bridge No. 70-44 on US-75.

5.2 Methods

At both sites, fresh concrete properties (before and after water addition) were measured and recorded. Samples for compressive strength were made according to ASTM C31 (2012). Samples for hardened air void analysis were also made. After casting, samples were stored in a cooler on site for the initial 24-hour curing period, and then transported to KSU laboratories and stored in the 100% moisture room at 72°F.

Similarly to mixes in the laboratory study, compressive strength was tested at 7 and 28 days (ASTM C39, 2012; ASTM C1231, 2014), and hardened air void analysis (including the automatic clustering evaluation) was carried out.

5.3 Materials, Mix Design, and Retempering

The same mix design (KDOT Mix No. 1PT0835A) was used in both cases. The design specifications are presented in Table 5.1. The retempering, however, was different for each project. For concrete delivered at Site I, two gallons of water per cubic yard of concrete were withheld at the batching plant and 1 gallon was later added to the concrete in the truck, while 2 gallons of water per cubic yard of concrete were withheld from the mix and added at Site II. Transformed into water-to-cement ratios, concrete from Site I had a w/c ratio of 0.38 and 0.40

before and after retempering, respectively. Ratios of water to cement on Site II were 0.37 and 0.40.

Table 5.1: Mix Design – 1PT0835A

Concrete Component	Specification	KDOT ID	Producer	Dosage
Cement (lbs/yd ³)	Type I/II	161060100	Central Plains Cement	521
Coarse Aggregate (lbs/yd ³)	SCA-3 Limestone	001270217	Mid-States Materials	1,586
Fine Aggregate (lbs/yd ³)	FA-A Natural Sand	001110008	Builders Choice	1,593
Admixture #1 (oz/yd ³)	AEA (BASF MB-90)	0410000000	BASF Construction Chemicals	3.0
Admixture #2 (oz/yd ³)	Water Reducer Type A (PolyHeed 900)	04201000A	BASF Construction Chemicals	20.0
Admixture #3 (oz/yd ³)	Water Reducer Type F (Glenium)	04204000F	BASF Construction Chemicals	20.0
Water (lbs/yd ³)				208
Designed w/c = 0.4				

Chapter 6: Results

6.1 Fresh Concrete Properties

As previously discussed in Section 4.2 Material Testing and Evaluation Methods, fresh concrete properties were determined for both mixes before and after retempering, as well as for all control mixes. Total air content is presented in Figure 6.1, Figure 6.2, and Figure 6.3.

Obtained values of other fresh concrete properties—slump, unit weight, and temperature—are shown in Table 6.1 for mixes before retempering, after retempering, and control mixes, respectively.

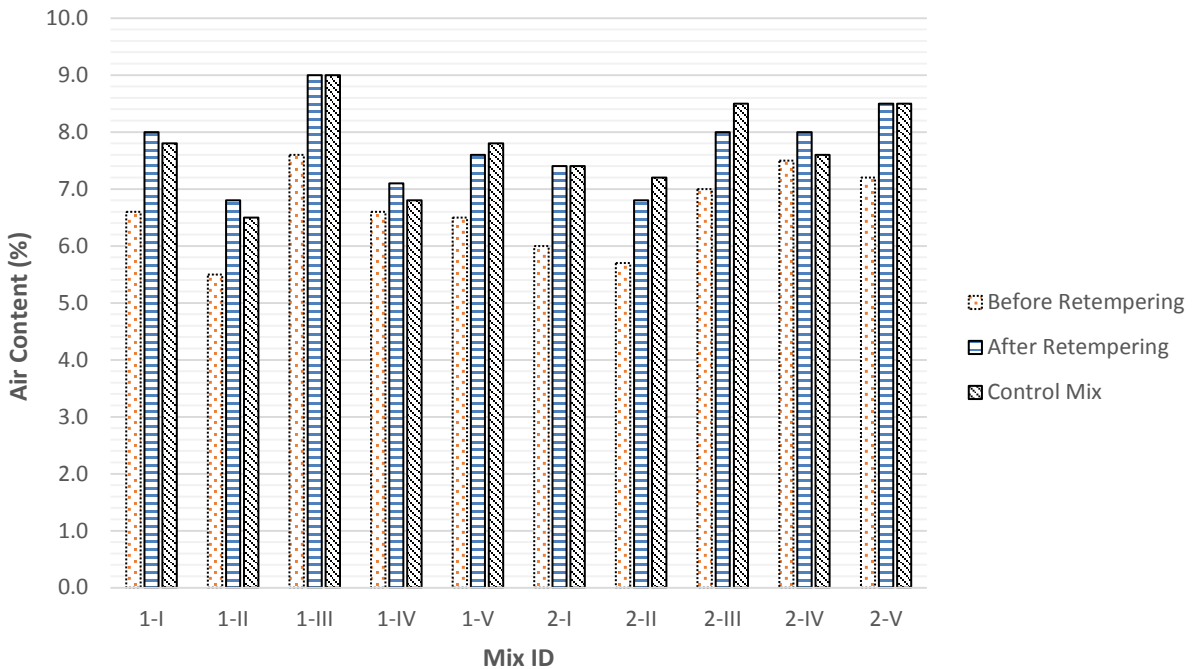


Figure 6.1: Air Content (Fresh) – Lincoln Quartzite

Note: 1=non-washed, 2=washed

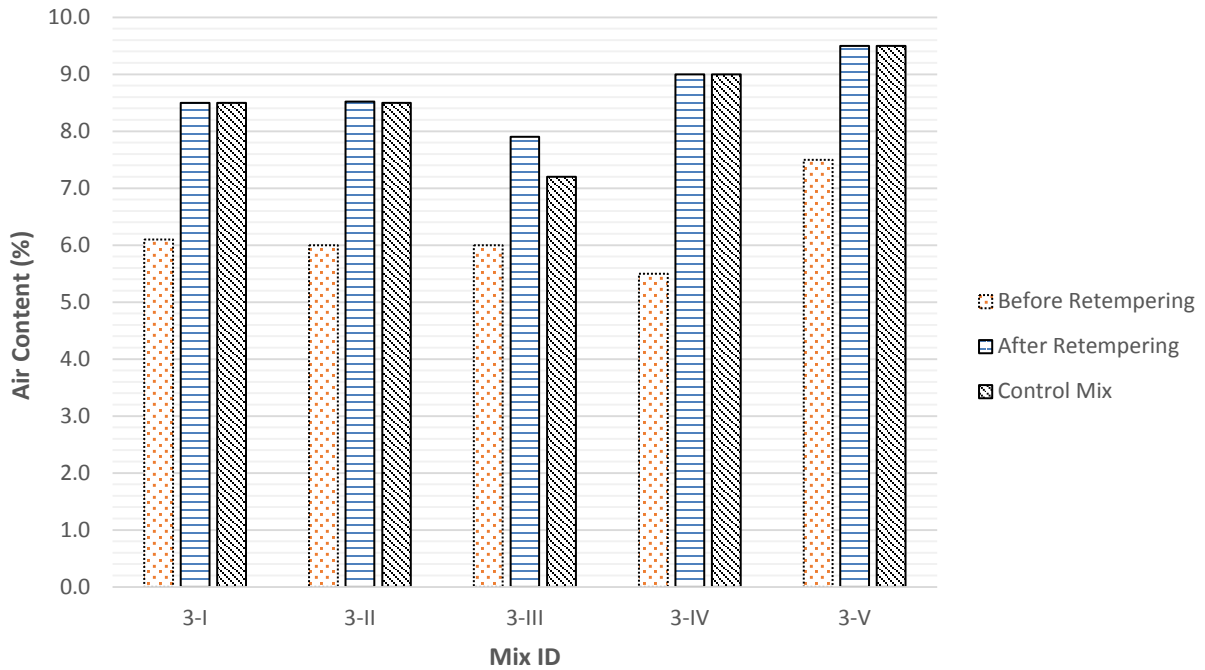


Figure 6.2: Air Content (Fresh) – Granite

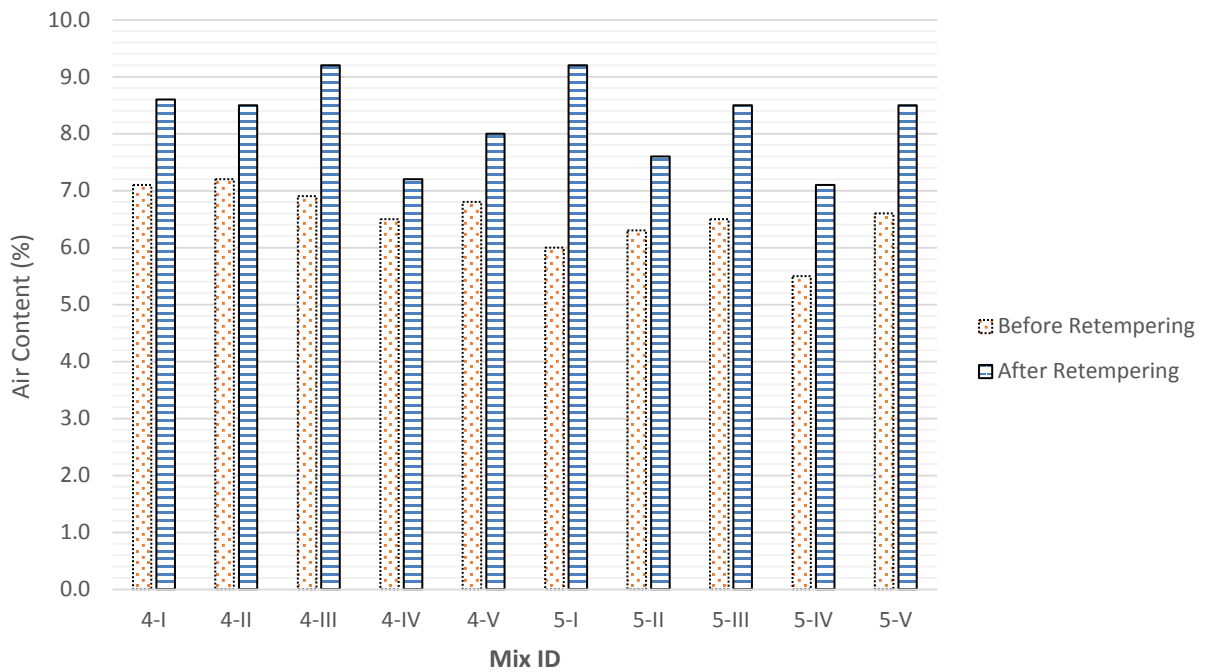


Figure 6.3: Air Content (Fresh) – Limestone and SD Quartzite

Table 6.1: Fresh Concrete Properties

ORIGINAL MIXES				RETEMPERED MIXES				CONTROL MIXES			
Mix ID	Slump	Unit Weight	Temp.	Mix ID	Slump	Unit Weight	Temp.	Mix ID	Slump	Unit Weight	Temp.
	<i>inches</i>	<i>lb/ft³</i>	<i>°F</i>		<i>inches</i>	<i>lb/ft³</i>	<i>°F</i>		<i>inches</i>	<i>lb/ft³</i>	<i>°F</i>
1-I	2.00	144	73	1-I-R	4.75	N/A	73	1-I-C	4.0	140	71
1-II	2.25	145	73	1-II-R	4.50	141	72	1-II-C	4.1	142	72
1-III	2.75	140	73	1-III-R	4.75	138	72	1-III-C	4.8	138	71
1-IV	2.50	143	72	1-IV-R	3.75	141	70	1-IV-C	4.1	142	73
1-V	2.25	143	75	1-V-R	3.50	140	74	1-V-C	4.2	140	71
2-I	2.50	144	73	2-I-R	4.25	141	72	2-I-C	4.0	141	73
2-II	2.75	144	74	2-II-R	4.25	141	73	2-II-C	4.1	141	72
2-III	3.50	142	74	2-III-R	4.50	139	73	2-III-C	4.8	139	73
2-IV	3.00	141	73	2-IV-R	4.50	139	72	2-IV-C	4.1	140	74
2-V	2.75	142	74	2-V-R	4.50	139	73	2-V-C	4.2	139	75
3-I	2.25	145	75	3-I-R	4.50	139	74	3-I-C	4.5	139	72
3-II	2.25	145	74	3-II-R	5.50	139	74	3-II-C	4.3	139	72
3-III	2.25	144	78	3-III-R	4.00	141	77	3-III-C	4.3	142	72
3-IV	2.00	146	74	3-IV-R	5.00	139	73	3-IV-C	4.0	139	73
3-V	2.50	142	74	3-V-R	4.75	137	73	3-V-C	4.8	138	73
4-I	2.00	141	79	4-I-R	3.00	137	77				
4-II	2.25	140	67	4-II-R	4.50	139	66				
4-III	2.25	142	75	4-III-R	3.75	139	74				
4-IV	2.00	142	72	4-IV-R	3.25	142	72				
4-V	2.00	141	70	4-V-R	4.25	139	69				
5-I	1.50	143	73	5-I-R	3.50	137	71				
5-II	1.00	143	67	5-II-R	2.75	140	66				
5-III	1.75	144	73	5-III-R	3.75	139	72				
5-IV	1.50	144	74	5-IV-R	3.00	141	74				
5-V	1.75	143	74	5-V-R	3.25	139	73				

6.2 Compressive Strength

Compressive strengths at 7 days are shown in Figure 6.4, Figure 6.5, and Figure 6.6, while values of compressive strength at 28 days are presented in Figure 6.7, Figure 6.8, and Figure 6.9. To recall, every testing sample consisted of three concrete cylinders (4x8 inches), and measured values were averaged over the number of tested cylinders in order to determine the final average value of compressive strength at a given time for a given mix.

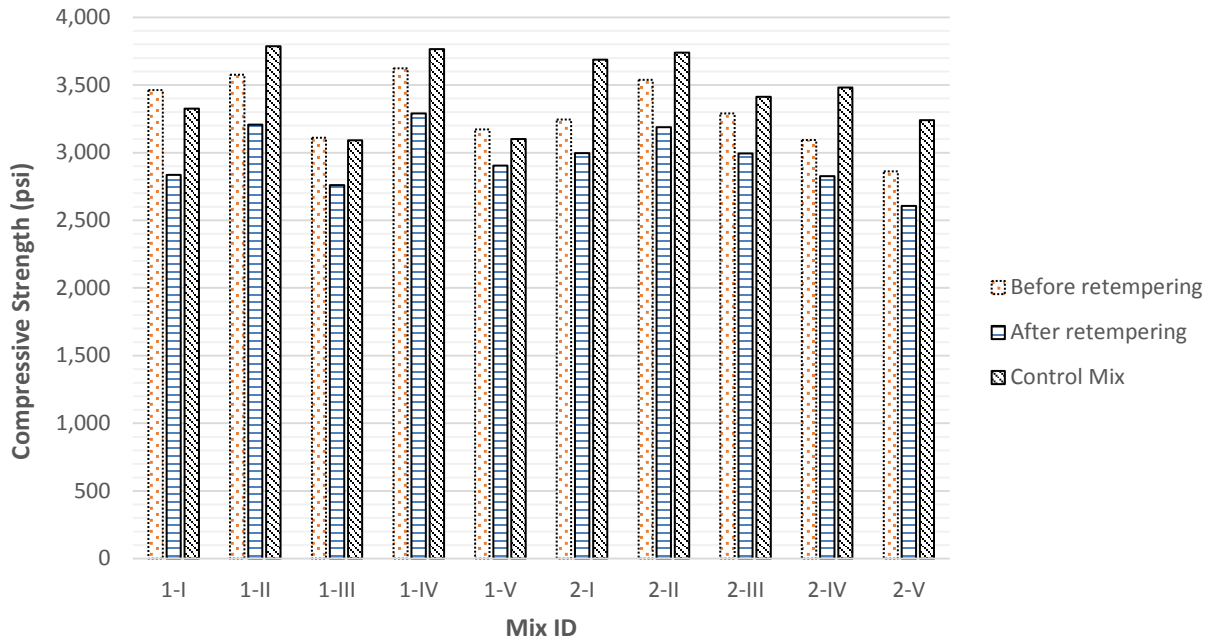


Figure 6.4: Compressive Strength at 7 Days – Lincoln Quartzite

Note: 1=non-washed, 2=washed

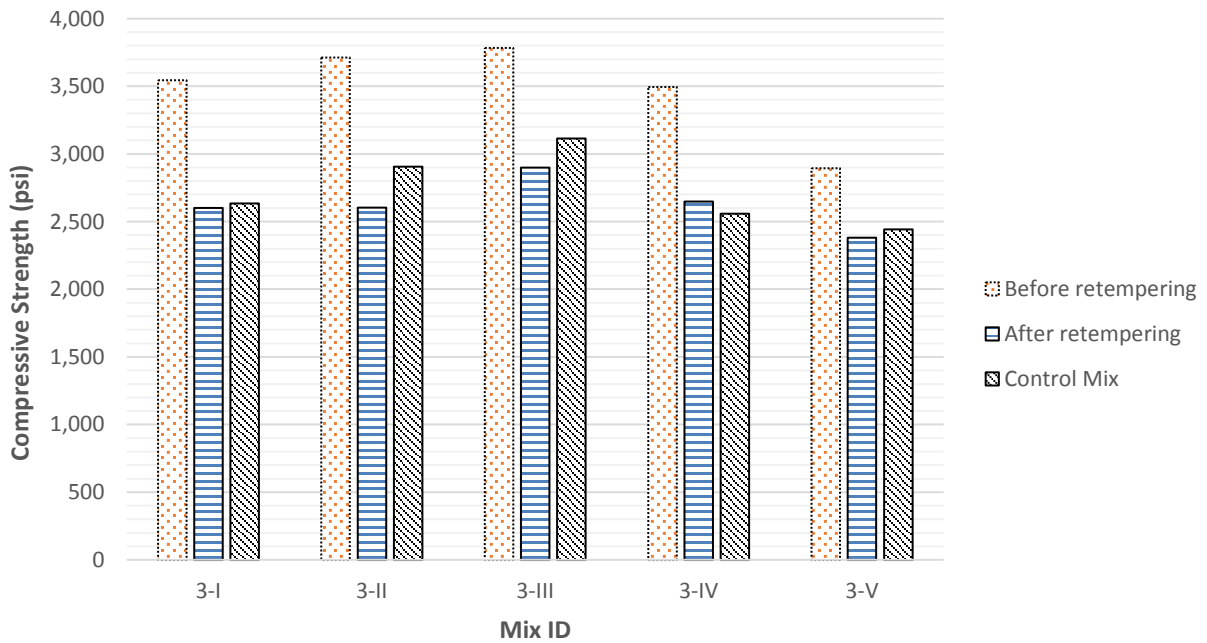


Figure 6.5: Compressive Strength at 7 Days – Granite

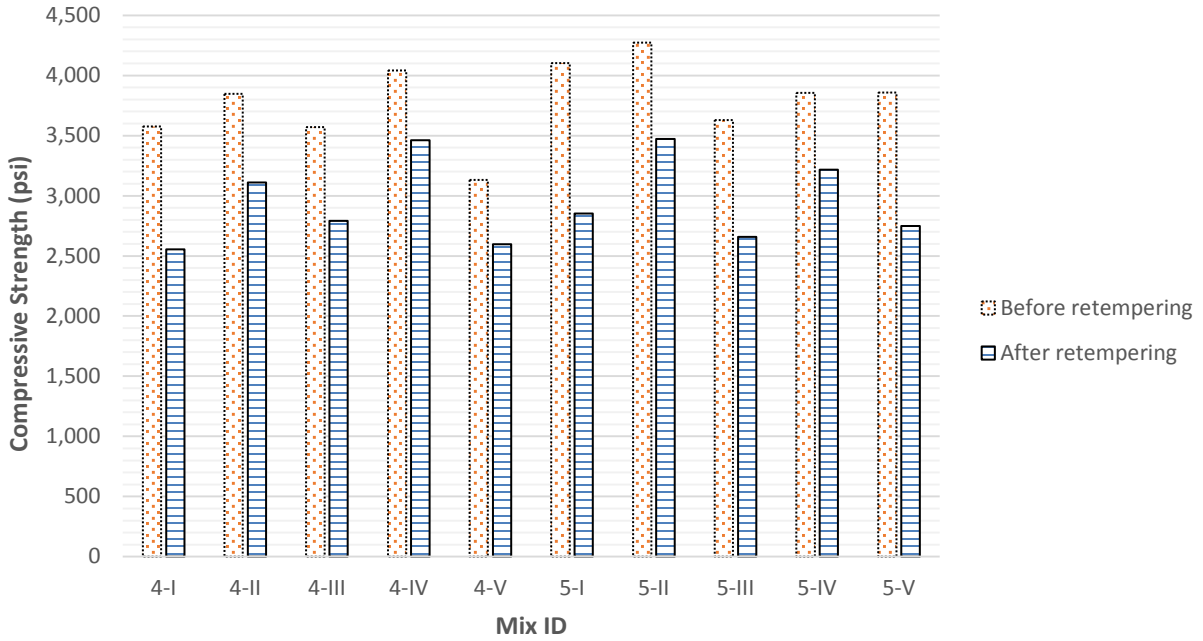


Figure 6.6: Compressive Strength at 7 Days – Limestone and SD Quartzite

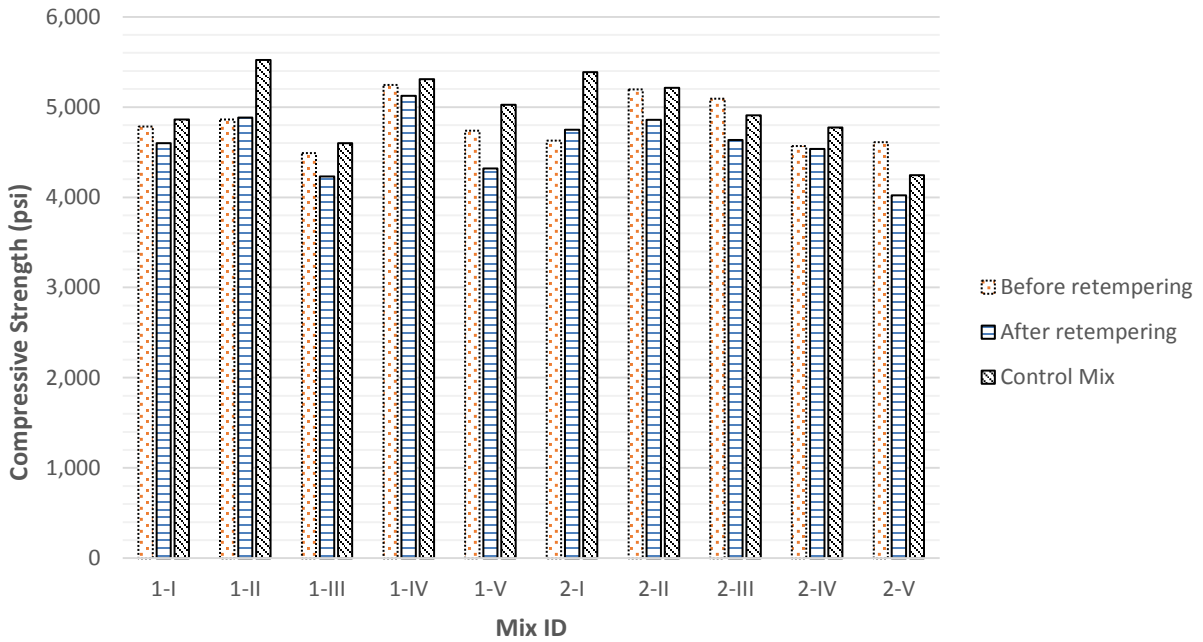


Figure 6.7: Compressive Strength at 28 Days – Lincoln Quartzite

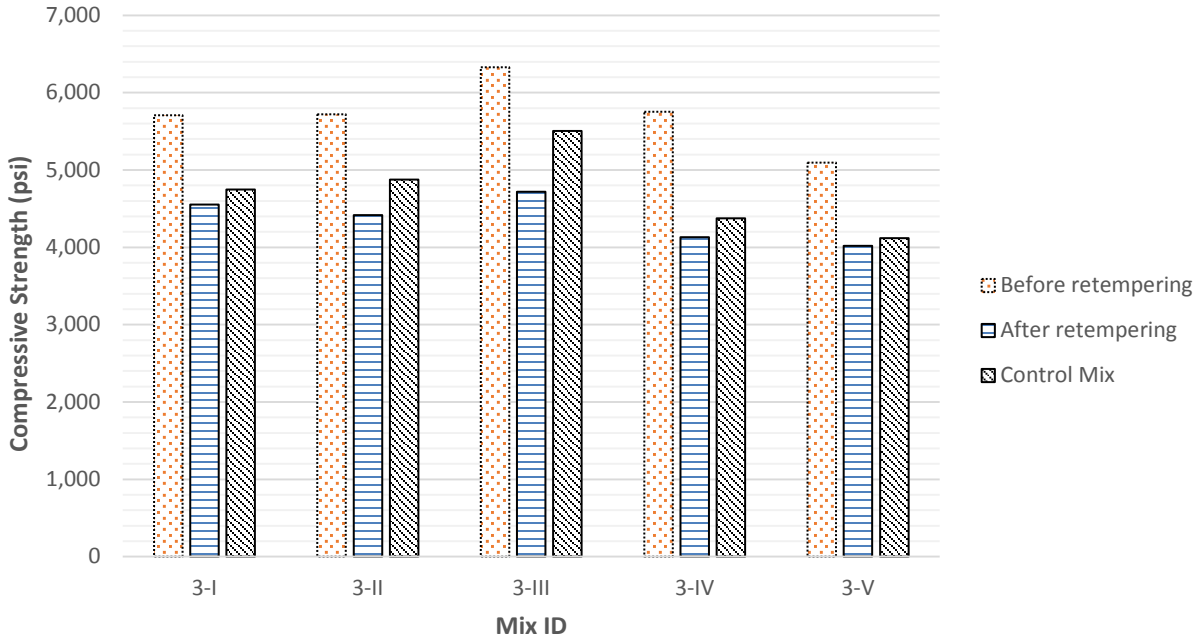


Figure 6.8: Compressive Strength at 28 Days – Granite

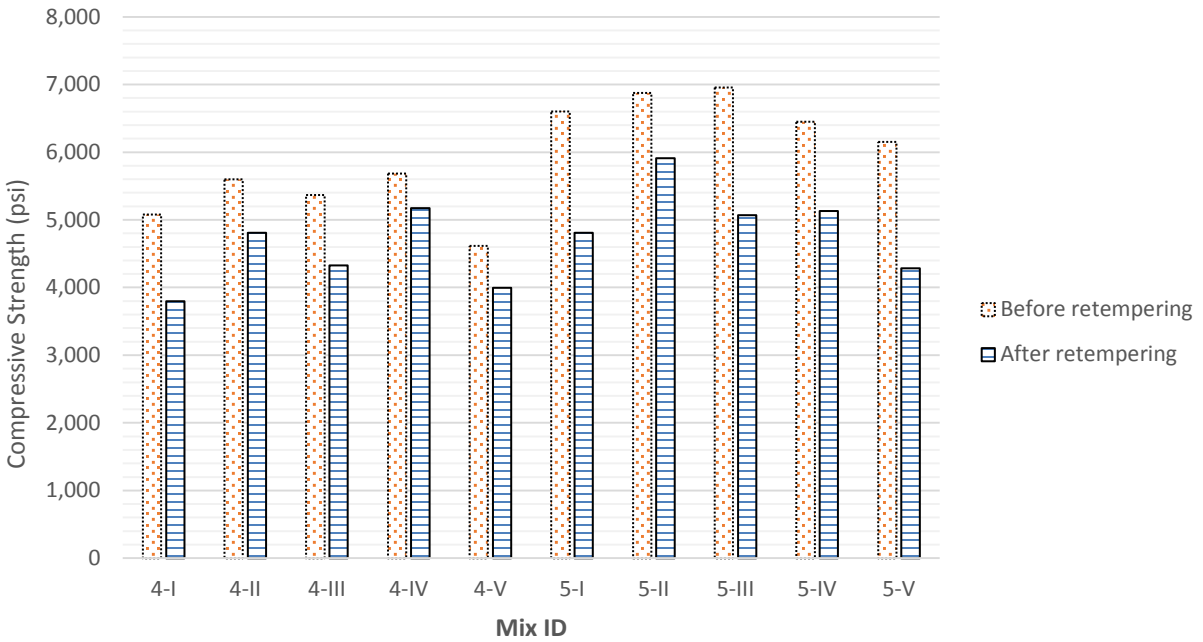


Figure 6.9: Compressive Strength at 28 Days – Limestone and SD Quartzite

6.3 Air Void Content of Hardened Concrete

Total air void content obtained from the hardened concrete analysis as described in Section 4.2.3 Air Void Analysis of Hardened Concrete is presented in Figure 6.10, Figure 6.11, and Figure 6.12. Corresponding spacing factors are shown in Figure 6.13, Figure 6.14, and Figure 6.15.

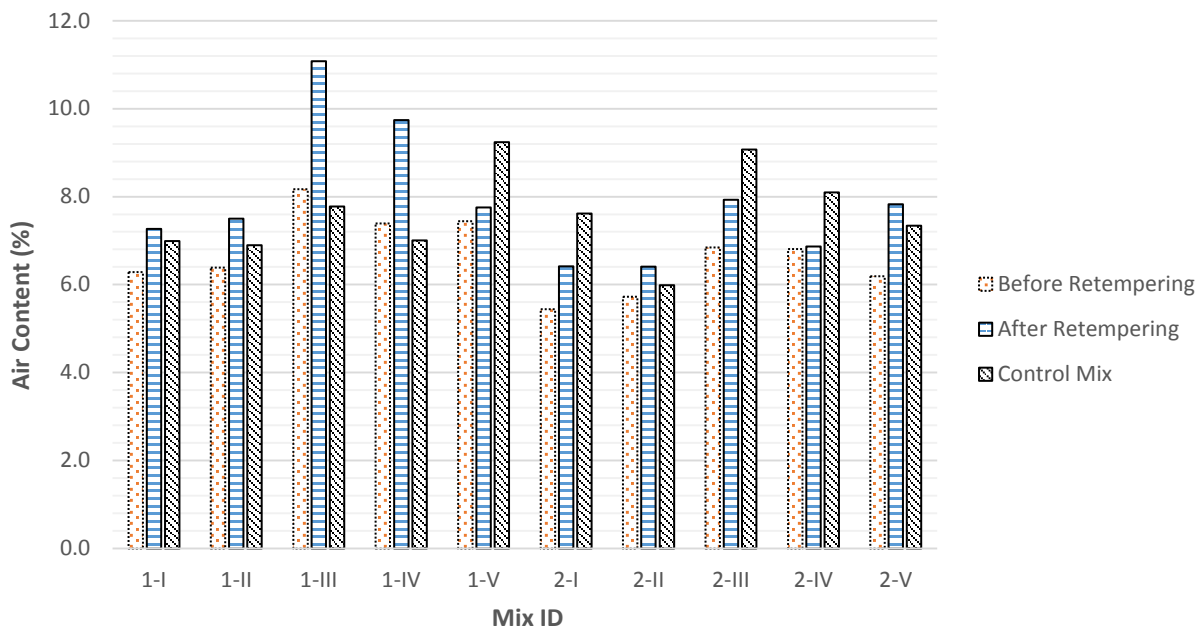


Figure 6.10: Air Content (Hardened) – Lincoln Quartzite

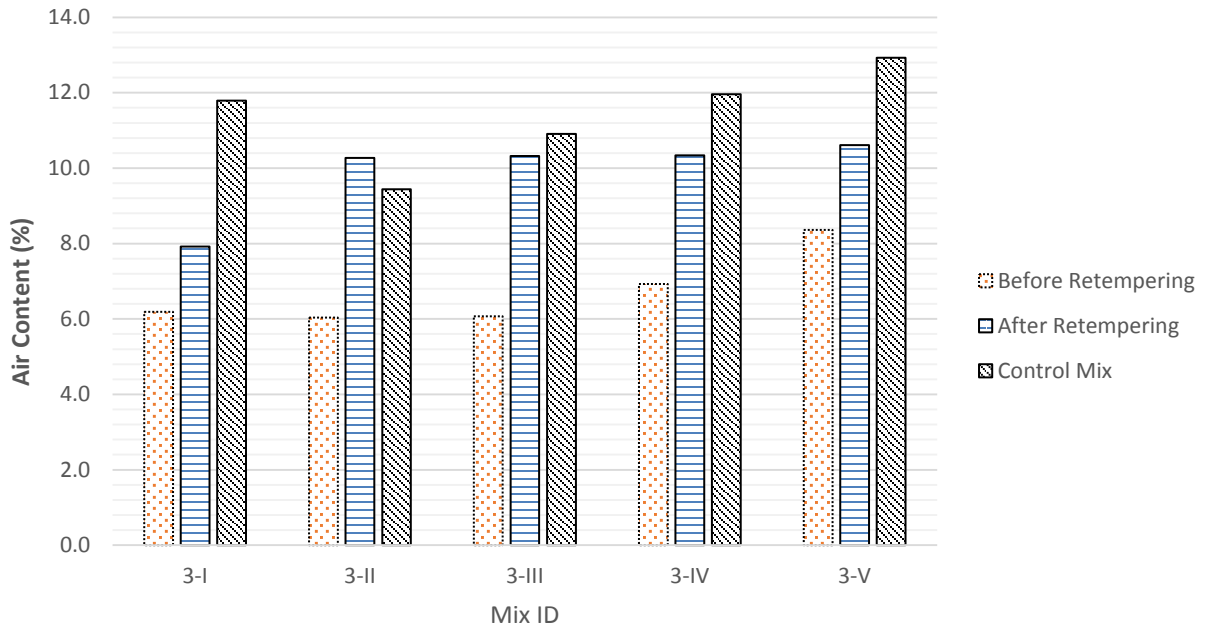


Figure 6.11: Air Content (Hardened) – Granite

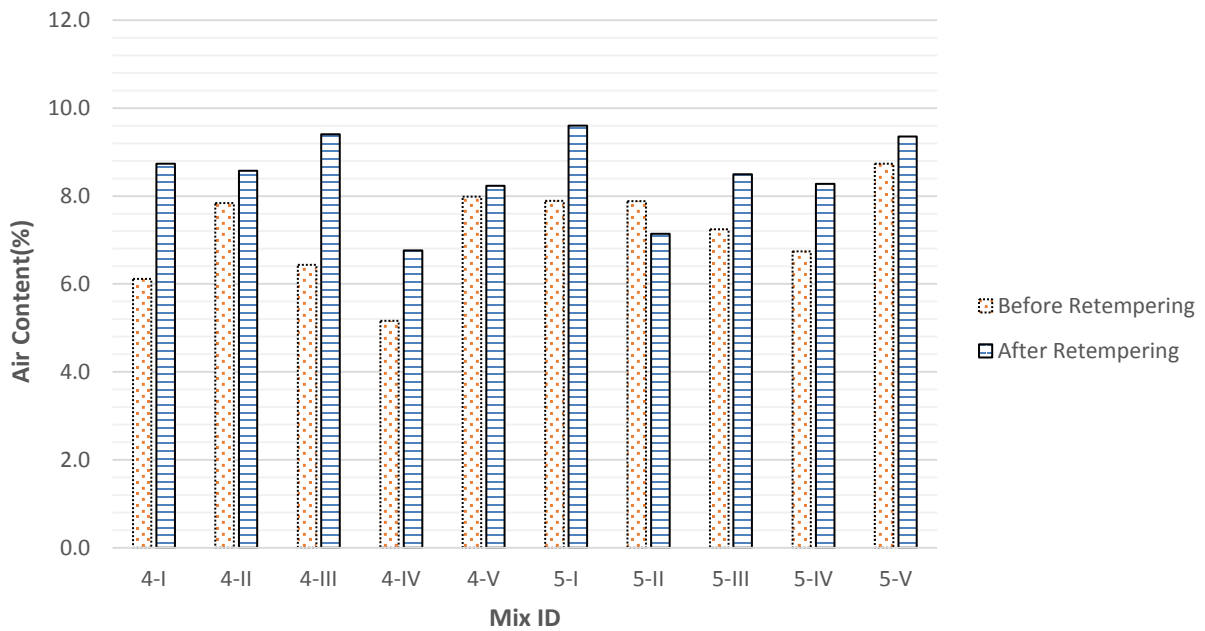


Figure 6.12: Air Content (Hardened) – Limestone and SD Quartzite

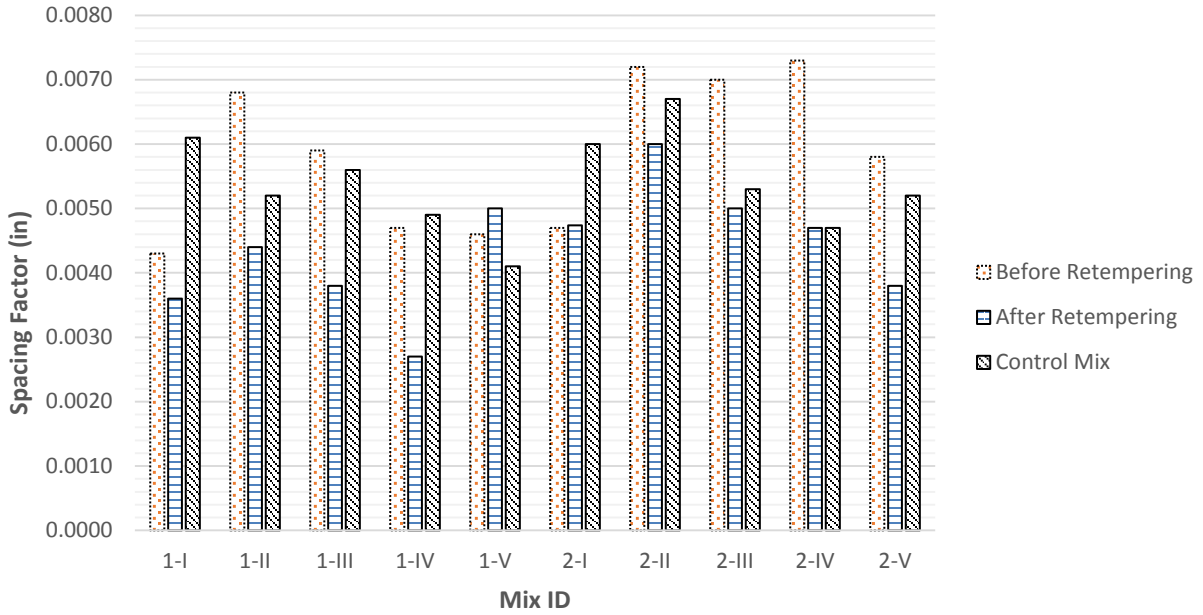


Figure 6.13: Spacing Factor – Lincoln Quartzite

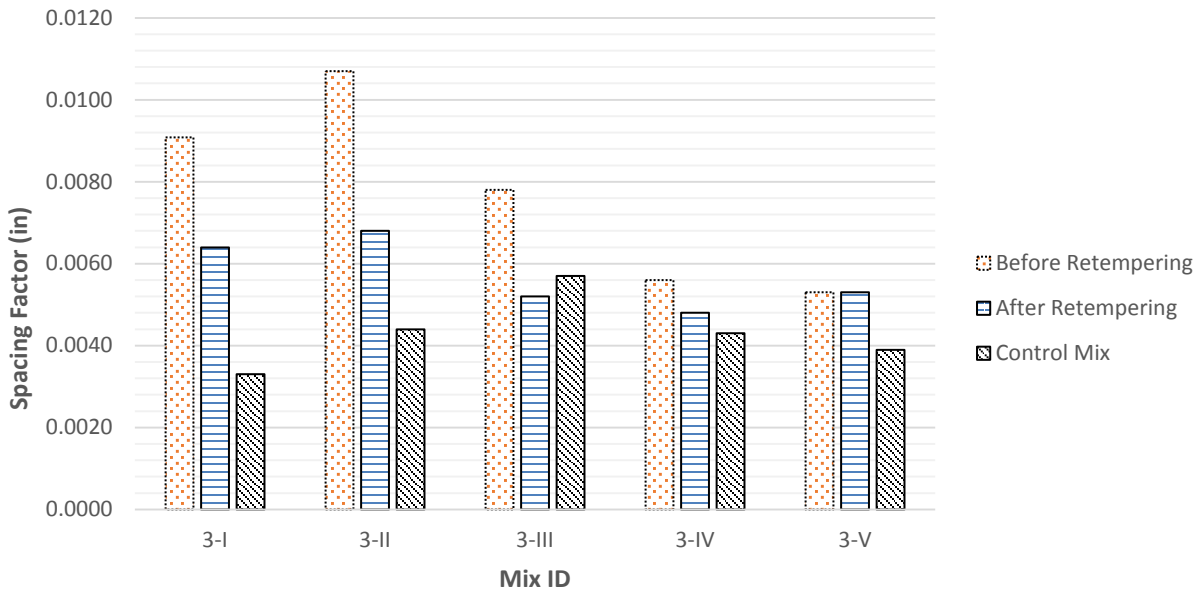


Figure 6.14: Spacing Factor – Granite

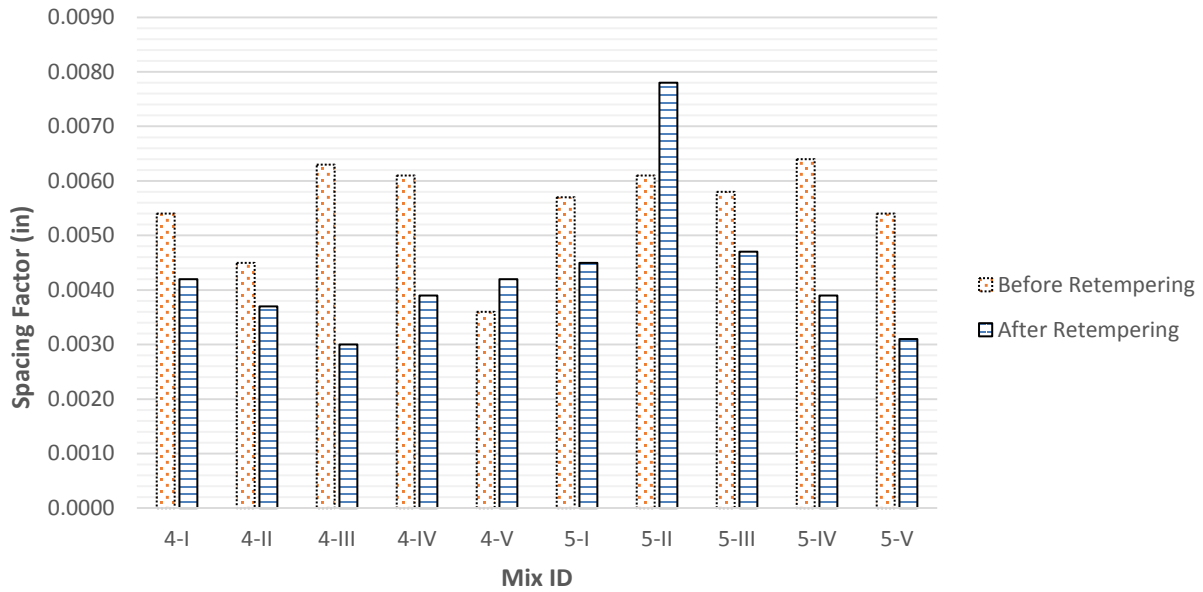


Figure 6.15: Spacing Factor – Limestone and SD Quartzite

6.4 Air Void Clustering

Results of the clustering analysis are presented in Figure 6.16, Figure 6.17, and Figure 6.18. Visual ratings of air void clustering obtained from the manual analysis are shown in Figure 6.19, Figure 6.20, and Figure 6.21.

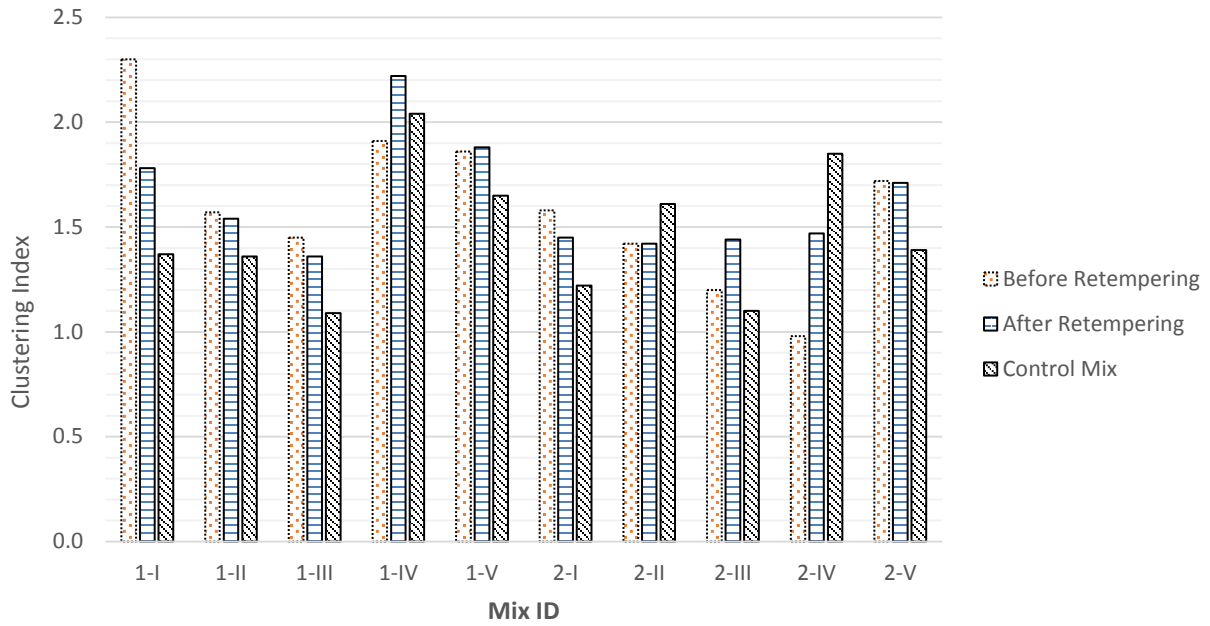


Figure 6.16: Clustering Index – Lincoln Quartzite

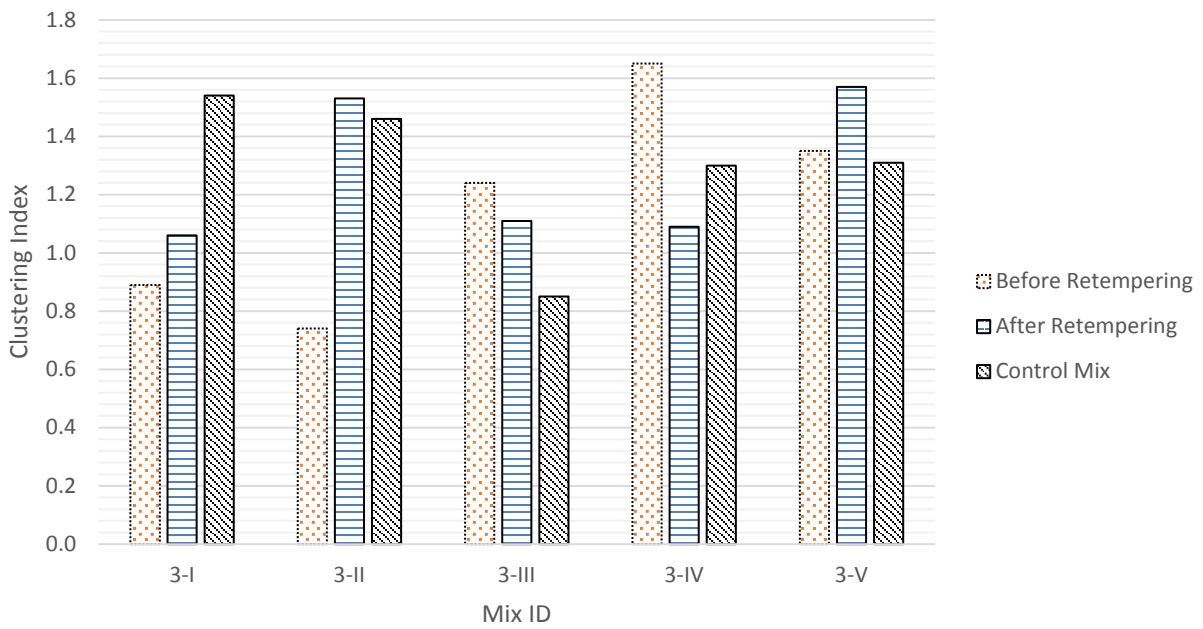


Figure 6.17: Clustering Index – Granite

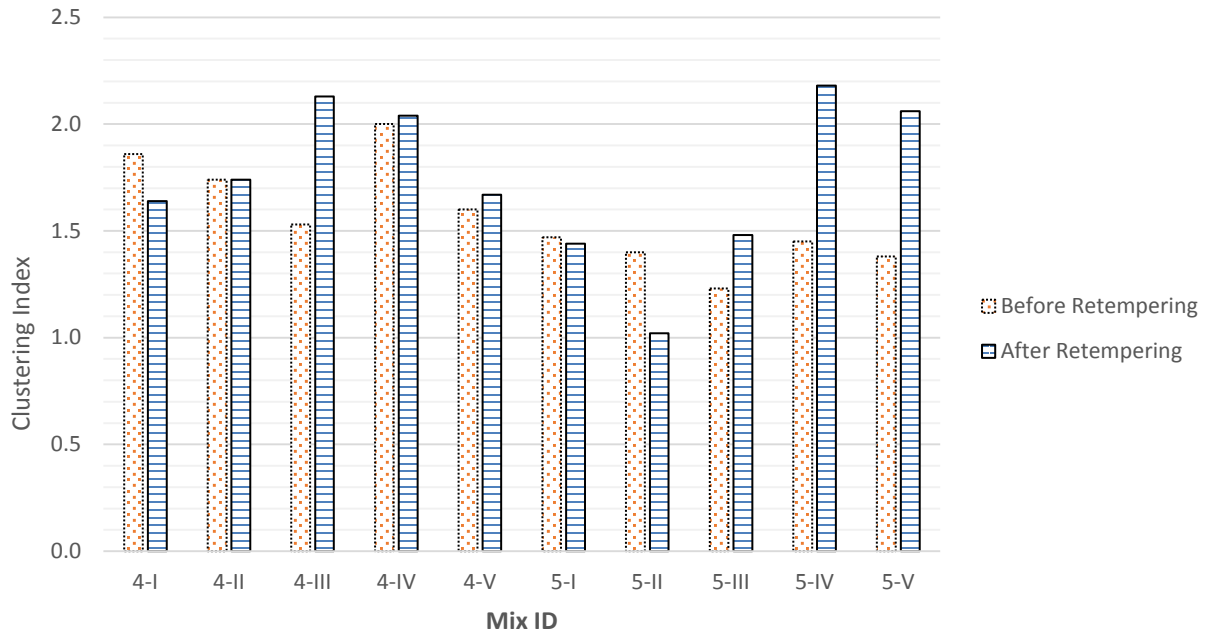


Figure 6.18: Clustering Index – Limestone and SD Quartzite

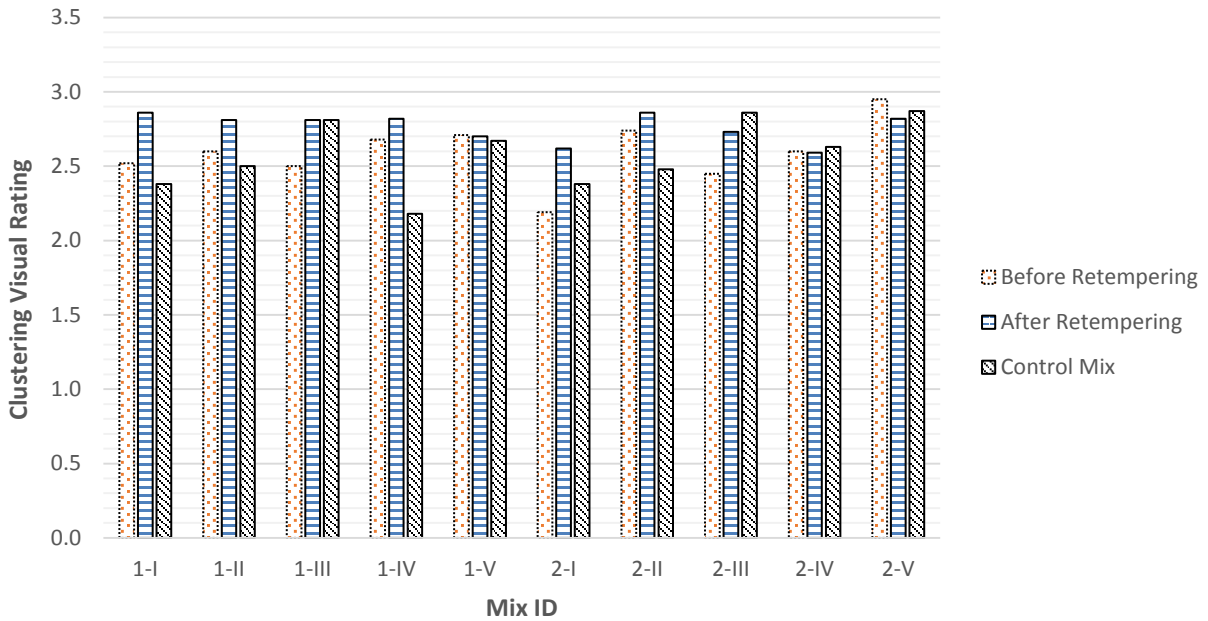


Figure 6.19: Clustering Index (Visual Rating) – Lincoln Quartzite

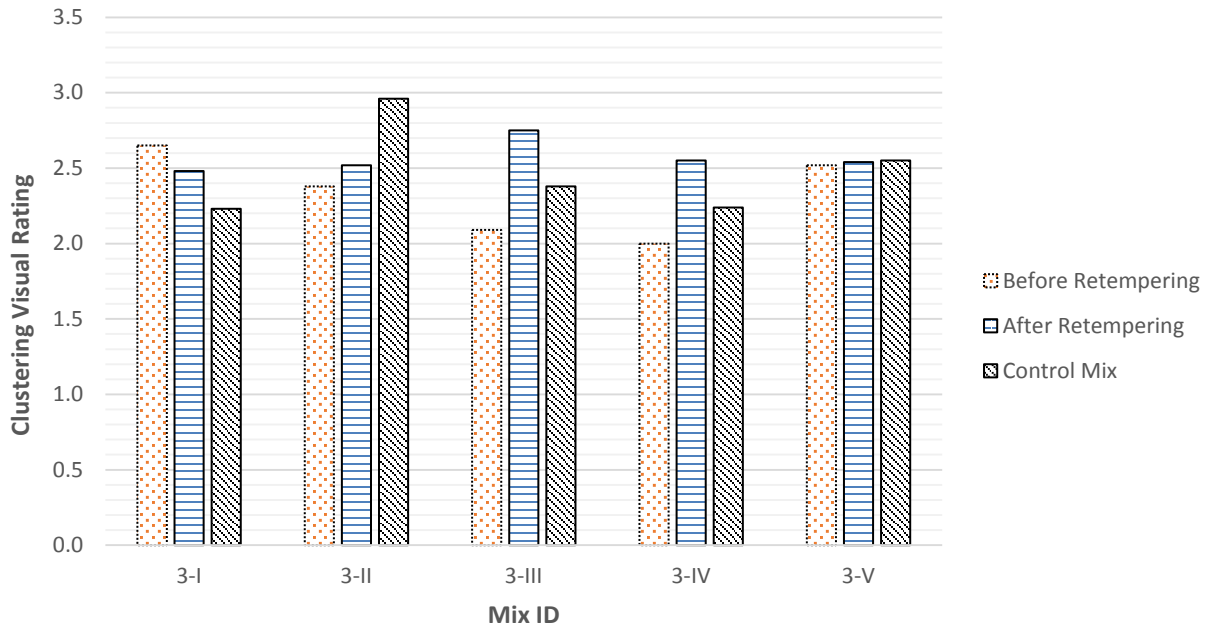


Figure 6.20: Clustering Index (Visual Rating) – Granite

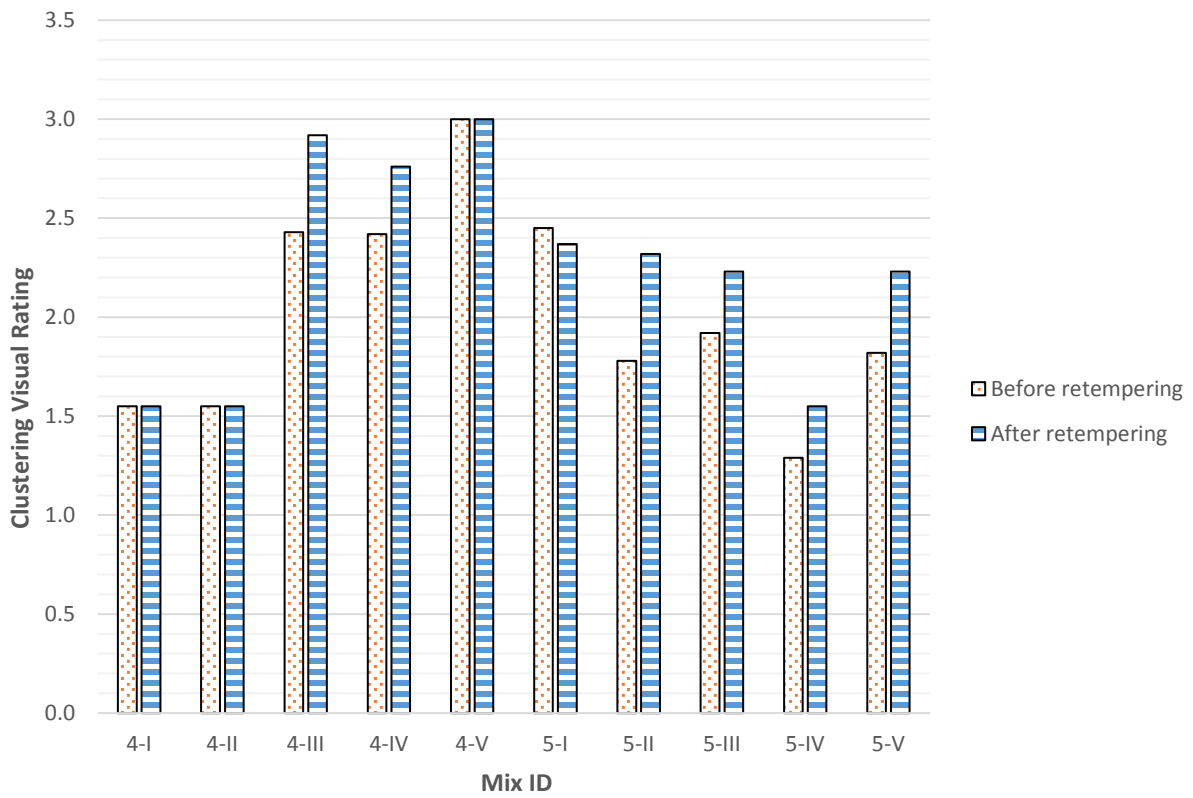


Figure 6.21: Clustering Index (Visual Rating) – Limestone and SD Quartzite

6.5 Field Samples

Fresh concrete properties of field mixes are presented in Table 6.2.

Table 6.2: Fresh Concrete Properties – Field Testing

Site	Slump	Air Content	Unit Weight	Temperature
	<i>inches</i>	<i>%</i>	<i>lb/ft³</i>	<i>°F</i>
Site I – Before Water Addition	3.25	6.2	144	84
Site I – After Water Addition	4.00	6.6	142	85
Site II – Before Water Addition	0.50	4.5	147	79
Site II – After Water Addition	1.50	5.8	145	81

Values of concrete compressive strength at both 7 and 28 days are shown in Figure 6.22 and Figure 6.23, respectively.

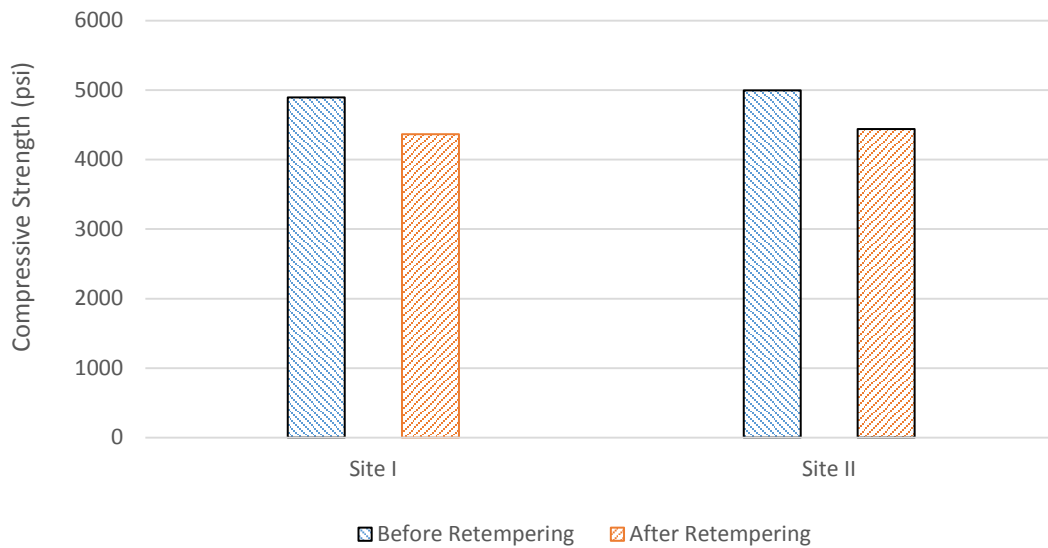


Figure 6.22: Compressive Strength at 7 Days – Field Testing

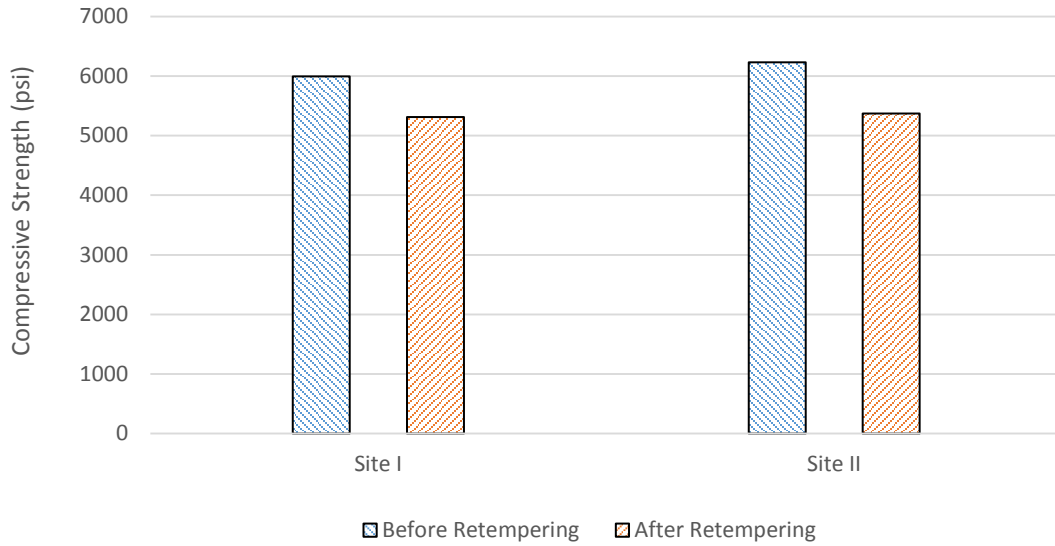


Figure 6.23: Compressive Strength at 28 Days – Field Testing

Results of the hardened air void analysis total air content and Clustering Index are presented in Figure 6.24 and Figure 6.25, respectively. A visual rating was not performed on the field samples, only the automated index analysis.

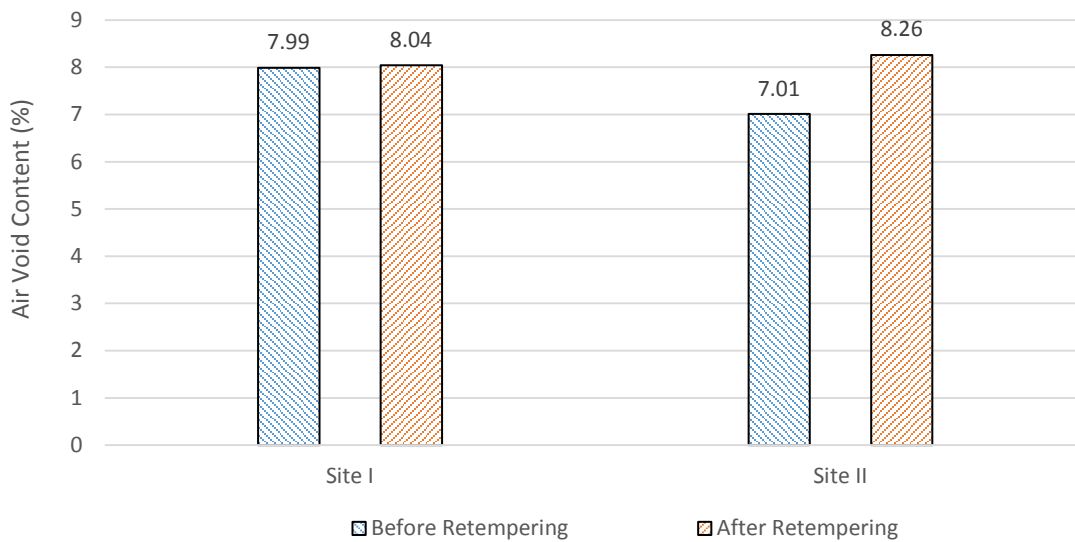


Figure 6.24: Hardened Air Void Content – Field Testing

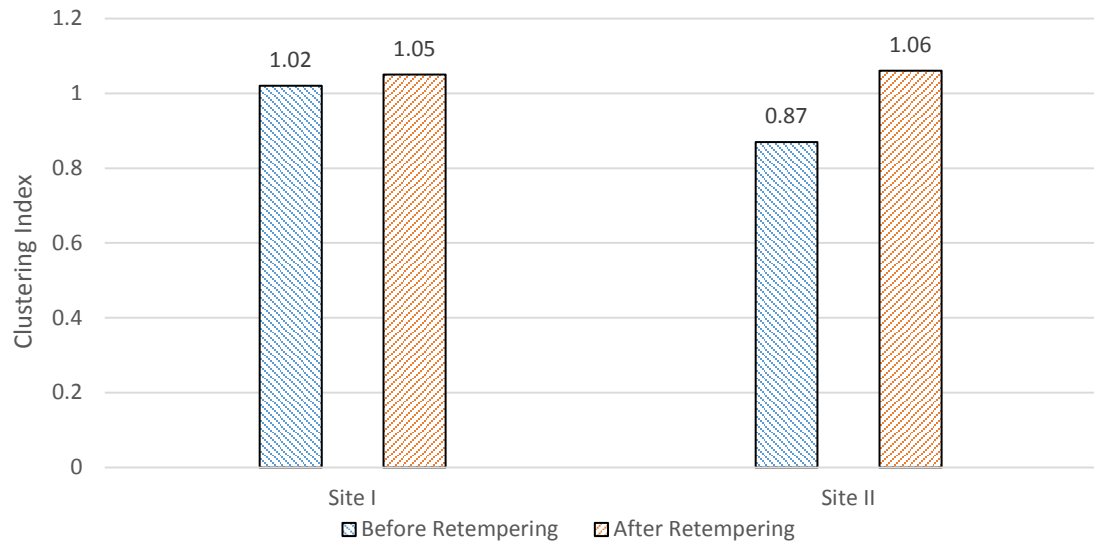


Figure 6.25: Clustering Index – Field Testing

Chapter 7: Discussion

Three variables were examined in this study: (1) retempering, (2) aggregate type, and (3) air entraining admixture type. Results with respect to all three investigated variables will be discussed in the following subsections.

7.1 Retempering

To recall, mixes with Lincoln quartzite had a water-to-cement ratio equal to 0.40 and 0.43 before and after retempering, respectively. Mixes utilizing granite, limestone and SD quartzite had a w/c ratio 0.42 and 0.45 before and after retempering. For all mixes, the additional mixing period during retempering was 2 minutes long.

Changes in concrete fresh properties before and after retempering corresponded to what was expected. In all cases, retempered mixes experienced an increase in slump and air content, as well as a decrease in unit weight. Concrete slump always increased after retempering (Figure 7.1), which is not surprising as one of the main reasons why the retempering practice is utilized in the industry is to increase concrete workability. The increase in slump as a percentage ranged from 44% to 175% (average value was 90% with standard deviation of 37%). Variation in slump values between retempered and control mixes was small. The difference can be attributed to small deviations from the targeted w/c after retempering because it was very difficult to determine the exact amount of concrete left in the batch after making cylinders for compressive strength before retempering. Small differences in the amount of concrete removed from the batch may have altered the final w/c for a given amount of water added during retempering, giving slight differences in the w/c in the retempered and control batches. Another possible cause of the difference in slump between the retempered and control mixtures was time from mixing. Retempered mixtures were tested at a slightly later age from the initial mixing, leading to a slight slump loss. Variation from the slump test procedure may have also contributed some to the difference.

Similarly, an increase in total air content was observed in all mixes after retempering, as shown in Figure 7.2. On average, air content increased by 1.6% after retempering (standard

deviation was 0.7%). The highest observed increase was 3.5% while the lowest value of air content increase was found to be 0.5%. The additional mixing action and higher concrete fluidity allowed more air to be folded into the concrete and be stabilized.

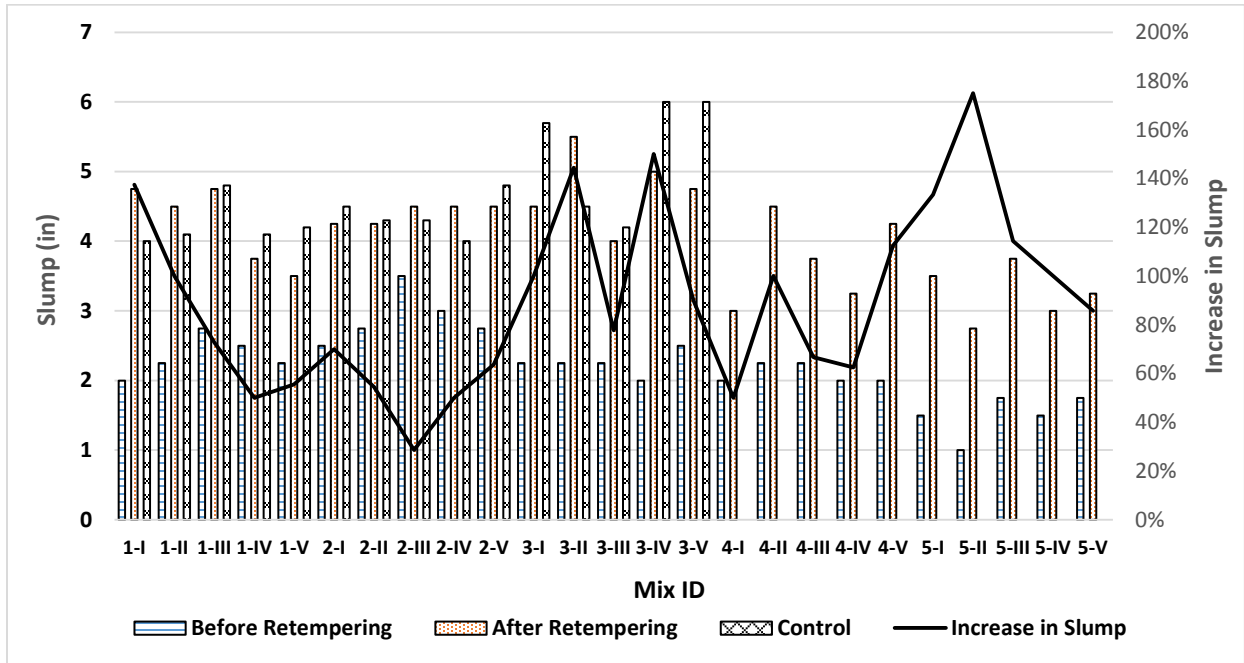


Figure 7.1: Slump Before and After Retempering

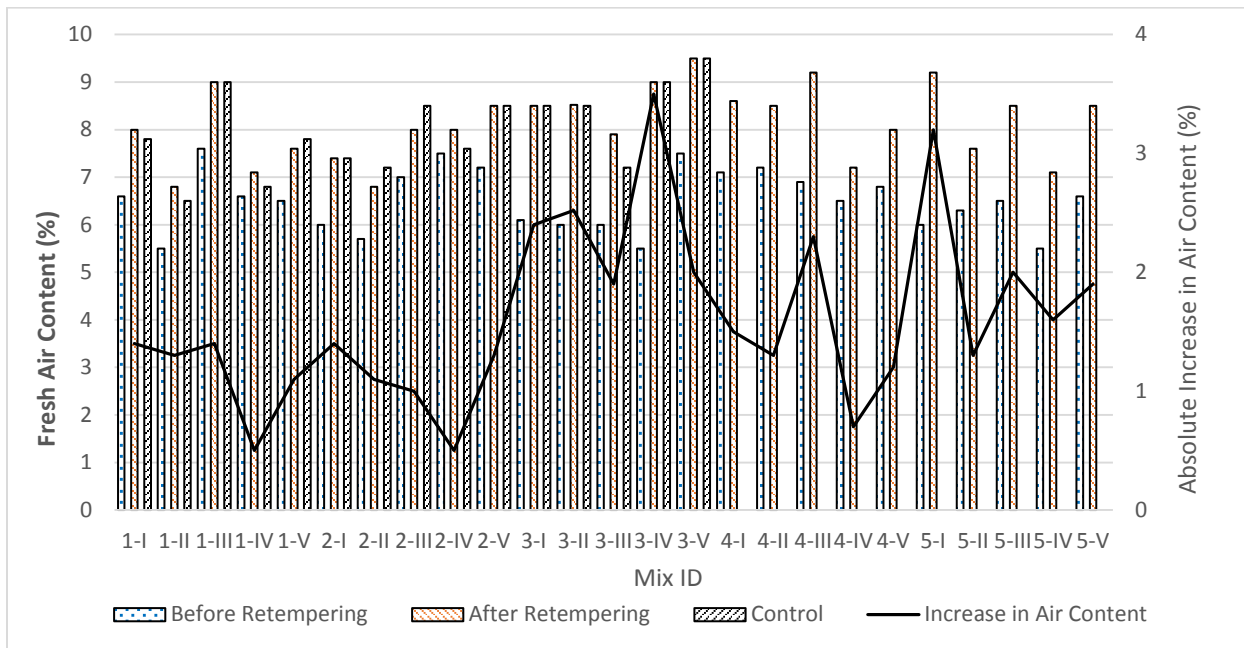


Figure 7.2: Fresh Air Content Before and After Retempering

Relationship between the air content of fresh concrete and unit weight is presented in Figure 7.3. Correlation can be seen between those two concrete properties, as R^2 values were 0.78, 0.69, and 0.94 for mixes before retempering, after retempering, and control mixes, respectively. The lower value of the R^2 coefficient for mixes after retempering is most likely caused by small differences in the paste-to-aggregate ratio from using some of the concrete in the mixture to make cylinders for strength that did not have the exact paste-to-aggregate ratio in the overall mixture or from small rounding of measured air contents as required.

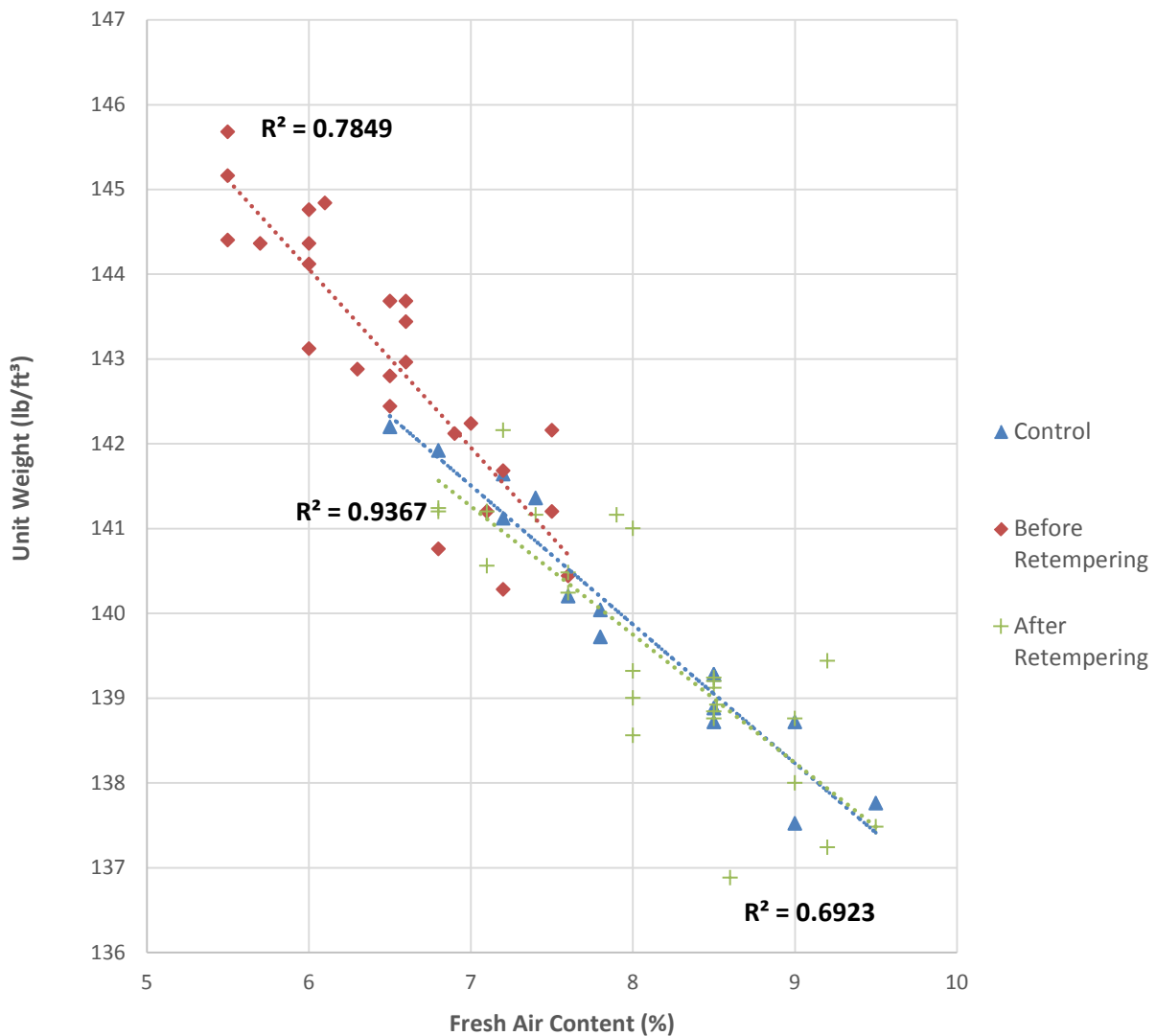


Figure 7.3: Air Content vs Unit Weight

Retempering has been previously associated with air void clustering (Naranjo, 2007; Kozikowski et al., 2005). Therefore, it was predicted that retempered mixes should have higher levels of air void clustering than non-retempered mixes. Despite the predictions, many mixes showed less clustering activity after retempering (10 out of 25), as presented in Figure 7.4. Average change in clustering index before and after retempering was only 10% (standard deviation equaled to 31%). The maximal observed increase in clustering after retempering was 107% whereas the highest decrease was by 34%.

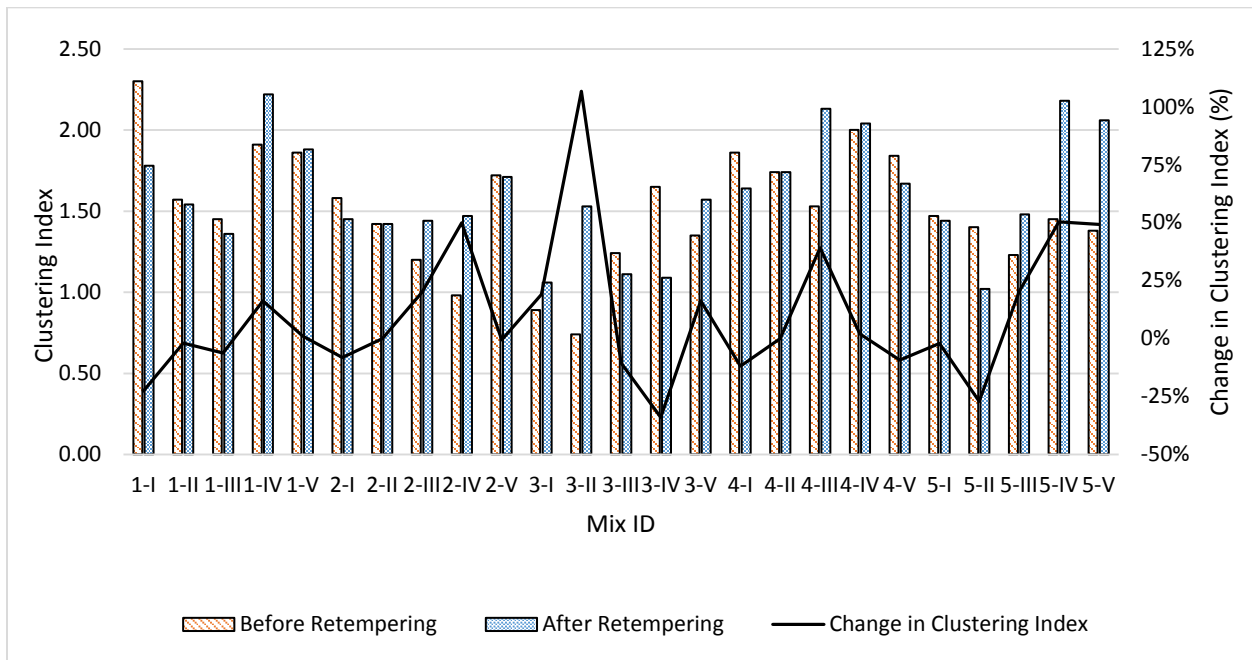


Figure 7.4: Clustering Index – Before and After Retempering

Comparison of clustering indexes of mixes after retempering and control mixes is provided in Figure 7.5. It is evident that the majority of mixes after being retempered showed a higher clustering rate than corresponding control mixes (11 out of 15). However, the retempered mixes had an average clustering index increase of only 9% (standard deviation was 20%).

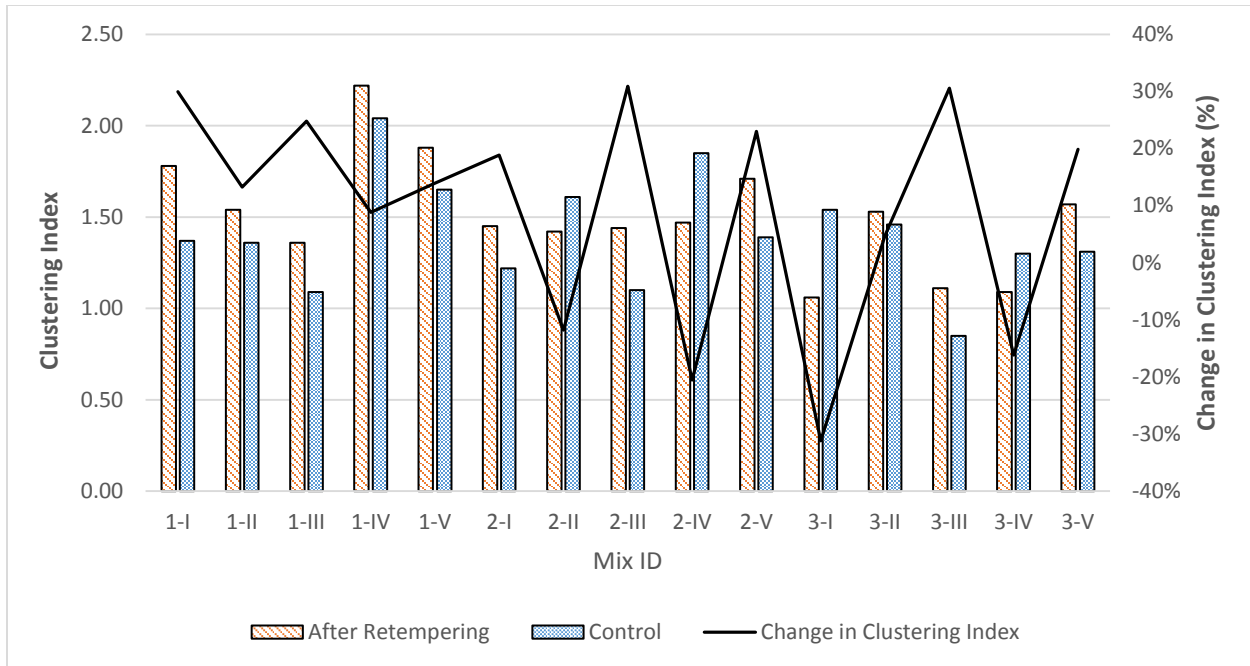


Figure 7.5: Clustering Index – After Retempering and Control Mixes

Based on the presented data, it seems that retempering might have had some influence on the formation of air void clusters around the coarse aggregate. However, the increase in the clustering rate was relatively small, as the change in the clustering rate between retempered and control mixes was only 9% in average.

On the other hand, compressive strength at both 7 and 28 days very much corresponded to what was expected. Compressive strength in all but 2 cases (out of 50) decreased after retempering, as shown in Figure 7.6 (7 days) and Figure 7.7 (28 days). At 7 days, the average decrease in strength after the concrete mix was retempered was 15% (standard deviation 8%), while at 28 days, the average decrease was 11% with a standard deviation of 10%. The maximum decrease in strength was 30% and 28% for strengths at 7 and 28 days, respectively. The lowest decrease was 8% at 7 days and, surprisingly, one mix showed similar compressive strength after retempering at 28 days (3% higher than the non-retempered mixture).

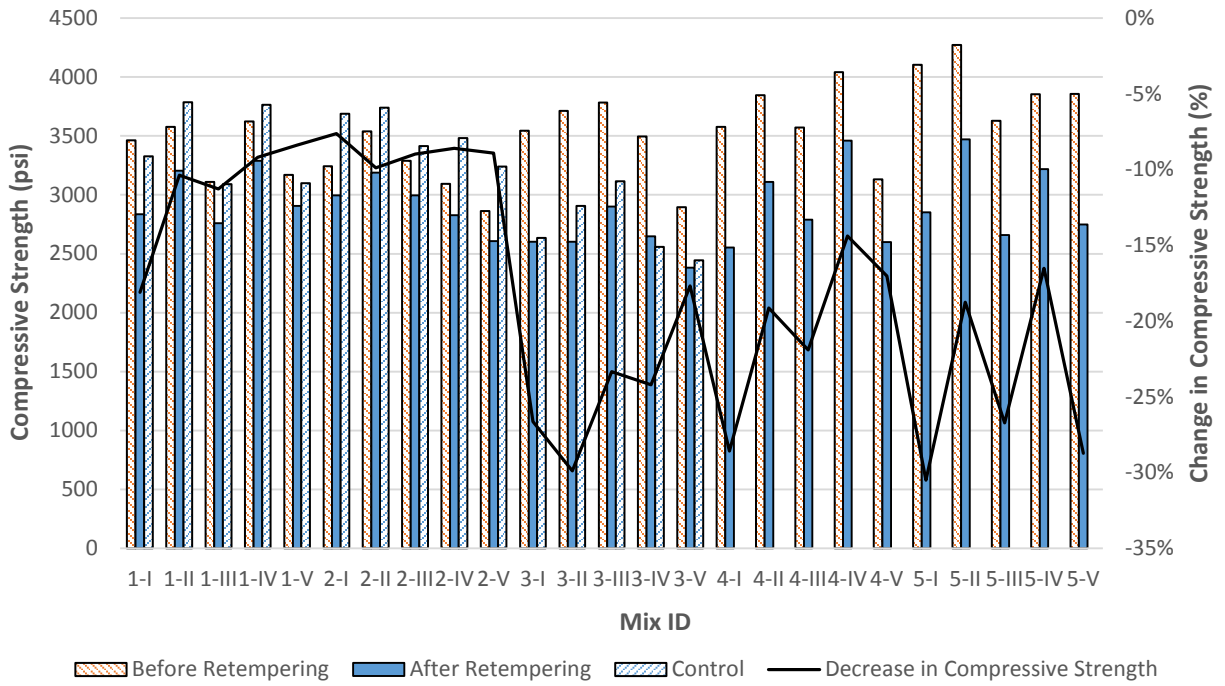


Figure 7.6: Compressive Strength at 7 Days

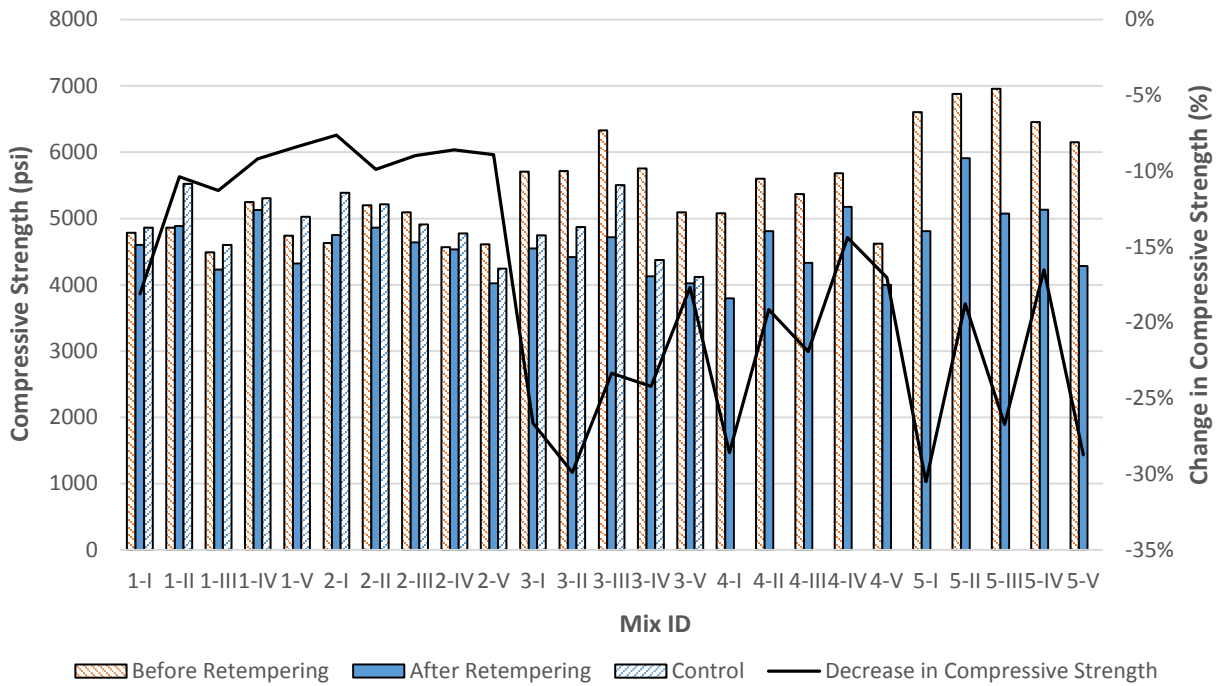


Figure 7.7: Compressive Strength at 28 Days

A comparative analysis, taking into account the increase in the water-cement ratio as well as the increase in the total air content in retempered mixes, has been carried out to evaluate the effect of retempering on the compressive strength. A common rule of thumb used in the concrete industry is that every extra percent of air content will reduce the compressive strength of concrete by 5% for a mix with a constant water-cement ratio. For instance, consider two identical mixes, one with 6% of air and another with 9%; the second mix should have the compressive strength at 28 days lowered by 15% (3 x 5%). Additionally, the alteration of the w/c must be considered. It has been reported that a w/c increase by 0.03 (which was done by retempering concrete mixes in this study) can result in a decrease in the compressive strength by approximately 8% (Kosmatka et al., 2003). Based on these two “rules of thumb,” an analysis comparing values of compressive strength of mixes before and after retempering was performed. For example, consider the mix 4-I and 4-I-R; the 1.5% increase in the total air content would theoretically result in 7.5% reduction in the compressive strength. Together with the 8% decrease due to w/c change, a decrease in the compressive strength of 15.5% can be theoretically predicted in the retempered mix. For comparison, the difference in compressive strength values based on the experimental data was 25.26%. The disagreement between the theoretical calculation and experimental values is then only about 10%. Results of this analysis are presented in Table 7.1. Moreover, it is important to keep in mind that the theoretical calculations are based on recommended general “rules of thumb,” therefore these calculations might be slightly inaccurate. For this reason, the control mixtures were made to compare the retempered concrete mixture to concrete made with similar air content and w/c.

Table 7.1: Compressive Strength – Comparative Analysis

Mix ID	Change in air content	Change in compressive strength due to increase in air content	Change in compressive strength due to increase in w/c	Theoretical change in compressive strength	Experimental change in compressive strength	Difference
	%	%	%	%	%	%
1-I	1.4	7.0	8.0	-15.00	-3.87	11.13
1-II	1.3	6.5	8.0	-14.50	0.47	14.97
1-III	1.4	7.0	8.0	-15.00	-5.77	9.23
1-IV	0.5	2.5	8.0	-10.50	-2.32	8.18
1-V	1.1	5.5	8.0	-13.50	-8.86	4.64
2-I	1.4	7.0	8.0	-15.00	2.63	17.63
2-II	1.1	5.5	8.0	-13.50	-6.48	7.02
2-III	1.0	5.0	8.0	-13.00	-8.95	4.05
2-IV	0.5	2.5	8.0	-10.50	-0.74	9.76
2-V	1.3	6.5	8.0	-14.50	-12.77	1.73
3-I	2.4	12.0	8.0	-20.00	-20.28	-0.28
3-II	2.5	12.6	8.0	-20.60	-22.75	-2.15
3-III	1.9	9.5	8.0	-17.50	-25.41	-7.91
3-IV	3.5	17.5	8.0	-25.50	-28.24	-2.74
3-V	2.0	10.0	8.0	-18.00	-21.10	-3.10
4-I	1.5	7.5	8.0	-15.50	-25.26	-9.76
4-II	1.3	6.5	8.0	-14.50	-14.14	0.36
4-III	2.3	11.5	8.0	-19.50	-19.34	0.16
4-IV	0.7	3.5	8.0	-11.50	-8.95	2.55
4-V	1.2	6.0	8.0	-14.00	-13.44	0.56
5-I	3.2	16.0	8.0	-24.00	-27.18	-3.18
5-II	1.3	6.5	8.0	-14.50	-14.07	0.43
5-III	2.0	10.0	8.0	-18.00	-27.08	-9.08
5-IV	1.6	8.0	8.0	-16.00	-20.50	-4.50
5-V	1.9	9.5	8.0	-17.50	-30.37	-12.87

Based on the previous analysis, it was concluded that the decrease in compressive strength can be credited to the increase in both the water-cement ratio and the total air content. Moreover, suggestions have been previously made (Cross et al., 2000; Kozikowski et al., 2005) that air void clustering can be a factor affecting the compressive strength of retempered mixes. However, data obtained in this laboratory study does not confirm this hypothesis. As shown in Figure 7.8 and Figure 7.9, neither mixes, before nor after retempering, exhibit any kind of correlation between the compressive strength and the clustering index.

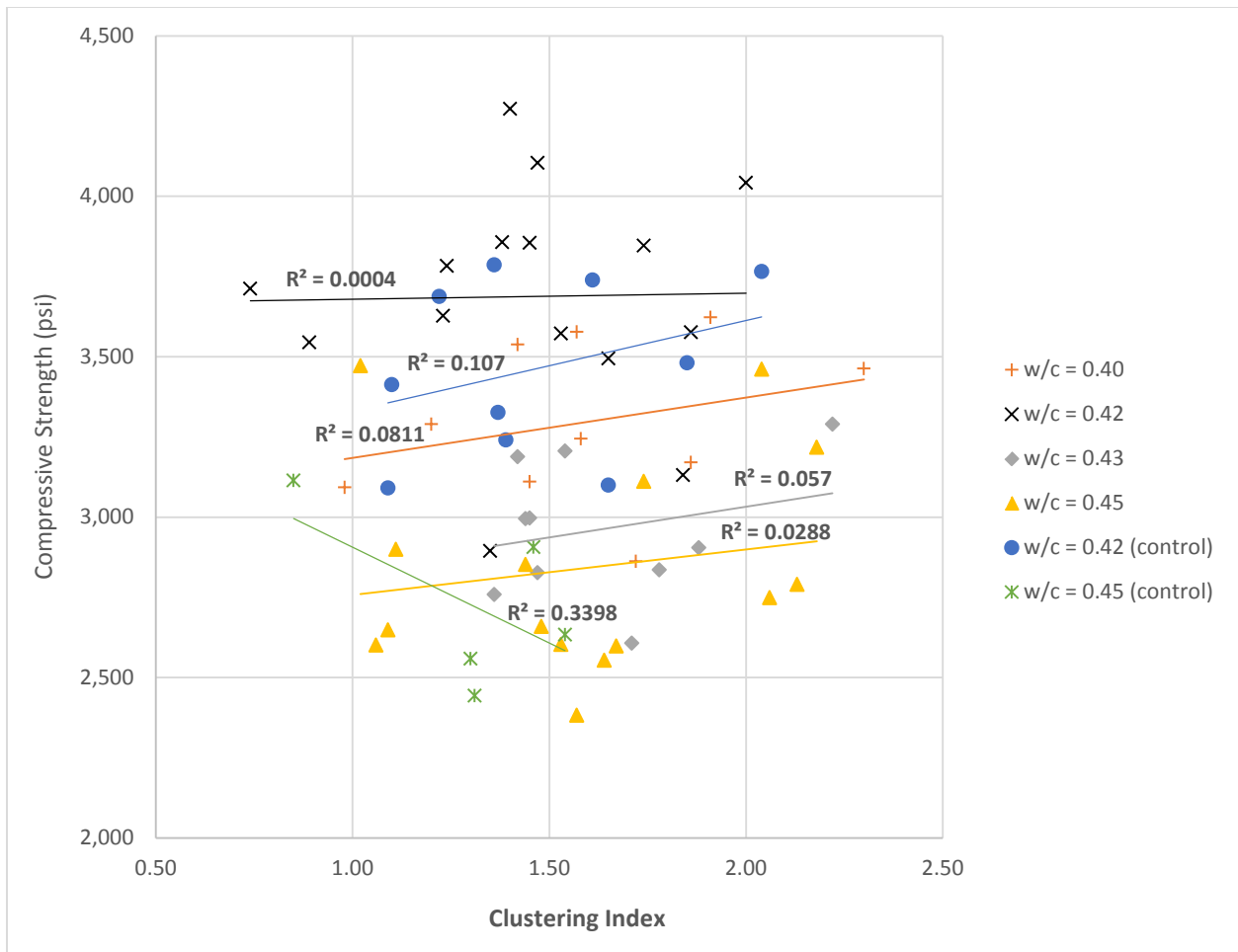


Figure 7.8: Clustering Index vs Compressive Strength at 7 Days

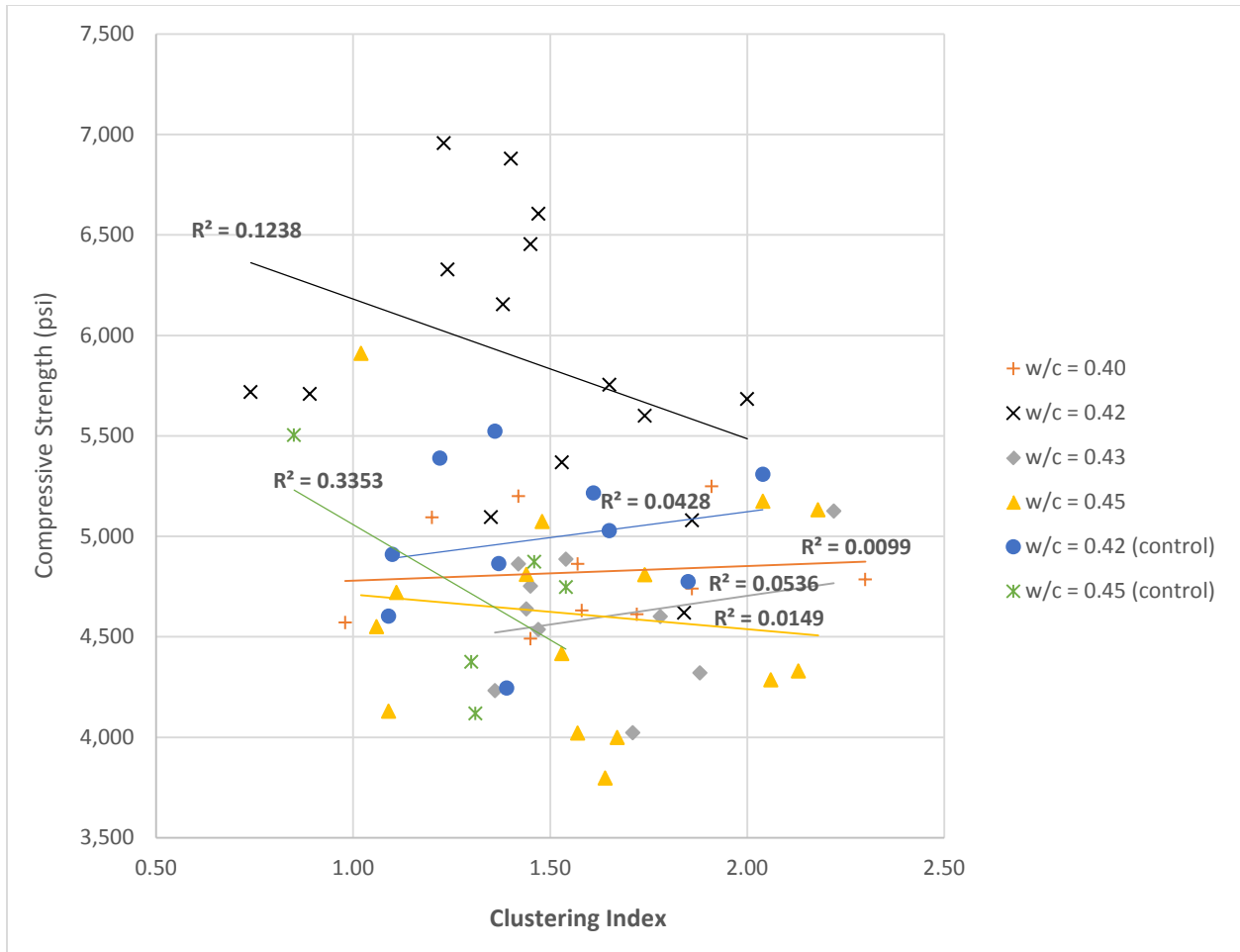


Figure 7.9: Clustering Index vs Compressive Strength at 28 Days

Similarly, no relationship can be observed between the compressive strength and the visual clustering rating, as shown in Figure 7.10 and Figure 7.11 for concrete at 7 and 28 days, respectively.

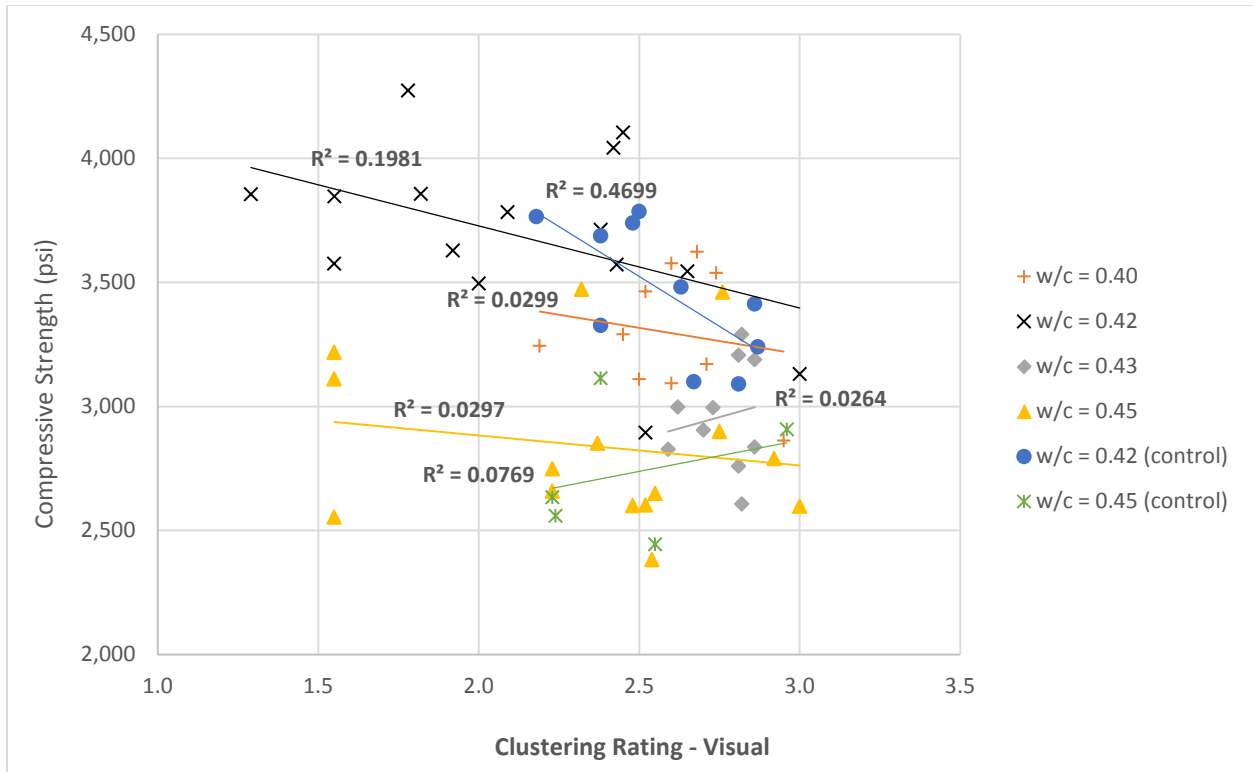


Figure 7.10: Visual Clustering Rating vs Compressive Strength at 7 Days

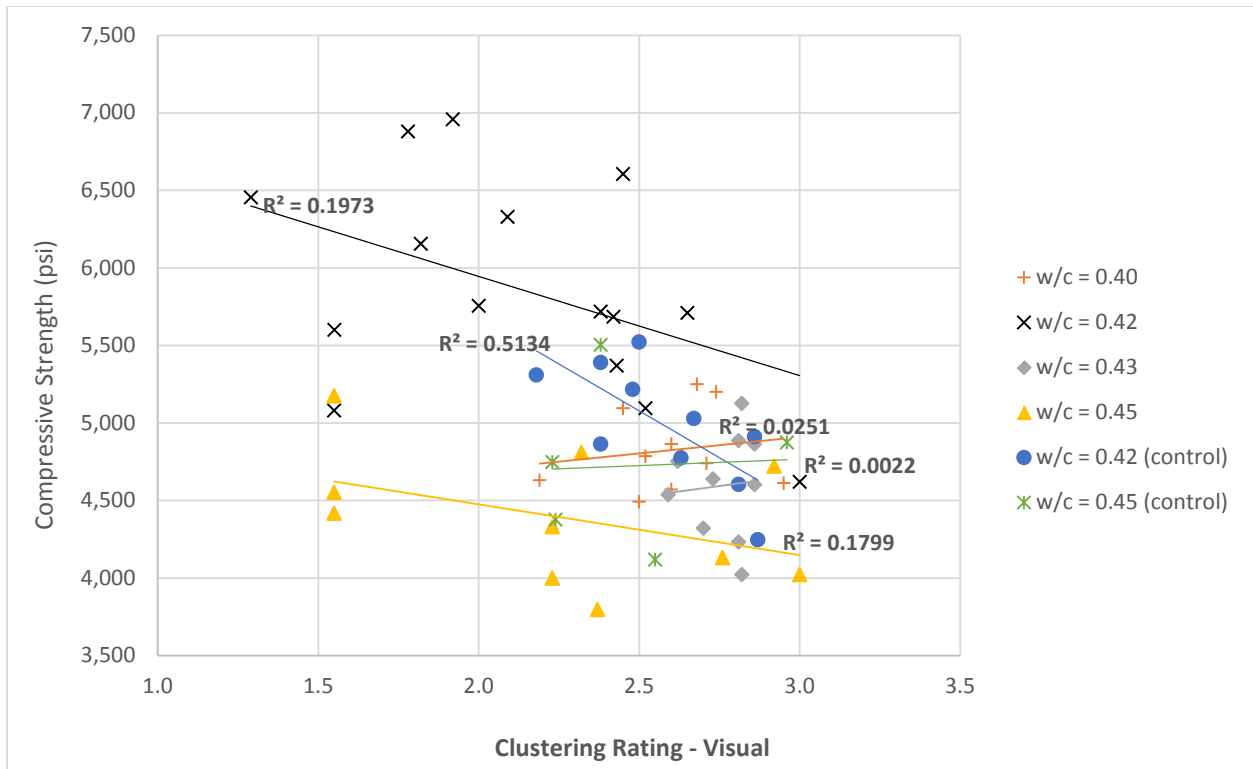


Figure 7.11: Visual Clustering Rating vs Compressive Strength at 28 Days

On the other hand, correlation was found between the air content and compressive strength for all mixes. Relationships are presented in Figure 7.12 and Figure 7.13 for data obtained at 7 and 28 days, respectively. A stronger correlation between the strength and air content was seen for 7-day compressive strength than 28-day compressive strength. This may be because at the higher strength values seen at 28 days, the strength of some aggregates started to limit the strength more than the paste strength which includes the air, reducing the correlation. The presented data includes all mixes and considers the variability in material properties, different water-cement ratios, as well as different chemical admixtures. Thus, it is more likely that the loss of compressive strength in mixes after retempering is a function of air content and water-cement ratio in addition to aggregate type, rather than the clustering rate.

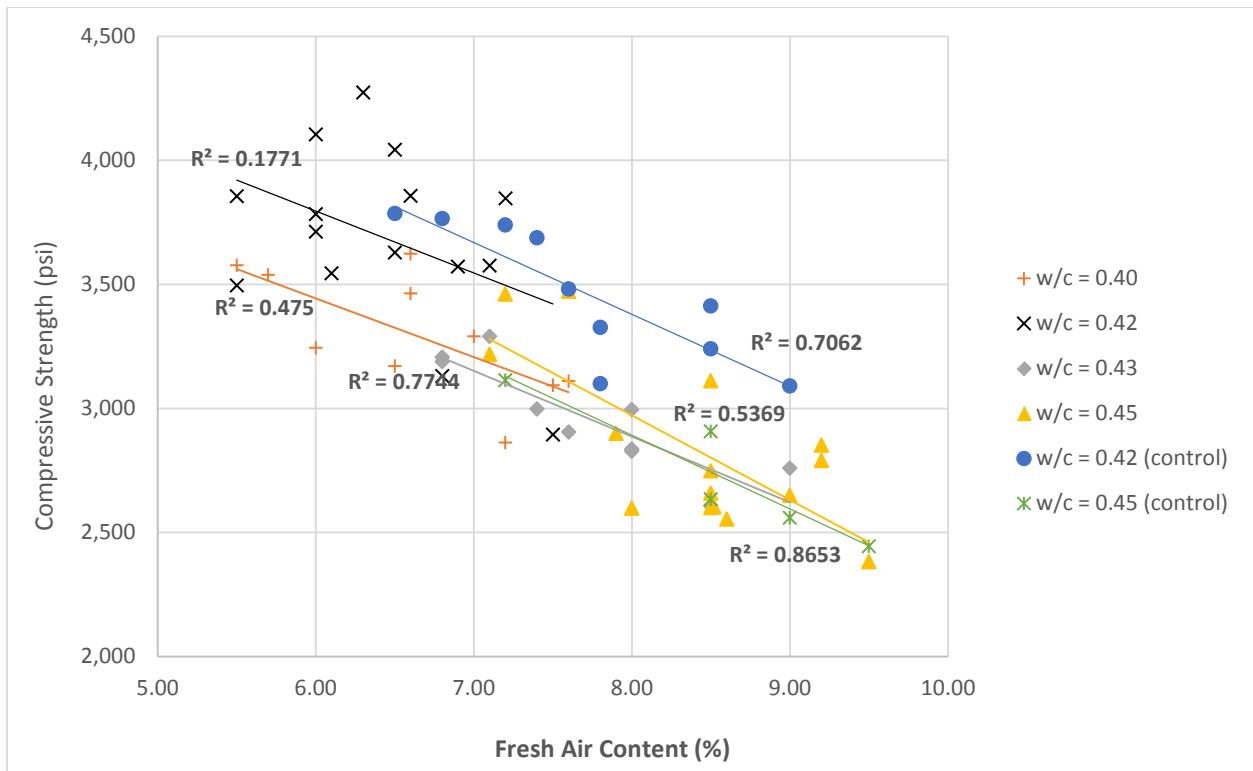


Figure 7.12: Fresh Air Content vs Compressive Strength at 7 Days

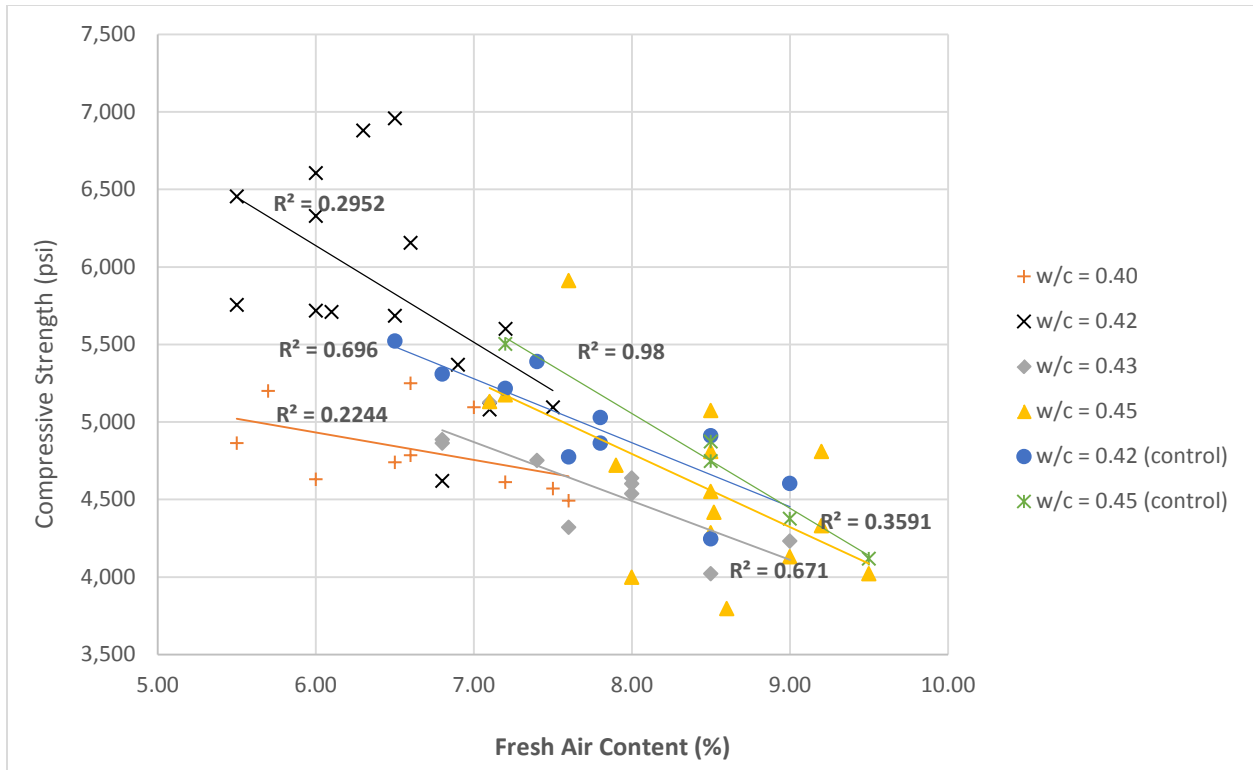


Figure 7.13: Fresh Air Content vs Compressive Strength at 28 Days

7.2 Aggregate Type

Absolute difference in slump between retempered and non-retempered mixes is presented in Figure 7.14. Granite shows the highest average increase. This is not very surprising since granite had the largest maximum size particles among the tested aggregate types and it is well known that increase in aggregate size generally results in slump increase. Additionally, the low porosity and different microtexture of the aggregates contributed to differences in slump increase.

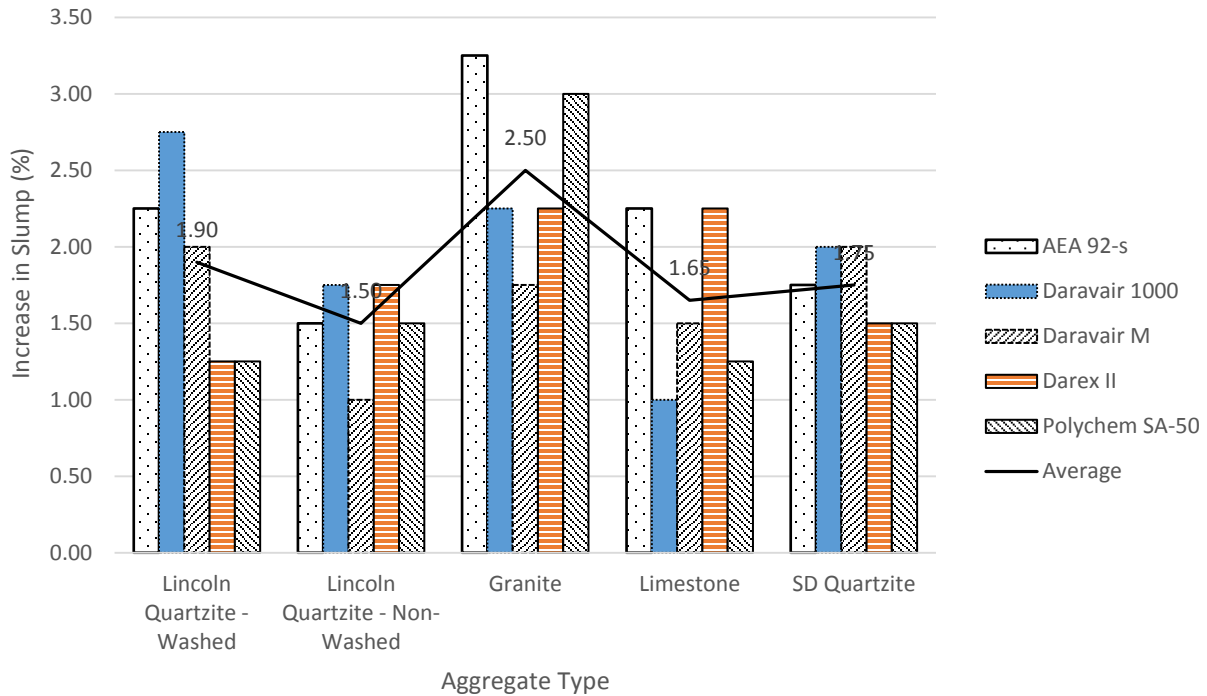


Figure 7.14: Slump Change After Retempering

The difference in the total air content before and after retempering with respect to the type of aggregate used is shown in Figure 7.15. Results show that increases in total air content for mixes containing Lincoln quartzite and limestone were rather similar—on average 18%, 16%, and 20% for non-washed quartzite, washed quartzite, and limestone, respectively. However, mixes utilizing granite and SD quartzite saw average increases in fresh air content of 41% and 33%, respectively. It is possible that the less porous SD quartzite and granite aggregates absorbed less AEA, giving a larger increase in air after retempering.

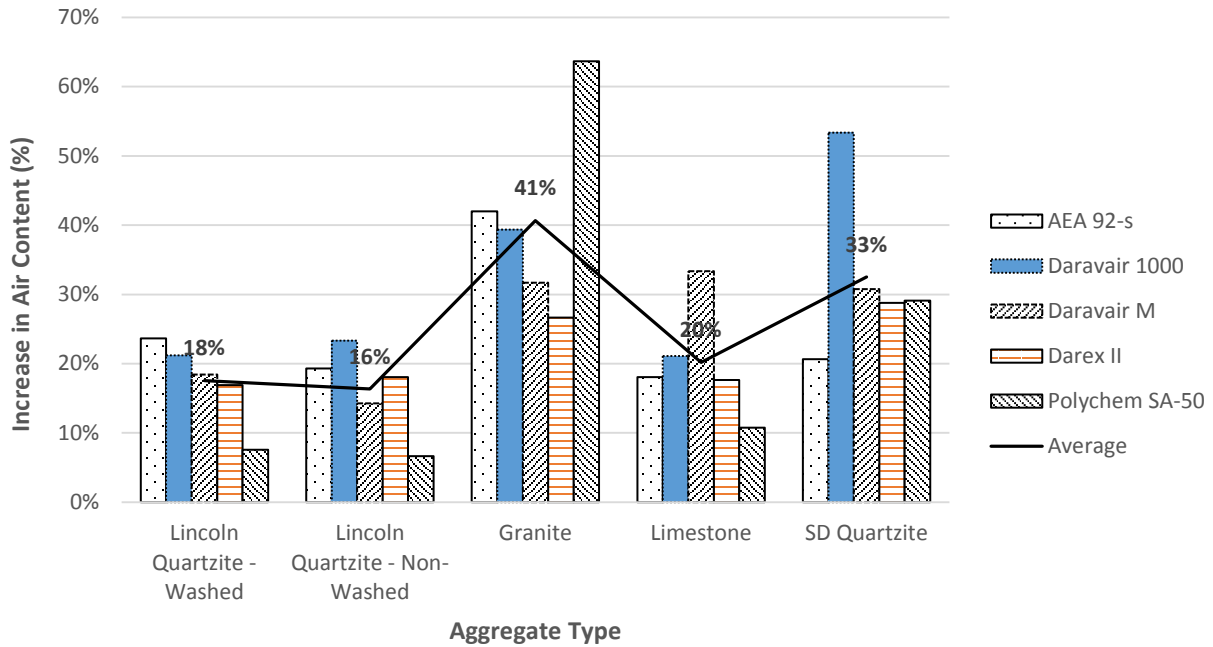


Figure 7.15: Increase in Air Content after Retempering by Aggregate Type

Clustering indexes based on aggregate type are presented in Figure 7.16 through Figure 7.20. In the case of Lincoln quartzite, 12 out of 15 mixes showed higher clustering index for non-washed aggregate. However, this difference was in average only 0.3, thus it is not possible to draw any strong conclusion, although results could suggest that the dirty aggregate is more prone to air void clustering. No other particular relationship between clustering and aggregate type was observed. This indicates that the aggregate itself has very little or no effect on formation of air void clusters around its particles.

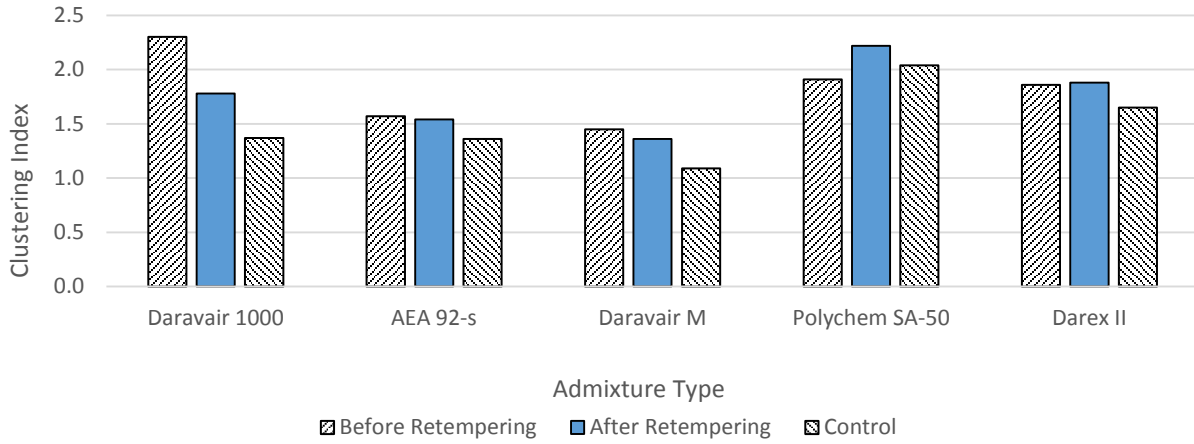


Figure 7.16: Clustering Index – Non-Washed Lincoln Quartzite

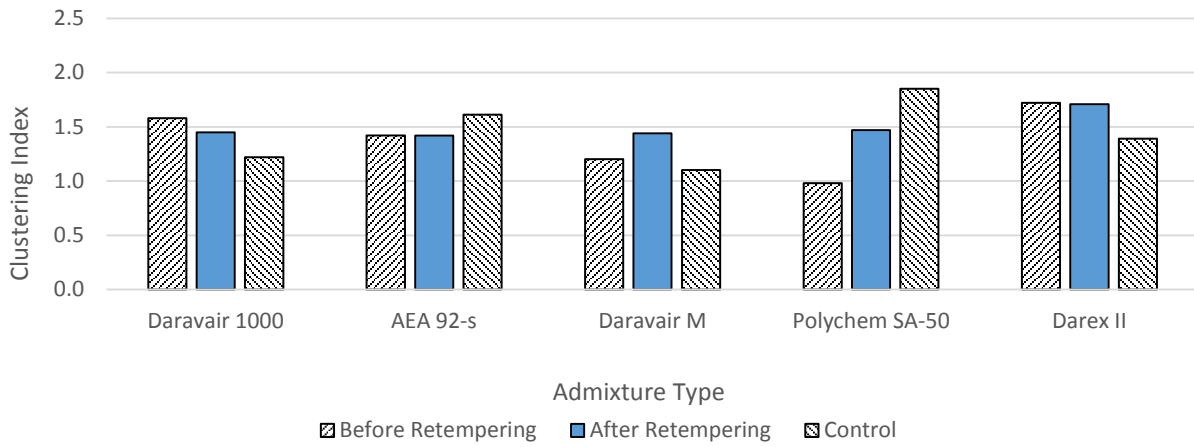


Figure 7.17: Clustering Index – Washed Lincoln Quartzite

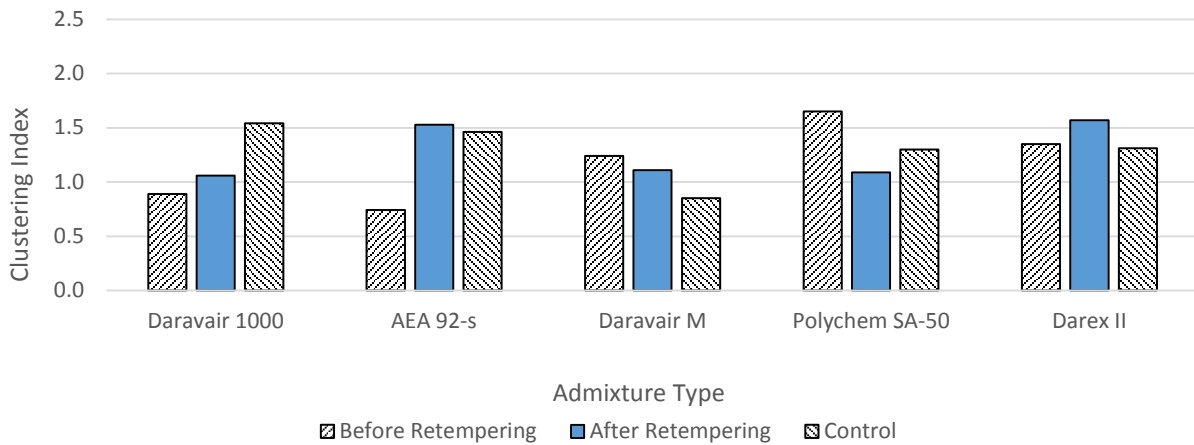


Figure 7.18: Clustering Index – Granite

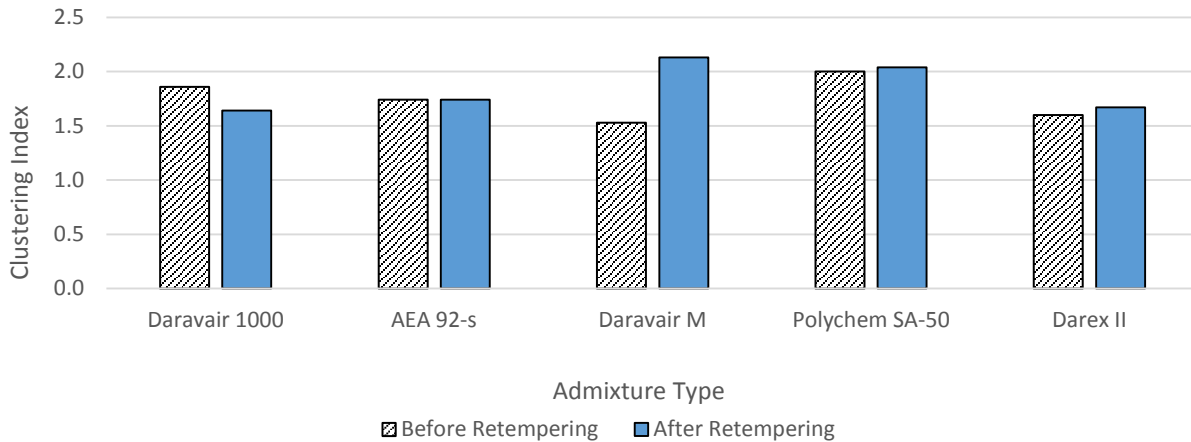


Figure 7.19: Clustering Index – Limestone

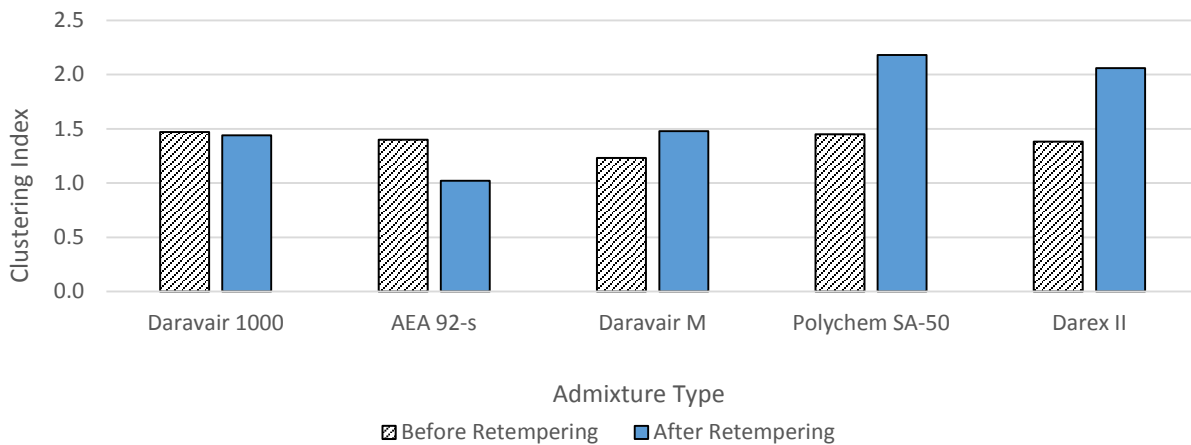


Figure 7.20: Clustering Index – SD Quartzite

Plots of changes in compressive strengths versus clustering indexes based on aggregate type are shown in Figure 7.21 through Figure 7.25. The highest R^2 value recorded was for values of compressive strength at 7 days for the non-washed Lincoln quartzite (0.75). However, such a high correlation was only observed in this case, and the other 9 sets of data do not indicate any significant relationship between clustering index and compressive strength values. This finding is in accordance with the observation made in Section 7.1 Retempering, namely that air void clustering has no effect on compressive strength. The effect the aggregate type has on the clustering rate and subsequently on the compressive strength seems to be alike.

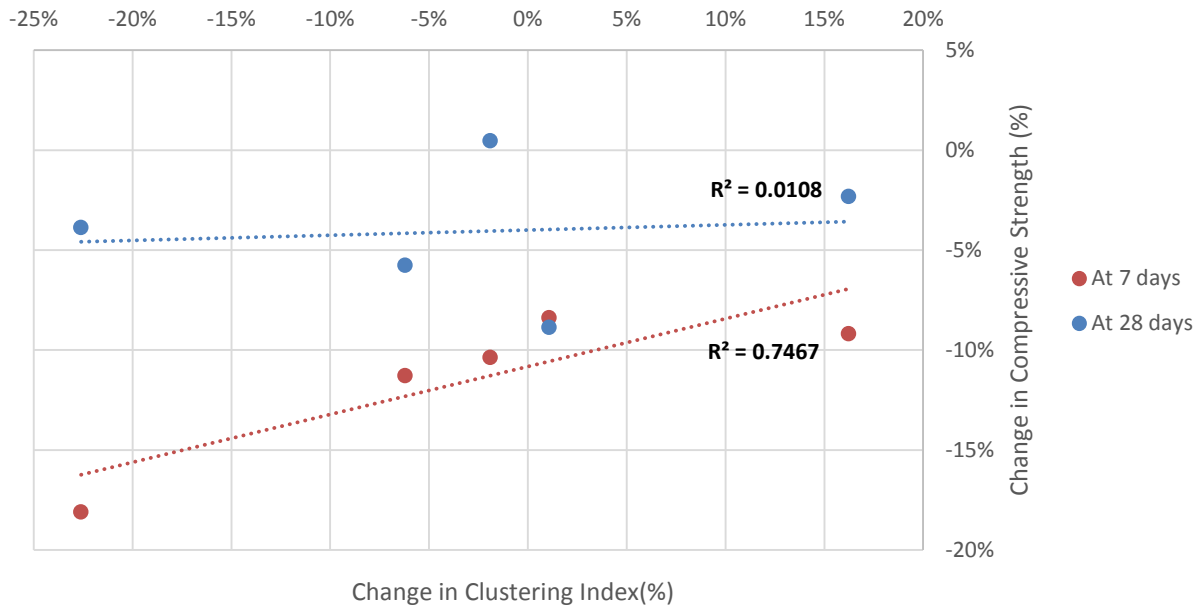


Figure 7.21: Clustering Index vs Compressive Strength – Non-Washed Lincoln Quartzite

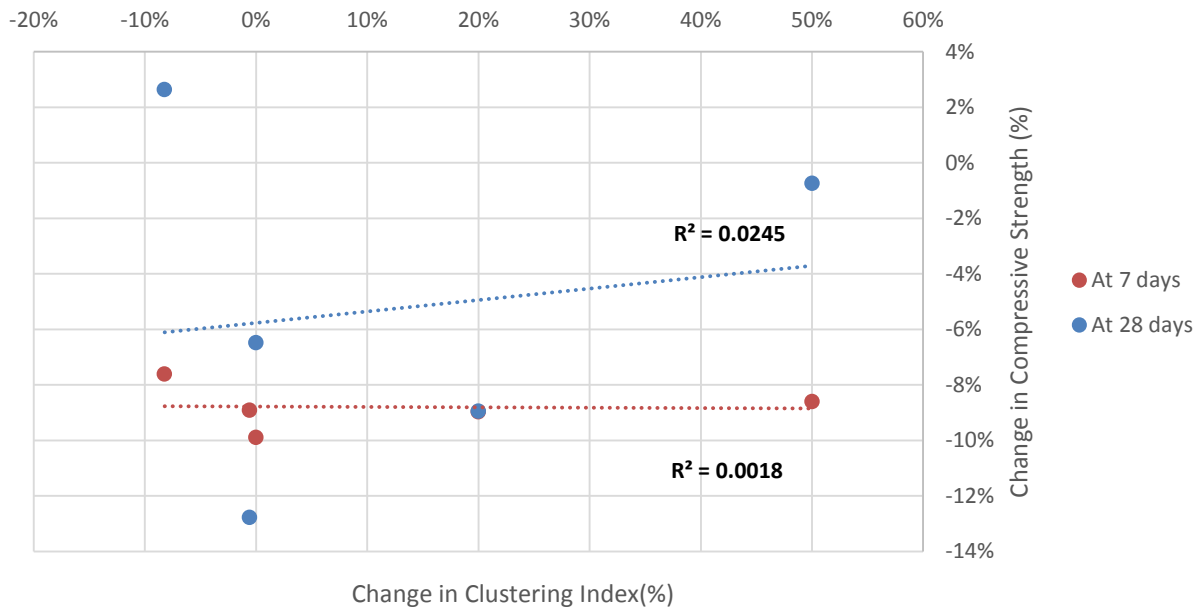


Figure 7.22: Clustering Index vs Compressive Strength – Washed Lincoln Quartzite

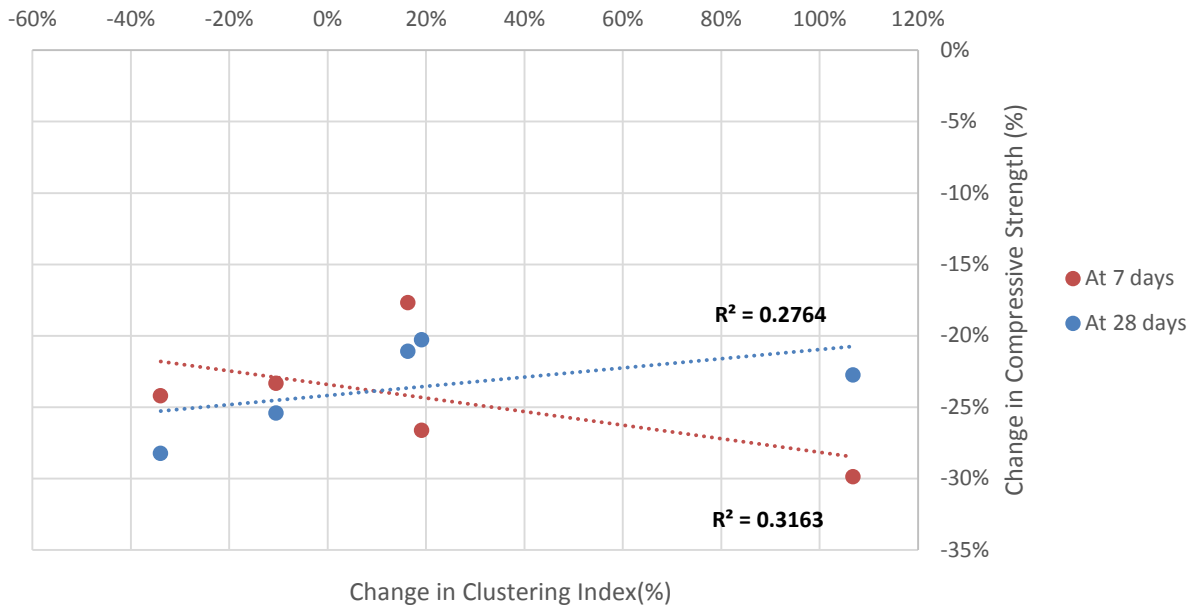


Figure 7.23: Clustering Index vs Compressive Strength – Granite

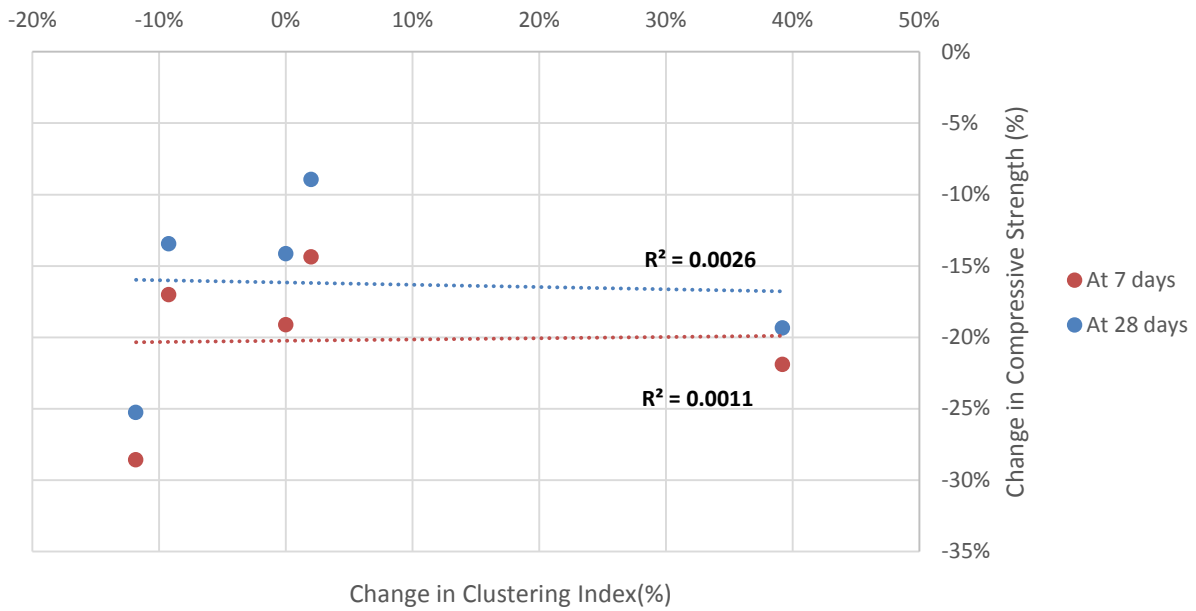


Figure 7.24: Clustering Index vs Compressive Strength – Limestone

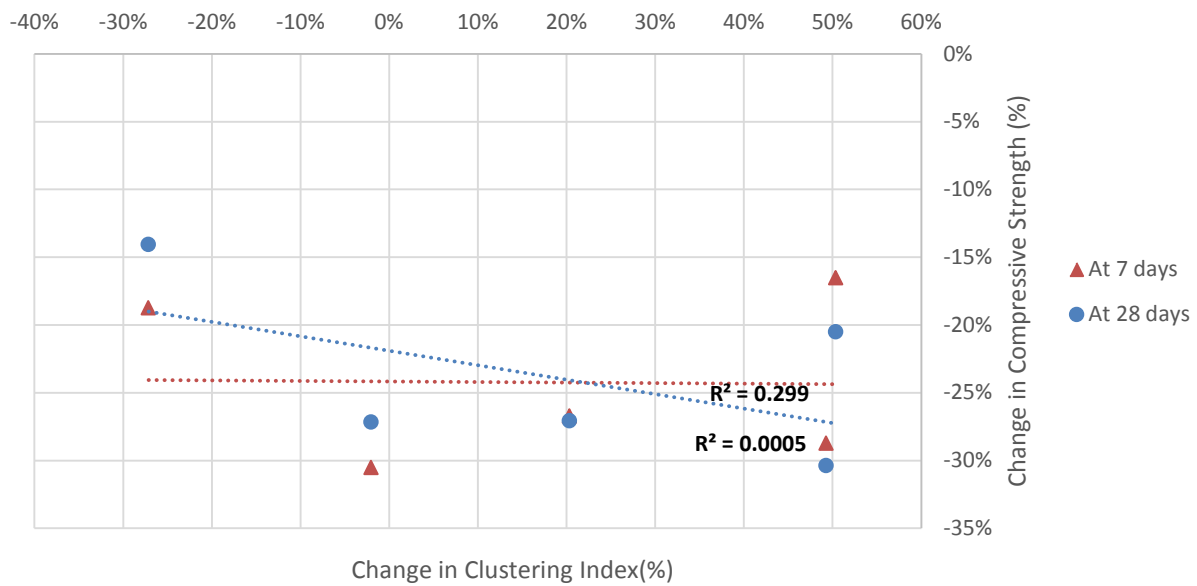


Figure 7.25: Clustering Index vs Compressive Strength – SD Quartzite

Concern with the performance of dirty Lincoln quartzite was expressed by KDOT in the past and was one of the reasons why this study was conducted. Particularly, compressive strength samples from a pavement project in Kansas, which utilized non-washed Lincoln quartzite, failed to meet the compressive strength requirements prescribed by KDOT. Several interesting observations regarding the behavior of washed and non-washed aggregate were made:

A lower dosage of AEA in mixes with washed aggregate was typically required to achieve the same air content as for the mixtures containing dirty rock, as shown in Figure 7.24. This was expected, as the dirty aggregate contains more fine particles and clay than washed rock, thus its specific surface is higher and potential for absorption by clay particles requires a higher dosage of an AEA to achieve the same total air content.

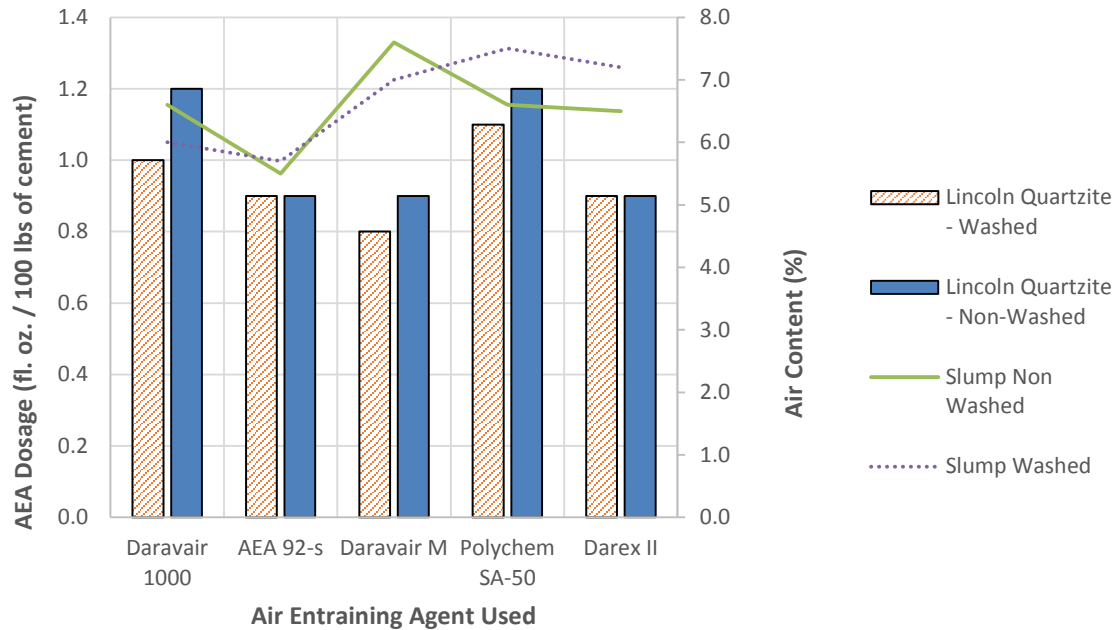


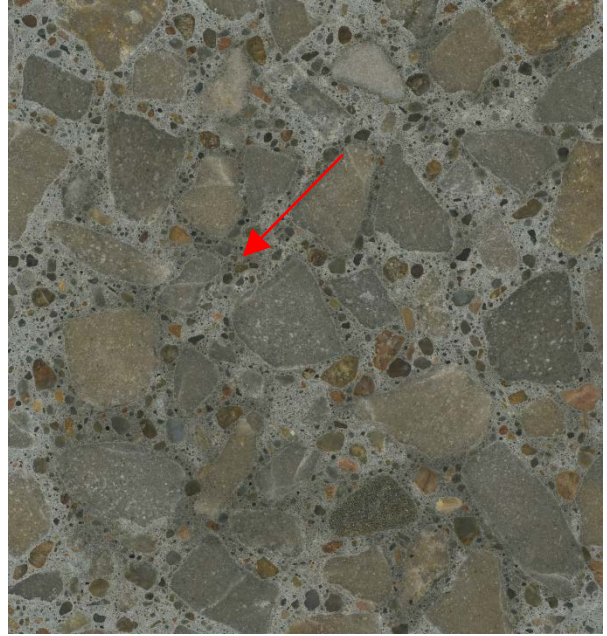
Figure 7.26: AEA Dosage vs Air Content – Lincoln Quartzite

As discussed in the Section 7.1 Retempering, mixes with Lincoln quartzite experienced a lower increase in slump and air content after rettempering than mixes containing the other types of coarse aggregate. This fact suggests that in order to restore the required workability of concrete with Lincoln quartzite in the field utilizing the rettempering technique, a considerably higher amount of additional water would be needed. Therefore, the loss of compressive strength due to increased water to cement ratio could be higher as well.

Dark regions of higher cement paste density were observed in various mixes with Lincoln quartzite. Those regions, typical for rettempered concrete, are areas of higher cement content and thus a lower water-to-cement ratio. If hydrated properly, these areas can be very strong. However, if dry cement particles are captured within those regions, their compressive strength will be very low and the area will form a zone of weakness (Walker et al., 2006). Examples of these zones observed in mixes with Lincoln quartzite are presented in Figure 7.27 and their occurrence in particular mixes is summarized in Table 7.2.



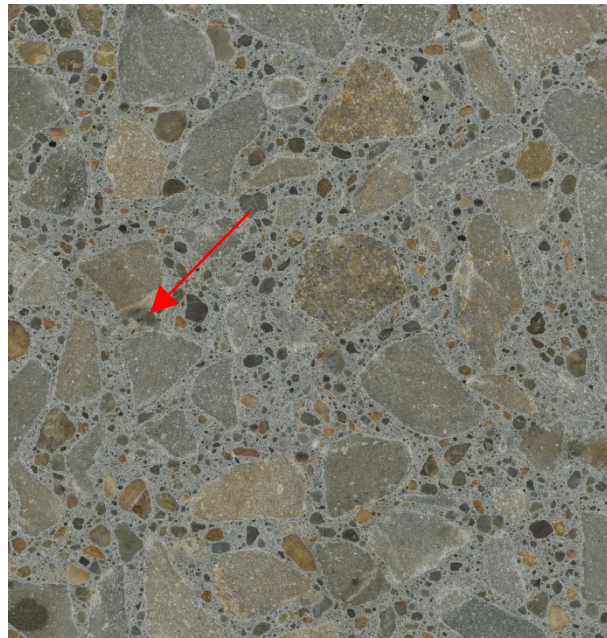
(a)



(b)



(c)



(d)

Figure 7.27: Higher Density Zones

(a) 1-II-R; (b) 2-II-R; (c) 1-III-R; (d) 1-I-C

Table 7.2: High Density Zones in Lincoln Quartzite

Mix ID	High Density Zone	Mix ID	High Density Zone	Mix ID	High Density Zone
Before Retempering		After Retempering		Control	
1-I	Y	1-I-R	Y	1-I-C	N
1-II	N	1-II-R	N	1-II-C	Y
1-III	N	1-III-R	Y	1-III-C	N
1-IV	N	1-IV-R	Y	1-IV-C	N
1-V	N	1-V-R	N	1-V-C	Y
2-I	Y	2-I-R	Y	2-I-C	Y
2-II	Y	2-II-R	Y	2-II-C	Y
2-III	Y	2-III-R	N	2-III-C	Y
2-IV	Y	2-IV-R	Y	2-IV-C	Y
2-V	Y	2-V-R	N	2-V-C	Y

Note that high density zones were present in all non-retempered mixes with washed Lincoln quartzite. This is very unusual, as those zones are typically seen in retempered concrete and it suggests that Lincoln quartzite as an aggregate can be generally susceptible to issues related with improper mixing. Although high density regions were observed in all control mixes with washed Lincoln quartzite as well, their severity (based on visual observation) was significantly lower. This could provide explanation for the unusual results of compressive strengths of the control mixes. One would expect the compressive strength of control mixes to be lower than values of mixes before retempering, as control mixes were produced with a higher water-to-cement ratio. However, some of the measured values showed the opposite trend, which indicates that observed dark paste in non-retempered mixes would be those with higher amounts of non-hydrated cement particles. This could result in lower compressive strength of those mixes and, despite the fact that those zones were presented in control mixes as well, their contribution to the compressive strength of control mixes was most likely insignificant due to their lower intensity.

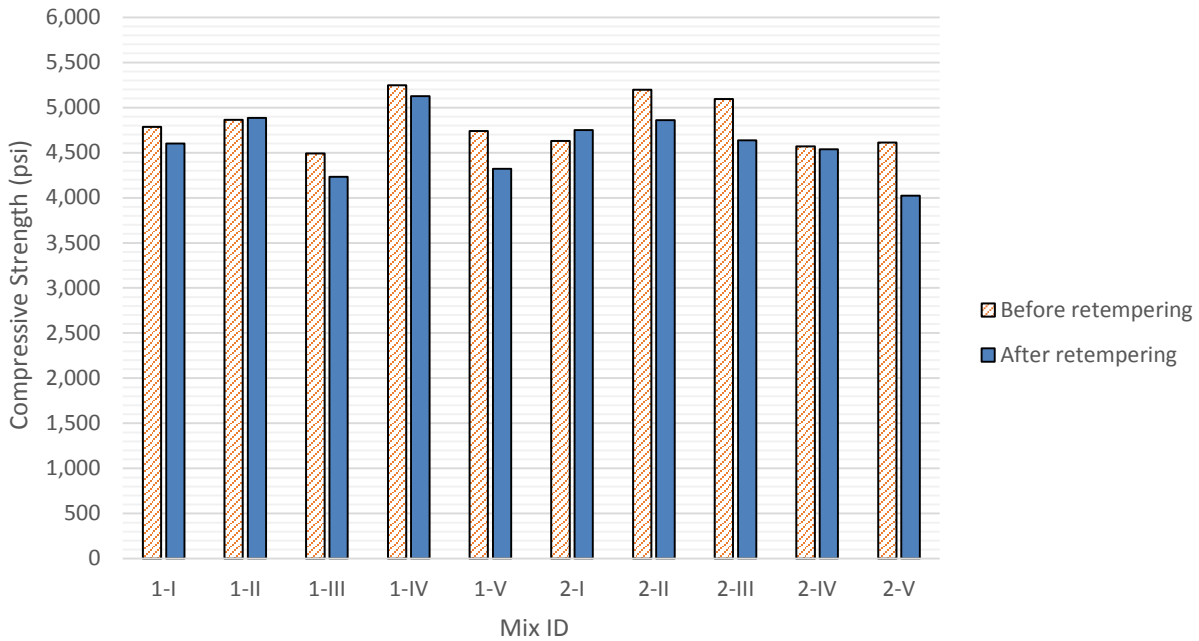


Figure 7.28: Compressive Strength – Lincoln Quartzite

Presence of low strength zones and lower dosages of AEA required to achieve similar fresh concrete properties for clean aggregate could provide explanation for the low compressive strength issues experienced by KDOT. First, if the dirty aggregate is used in concrete, it is very likely that locally some of the aggregate will be cleaner than the rest of the material (for example, if stored outdoors, rain can easily wash the upper layer of the aggregate pile). Certain portions of the batch containing this cleaner aggregate can then experience higher air content, hence lower compressive strength might occur.

At the same time, those “clean zones” can also experience issues related to the improper mixing of cement and water, so not only regions with higher air content, but also regions of higher cement content can be formed. Those two factors combined together could lead to the values of low compressive strengths.

7.3 Type of Air Entraining Agent

Figure 7.29 and Figure 7.30 show increase in slump and air content after retempering with respect to the air entraining agent used. It is evident that all mixes using an AEA performed rather similarly, as the average increase in slump varied from 1.6 to 2.1 inches and the average increase in the fresh air content after retempering ranged from 20-30%. Presented data suggests that the efficiency of retempering is more dependent on the type of used aggregate (as discussed in the Section 7.2 Aggregate Type), rather than on the chemical composition of AEA.

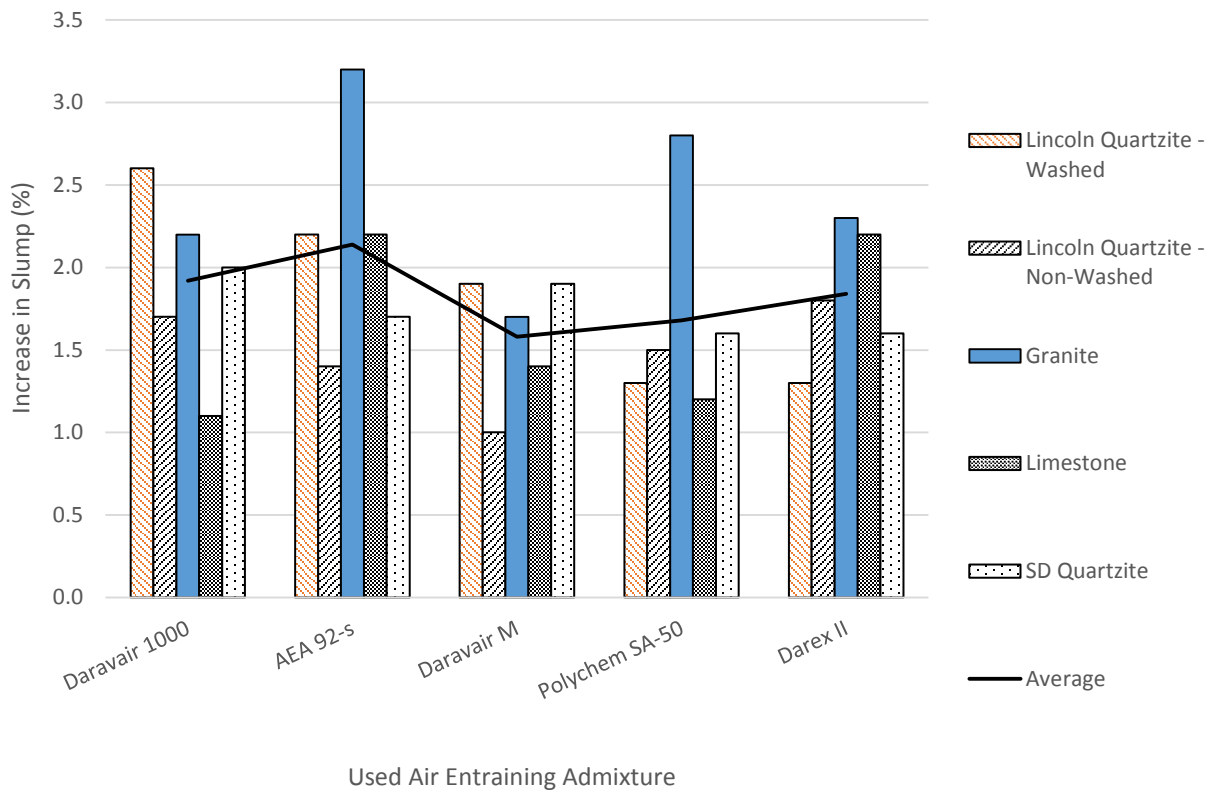


Figure 7.29: Increase in Slump After Retempering by Used AEA

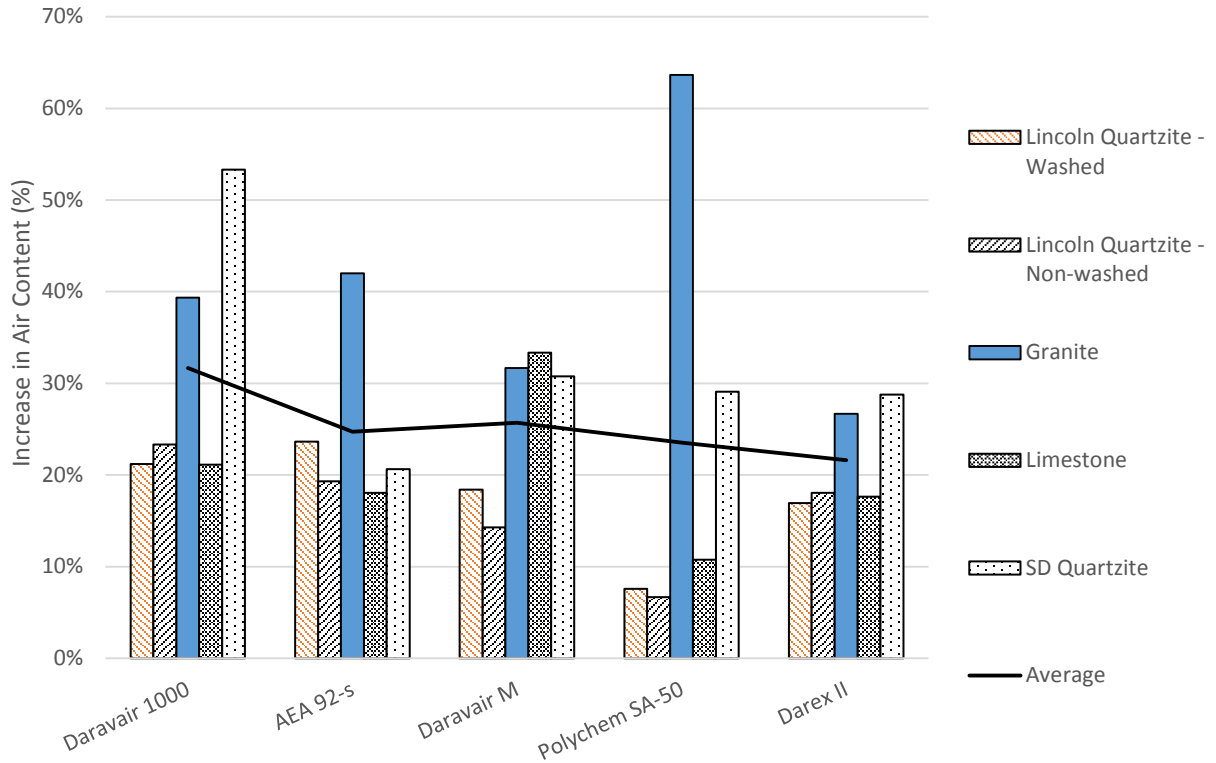


Figure 7.30: Increase in Air Content After Retempering by Used AEA

As shown in Figure 7.31 through Figure 7.35, the change in the clustering index before and after retempering was not typically affected by the type of air entraining admixture, as both an increase and a decrease were observed for different types of AEA. Polychem SA-50 showed the highest average values of the clustering index (Figure 7.36); however, the difference with respect to the other AEAs was very small. Thus, it is evident that the type of AEA that is used to generate the air void system did not have a statistically significant effect on the clustering rate. This finding is quite surprising since the synthetic (non-vinsol resin) air entraining agents were often blamed for air void clustering in retempered mixes. AEA-92S (Euclid Chemical) was chosen as a representative of the non-organic group of AEAs in this study. Contrary to the popular belief, this admixture performed rather well as, in 4 out of 5 cases, the overall clustering index remained the same or decreased after retempering. In fact, only Daravair 1000 showed similar results, and no other admixture performed better than this synthetic AEA.

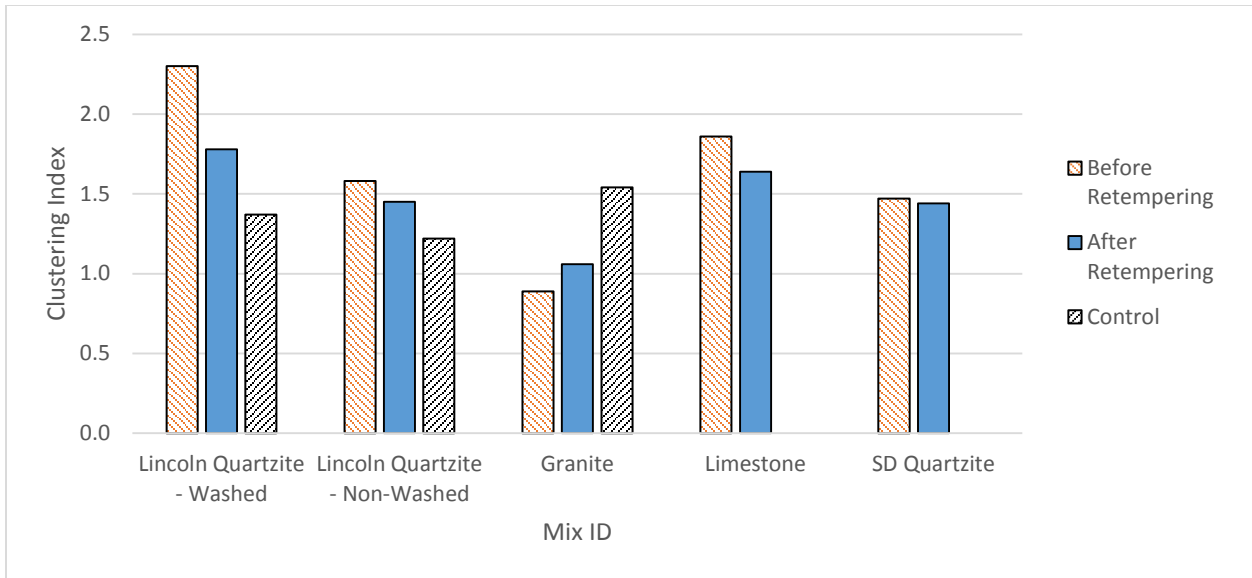


Figure 7.31: Clustering Index – Daravair 1000

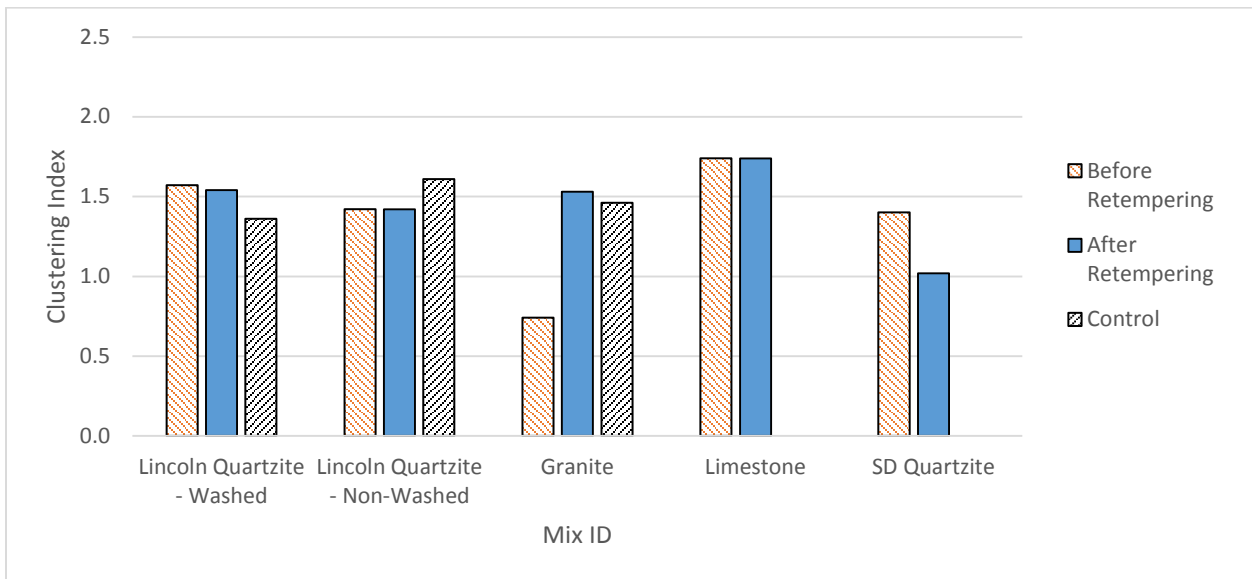


Figure 7.32: Clustering Index – AEA-92S

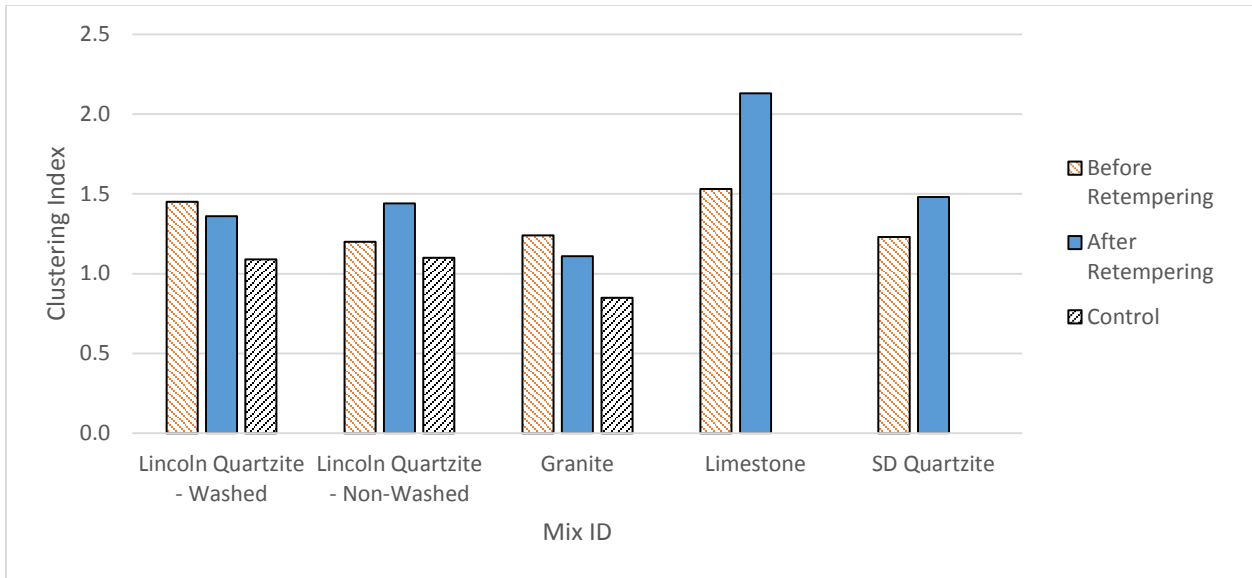


Figure 7.33: Clustering Index – Daravair M

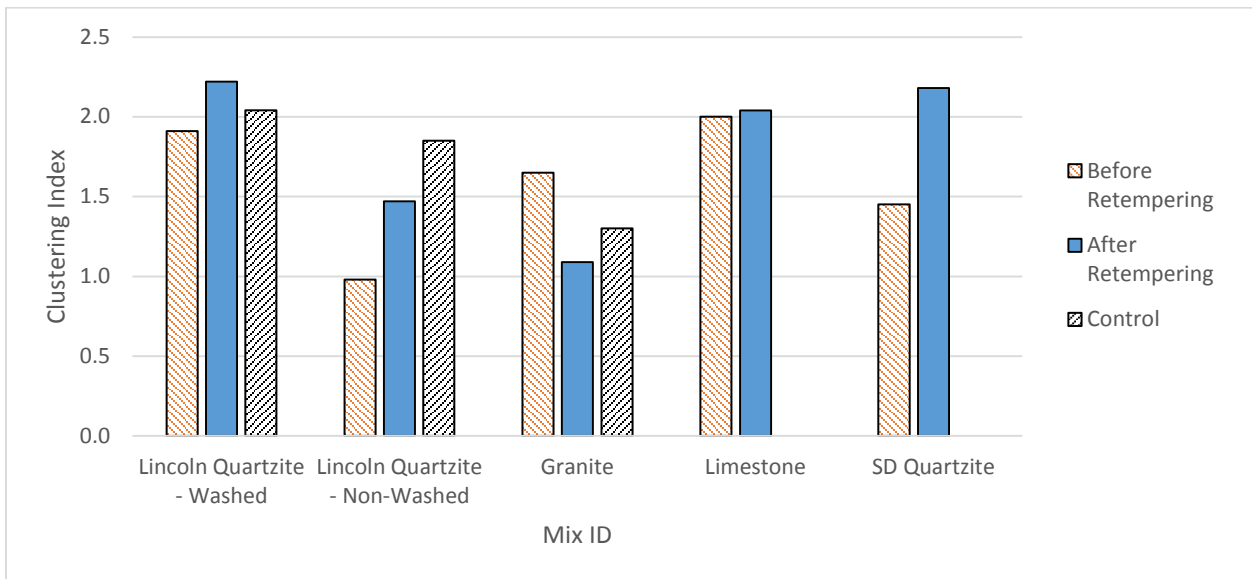


Figure 7.34: Clustering Index – Polychem SA-50

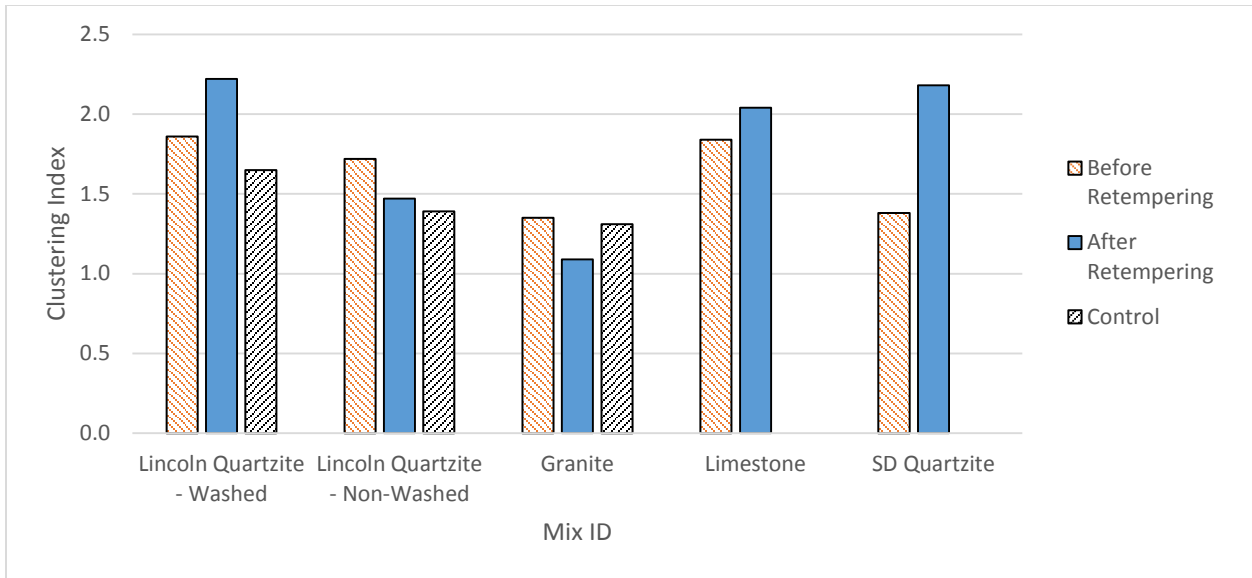


Figure 7.35: Clustering Index – Darex II

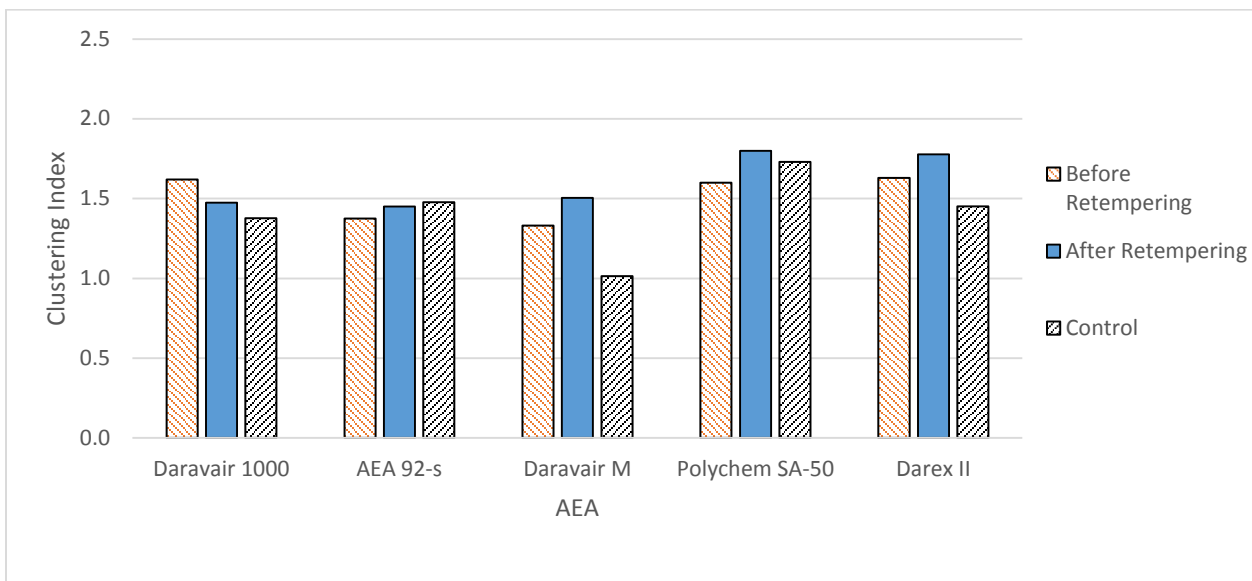


Figure 7.36: Clustering Index – Average by AEA

The relationship between change in the compressive strength at 28 days and change in the clustering index by the type of air entraining admixture used is presented in Figure 7.37 through Figure 7.41. A trend was observed for Darex II as the R^2 value was found to be 0.824, which could indicate there is a strong correlation between clustering and compressive strength for this particular admixture. When the change in compressive strength vs. change in fresh air content was plotted, a stronger correlation was seen than for clustering, however. It seems likely that the change in strength may be more related to the change in air content than clustering in this case. However, since only five data points were available for the regression analysis, definitive conclusions for this admixture are not possible.

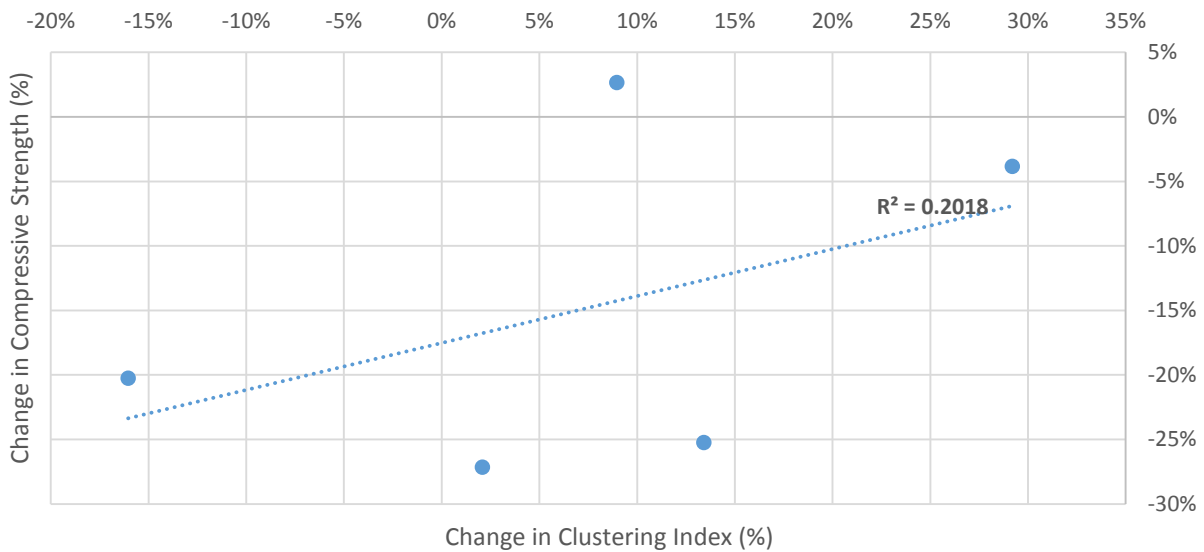


Figure 7.37: Compressive Strength vs Change in Clustering Index – Daravair 1000

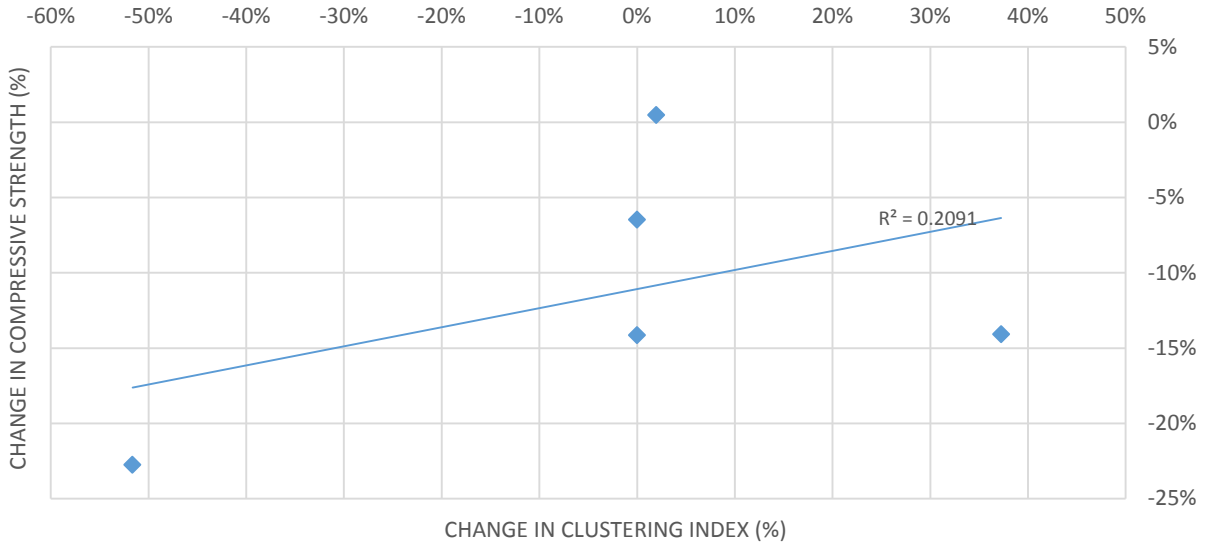


Figure 7.38: Compressive Strength vs Change in Clustering Index – AEA-92S

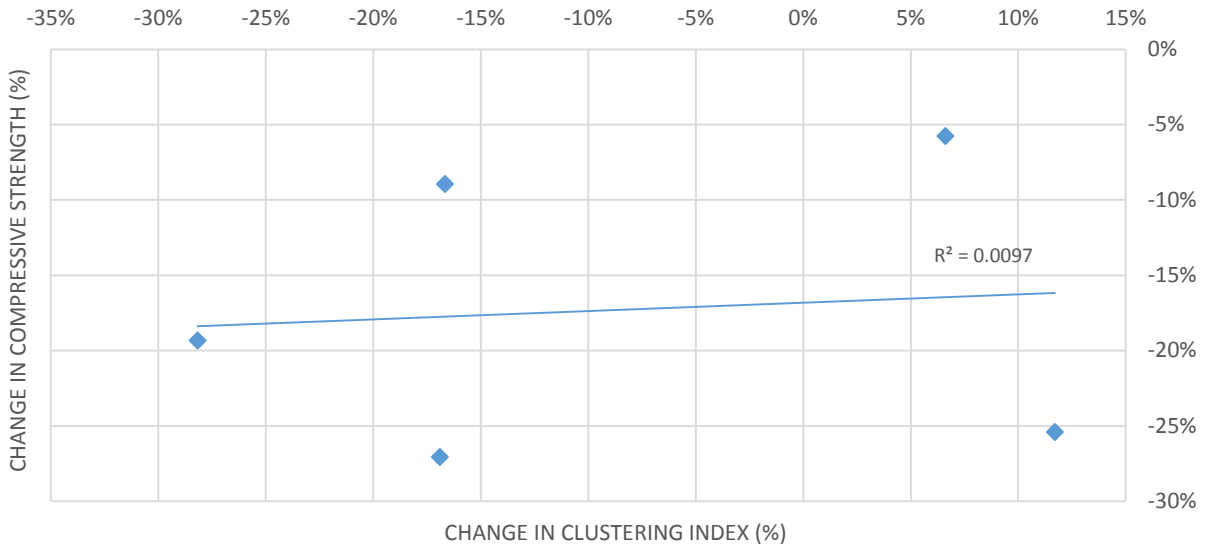


Figure 7.39: Compressive Strength vs Change in Clustering Index – Daravair M

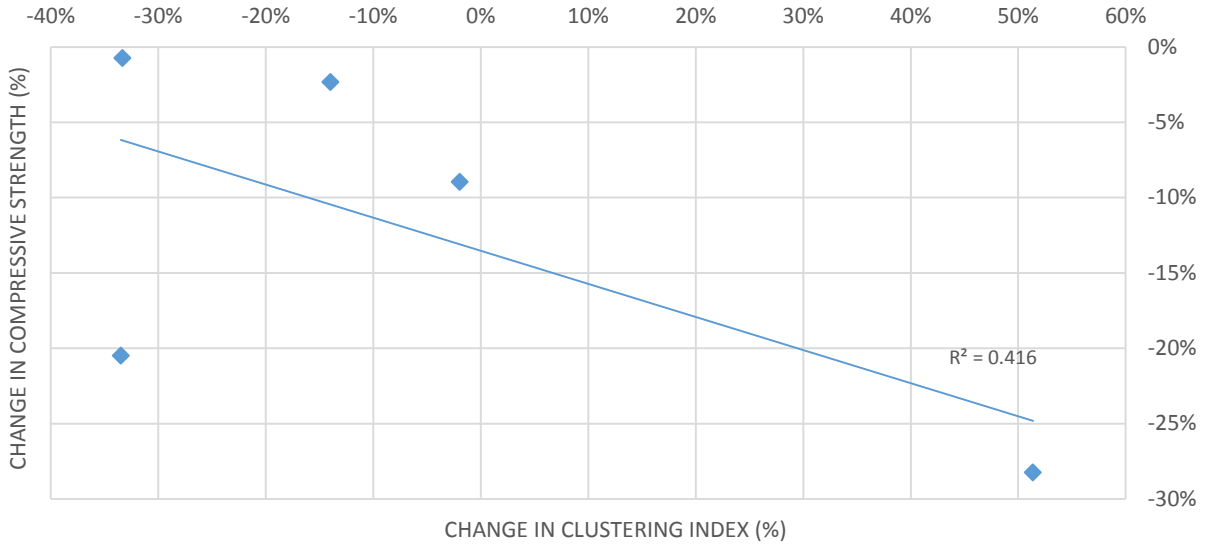


Figure 7.40: Compressive Strength vs Change in Clustering Index – Polychem SA-50



Figure 7.41: Compressive Strength vs Change in Clustering Index – Darex II

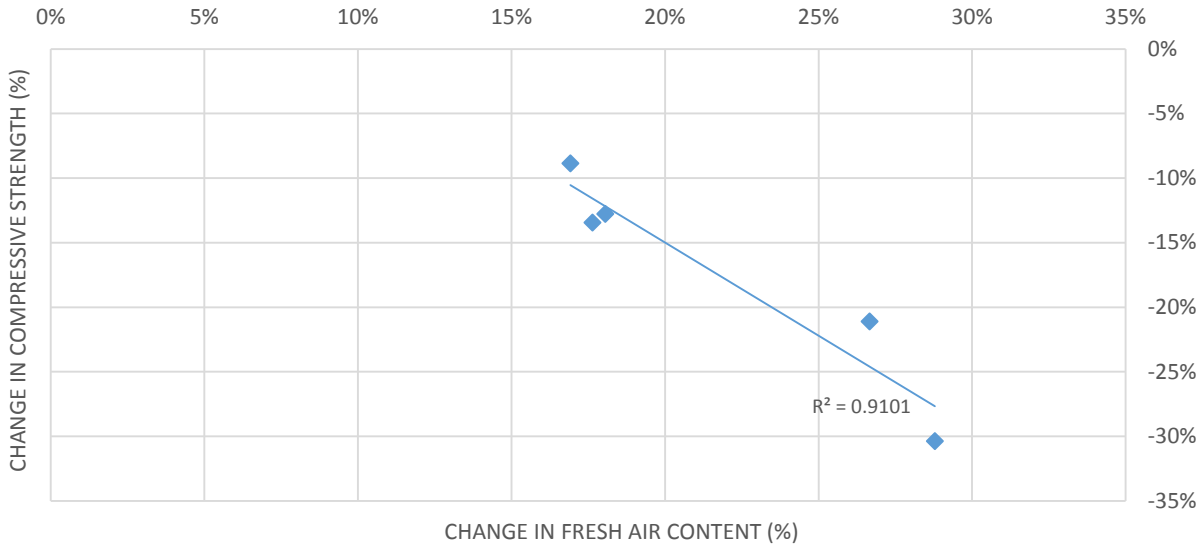


Figure 7.42: Compressive Strength vs Change in Fresh Air Content – Darex II

7.4 Visual Rating of Air Void Clustering

In addition to the clustering analysis using the image processing techniques, visual evaluation following the procedure developed by Kozikowski et al. (2005) was carried out, as shown in Figure 7.43. While there was agreement in the extent of clustering between the automated and manual methods, they did not agree 100% of the time. The results of the manual evaluation followed, in most of the cases, the expected trend of a higher clustering rate in retempered concrete. However, the evaluation has been assembled based on a visual investigation with a reference frame that has not been defined, thus it was found that the manual analysis is rather subjective. Furthermore, it is more likely that for systems with higher air contents, a human operator might tend to overrate the level of clustering present due to increased presence of air voids in cement paste. As all retempered samples but one had a higher total air content than samples taken before retempering, this observation would help explain the differences in the two performed analyses.

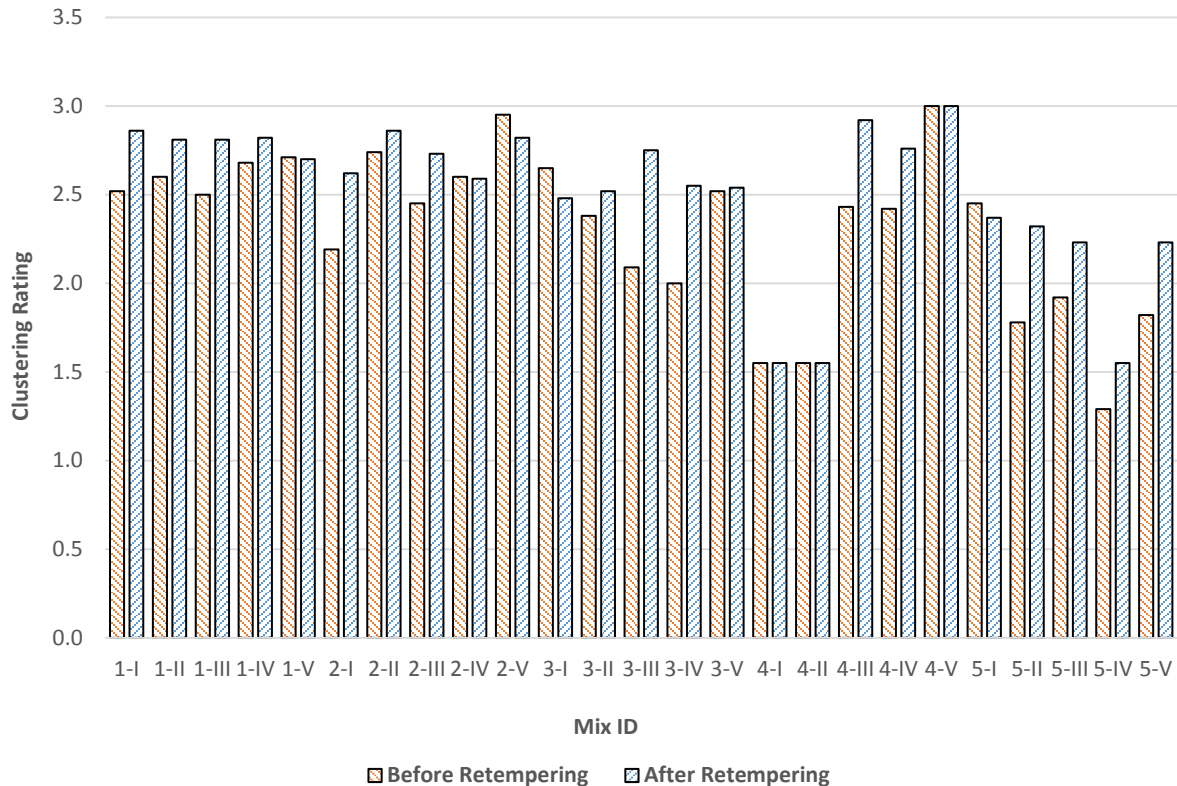


Figure 7.43: Visual Clustering Evaluation

7.5 Field Testing

Results obtained from the field testing correspond to what was found in the laboratory environment. Increases in fresh concrete properties (slump, air content) in mixes after retempering occurred in both cases. Samples obtained from Site I, where concrete was retempered with only 1 gallon of mixing water per cubic yard of concrete, experienced smaller changes than samples from Site II. The hardened air void content followed a similar pattern, as a very small change in the air content (7.99% vs 8.04%) was observed in mixes from Site I. For Site II, the hardened air void content was 7.01% before retempering and 8.26% after additional water was added.

As for the clustering activity, retempering in both cases did not cause any significant increase in the clustering index. Again, the change in the clustering rate before and after water addition was higher for samples from Site II; however, it was still insignificant (change from

0.87 to 1.06) as shown in Figure 6.24 and Figure 6.25. MasterAir AE 90 (formerly MB-AE 90) air entraining admixture was used. Although this admixture is rosin-based (organic), the manufacturer warns regarding the possibility of air void clustering in the product information sheet, as some clustering concerns were raised in the past (Kozikowski et al., 2005). However, those concerns were not found to be justified for mixes used in this study.

Compressive strength at 7 days decreased by 11% in the retempered samples from both locations, and by 11% and 14% at 28 days for the Site I and Site II samples, respectively. These values are in the range that were observed in the laboratory study and occurred because of the increase in the w/c ratio and retempering, not air void clustering. It is interesting to see an almost uniform strength drop, although the amount of retempering water was different for Site I and Site II. However, caution should be exercised in drawing conclusions too strongly from this because of the small sample size (two field sites).

Chapter 8: Conclusions and Recommendations

8.1 Conclusions

Based on the results of the laboratory study presented and discussed in the previous sections, the following conclusions have been made:

- Air void clustering is reproducible in the laboratory environment, as it was observed in several mixes. The highest value of the clustering index was 2.3 and 2.2 for mixes before and after retempering, respectively.
- A correlation between the air void clustering and compressive strength was not found. Instead, the loss in compressive strength after retempering seems to be simply a function of the air void content and the water-to-cement ratio.
- Air void clustering was not significantly affected by retempering. Ten out of 25 mixes experience a decrease in clustering activity after retempering, and only a small increase was observed in the remaining 15 mixes.
- Granite and SD quartzite showed a higher increase in both slump and air content after retempering than the other aggregates. Lincoln quartzite, on the other hand, experienced a lower increase in slump and air content after retempering than mixes containing the other types of coarse aggregate. This fact suggests that in order to restore the required workability of concrete with Lincoln quartzite in the field utilizing the retempering technique, a considerably higher amount of additional water would be needed. Therefore, the loss of compressive strength due to increased water to cement ratio could be higher as well.
- High density zones of cement paste were observed in mixes with Lincoln quartzite, especially mixes that utilized the washed aggregate. Presence of those zones could explain low compressive strengths experienced in some projects where Lincoln quartzite was used.
- A lower dosage of AEA was found to be required for clean Lincoln quartzite to achieve the same level of workability as the non-washed aggregate.

- The hypothesis that retempering of concrete with a non-organic air entraining admixture will cause air void clustering was not confirmed. In fact, AEA-92S, a synthetic air entraining agent used in the study, showed one of the best performances of all the AEAs used, as 4 out of 5 mixes with this admixture experienced a decrease or no change in the clustering index after retempering.
- The visual rating of air void clustering provided by Kozikowki et al. (2005) agreed in many but not all cases with the automated, analytical method developed and implemented as part of the KSU Air Void Analyzer software. However, it is felt that the automated method removes results bias, and it seems that air void clustering tends to be overrated in concrete systems with high air content if this method is used.
- Concrete obtained from pavement projects during placement show similar behavior to concrete prepared under laboratory conditions.

8.2 Recommendations

Lincoln quartzite showed some behavior different than other aggregates (high density paste zone, low increase in slump and air content after retempering). Retempering of concrete with Lincoln quartzite should be avoided.

8.3 Future Research Needs

The effect of temperature on the clustering of air voids is still unclear. Further research investigating this factor is needed to better understand the phenomena of air void clustering.

Fine aggregate is known to have a strong impact on the performance of air entraining agents, thus its effect on air void clustering and retempering should be scrutinized.

Further testing of Lincoln quartzite, especially with focus on the formation of high density paste zones, is needed.

References

- ASTM Standard C31 / C31M-12. (2012). *Standard practice for making and curing concrete test specimens in the field*. West Conshohocken, PA: ASTM International. DOI: 10.1520/C0031_C0031M-12, www.astm.org.
- ASTM Standard C39 / C39M-12. (2012). *Standard test method for compressive strength of cylindrical concrete specimens*. West Conshohocken, PA: ASTM International. DOI: 10.1520/C0039_C0039M-12, www.astm.org.
- ASTM Standard C127-12. (2012). *Standard test method for density, relative density (specific gravity), and absorption of coarse aggregate*. West Conshohocken, PA: ASTM International. DOI: 10.1520/C0127-12, www.astm.org.
- ASTM Standard C128-12. (2012). *Standard test method for density, relative density (specific gravity), and absorption of fine aggregate*. West Conshohocken, PA: ASTM International. DOI: 10.1520/C0128-07A, www.astm.org.
- ASTM Standard C136-06. (2006). *Standard test method for sieve analysis of fine and coarse aggregates*. West Conshohocken, PA: ASTM International. DOI: 10.1520/C0136-06, www.astm.org.
- ASTM Standard C138 / C138M-12. (2012). *Standard test method for density (unit weight), yield, and air content (gravimetric) of concrete*. West Conshohocken, PA: ASTM International. DOI: 10.1520/C0138_C0138M-12, www.astm.org.
- ASTM Standard C143 / C143M-12. (2012). *Standard test method for slump of hydraulic-cement concrete*. West Conshohocken, PA: ASTM International. DOI: 10.1520/C0143_C0143M-12, www.astm.org.
- ASTM Standard C150 / C150M-12. (2012). *Standard specification for portland cement*. West Conshohocken, PA: ASTM International. DOI: 10.1520/C0150_C0150M-12, www.astm.org.
- ASTM Standard C172 / C172M-10. (2010). *Standard practice for sampling freshly mixed concrete*. West Conshohocken, PA: ASTM International. DOI: 10.1520/C0172_C0172M-10, www.astm.org.

- ASTM Standard C173 / C173M-14. (2014). *Standard test method for air content of freshly mixed concrete by the volumetric method*. West Conshohocken, PA: ASTM International. DOI: 10.1520/C0173_C0173M, www.astm.org.
- ASTM Standard C192 / C192M-13. (2013). *Standard practice for making and curing concrete test specimens in the laboratory*. West Conshohocken, PA: ASTM International. DOI: 10.1520/C0192_C0192M, www.astm.org.
- ASTM Standard C231 / C231M-10. (2010). *Standard test method for air content of freshly mixed concrete by the pressure method*. West Conshohocken, PA: ASTM International. DOI: 10.1520/C0231_C0231M-10, www.astm.org.
- ASTM Standard C457 / C457M-12. (2012). *Standard test method for microscopical determination of parameters of the air-void system in hardened concrete*. West Conshohocken, PA: ASTM International. DOI: 10.1520/C0457_C0457M-12, www.astm.org.
- ASTM Standard C1231 / C1231M-14. (2014). *Standard practice for use of unbonded caps in determination of compressive strength of hardened concrete cylinders*. West Conshohocken, PA: ASTM International. DOI: 10.1520/C1231_C1231M-14, www.astm.org.
- Chatterji, S. (2003). Freezing of air-entrained cement-based materials and specific actions of air-entraining agents. *Cement and Concrete Composites*, 25(7), 759-765.
- Cross, W., Duke, E., Kellar, J., & Johnston, D. (2000). *Investigation of low compressive strengths of concrete paving, precast and structural concrete* (Report No. SD98-03-F). Pierre, SD: South Dakota Department of Transportation.
- Distlehorst, J. (2009). *Evaluation of air-void clustering in concrete pavement from Meade, Kansas* (Internal Report). Topeka, KS: Kansas Department of Transportation.
- Du, L., & Folliard, K. J. (2005). Mechanisms of air entrainment in concrete. *Cement and Concrete Research*, 35(8) 1463-1471.
- Garboczi, E. J., Bentz, D. P., Snyder, K. A., Martys, N. S., Stutzman, P. E., Ferraris, C. F., & Bullard, J. W. (2014). *An electronic monograph: Modeling and measuring the structure and properties of cement-based materials*. Gaithersburg, MD: Materials and Structural

- Systems Division, National Institute of Standards and Technology. Retrieved from <http://ciks.cbt.nist.gov/~garbocz/>.
- Kansas Department of Transportation. (2007). *Standard specifications for state road and bridge construction*. Topeka, KS: Kansas Department of Transportation.
- Kansas Department of Transportation. (2014). *List of non-reactive siliceous aggregate sources for concrete* (Revised 04/25/14). Retrieved from <http://ksdot1.ksdot.org/burmatres/pql/default.asp>.
- Kosmatka, S. H., Kerkhoff, B., & Panarese, W. C. (2003). *Design and control of concrete mixtures* (14th ed.). Skokie, IL: Portland Cement Association.
- Kozikowski, R. L., Jr., Vollmer, D.B., Taylor, P.C., and Gebler, S.H. (2005). *Factors affecting the origin of air-void clustering* (PCA R&D Serial No. 2789). Skokie, IL: Portland Cement Association.
- Ley, M. T. (2007). *The effects of fly ash on the ability to entrain and stabilize air in concrete* (Doctoral dissertation). The University of Texas at Austin, Austin, TX.
- Litvan, G. (1973). Frost action in cement paste. *Materials and Structures*, 6(4), 293-298.
- Naranjo, A. (2007). *Clustering of air voids around aggregates in air entrained concrete* (Master's thesis). The University of Texas at Austin, Austin, TX.
- Peterson, K. (2008). *Automated air-void system characterization of hardened concrete: helping computers to count air-voids like people count air-voids – Methods for flatbed scanner calibration* (Doctoral dissertation). Michigan Technological University, Houghton, MI.
- Pigeon, M., & Pleau, R. (1995). *Durability of concrete in cold climates*. London: E. & F.N. Spon.
- Pomeroy, D. (1987). Concrete durability: From basic research to practical reality. *American Concrete Institute Special Publication*, 100, 111-130.
- Powers, T. C., & Helmuth, R. A. (1953). Theory of volume changes in hardened portland-cement paste during freezing. *Proceedings of the Thirty-Second Annual Meeting of the Highway Research Board, Washington, D.C., January 13-16, 1953* (pp. 285-297). Washington, DC: Highway Research Board.

- Powers, T. C., & Willis, T. F. (1950). The air requirement of frost resistant concrete. *Proceedings of the Twenty-Ninth Annual Meeting of the Highway Research Board Held at Washington, D.C. December 13-16, 1949* (pp. 184-211). Washington, DC: Highway Research Board.
- Ramachandran, V. S. (1997). *Concrete admixtures handbook* (2nd ed.). Park Ridge, NJ: Noyes Publications.
- Torrans, P. H., & Ivey, D. L. (1968). *Review of literature on air-entrained concrete* (Report No. 103-1). College Station, TX: Texas Transportation Institute, Texas A&M University.
- Walker, H. N., Lane, D. S., & Stutzman, P. E. (2006). *Petrographic methods of examining hardened concrete: A petrographic manual* (Report No. FHWA-HRT-04-150). McLean, VA: Federal Highway Administration.
- Whiting, D. A., & Nagi, M. A. (1998). *Manual on Control of Air Content in Concrete*. Skokie, IL: Portland Cement Association.

K-TRAN

KANSAS TRANSPORTATION RESEARCH AND NEW-DEVELOPMENT PROGRAM

